Spectrum Sharing under Interference Constraints

Abdoulaye Bagayoko

Orange Labs

Ph.D. THESIS

presented to

University of Cergy-Pontoise
École Doctorale Sciences et Ingénierie

to obtain the title of

Doctor of Science of the University of Cergy-Pontoise
***Specialty:* Sciences and Technologies of Information and Communication**

Defended by

Abdoulaye Zana BAGAYOKO

Spectrum Sharing under Interference Constraints

prepared at
Orange Labs (France Telecom R&D) Issy-les-Moulineaux.
Équipes Traitement de l'Information et Systèmes (ETIS) - UMR 8051
ENSEA - Université de Cergy-Pontoise - CNRS

defended on October 29, 2010

Jury:

President:	Prof.	Mérouane DEBBAH	Supélec/Alcatel Lucent
Reviewers:	Prof.	Philippe GODLEWSKI	Telecom-Paritech
	Dr.	David GESBERT	EURECOM Sophia Antipolis
Examinator:	Dr.	Christophe LE MARTRET	THALES
Advisor:	Prof.	Inbar FIJALKOW	ETIS/ENSEA-UCP-CNRS
Co-advisor:	M.	Patrick TORTELIER	Orange Labs (France Telecom R&D)
Invited:	Dr.	Berna SAYRAC	Orange Labs (France Telecom R&D)

A ma mère, Korotoumou BAGAYOKO,
que j'adore.

"L'écriture est une chose et le savoir en est une autre. L'écriture est la photographie du savoir, mais elle n'est pas le savoir lui-même. Le savoir est une lumière qui est en l'homme; héritage de ce qui lui a été transmis."

Amadou Hampaté Bâ.

Résumé

Le spectre électromagnétique est une ressource naturelle dont l'usage doit être optimisé. Un grand nombre de travaux actuels visent à améliorer l'utilisation des fréquences radio en y introduisant un degré de flexibilité rendu possible par l'agilité en forme d'onde et en fréquence permise par la radio logicielle (SDR), ainsi que par les méthodes de traitement intelligent du signal (radio cognitive). Cette thèse se place dans ce contexte. Concrètement, nous considérons le problème de partage du spectre électromagnétique entre plusieurs utilisateurs sous contraintes d'interférence mutuelle. Notre objectif est de contribuer à l'évaluation du gain de partage de cette ressource rare qu'est le spectre électromagnétique. En étudiant le canal gaussien d'interférence avec l'interférence traitée comme du bruit additif gaussien aux différents récepteurs, nous avons trouvé une description géométrique et plusieurs caractérisations de la région des débits atteignables. Ensuite, considérant un cas plus réaliste où chaque utilisateur a une certaine qualité de service, nous avons trouvé une condition nécessaire et suffisante pour permettre la communication simultanée à travers le canal gaussien d'interférence pour deux utilisateurs. Dans un scénario de partage entre un utilisateur primaire ayant une plus grande priorité d'accès au spectre et un utilisateur secondaire, après avoir déterminé des bornes minimales pour le débit du primaire en fonction du schéma d'allocation de puissance de l'utilisateur secondaire, nous avons proposé une technique originale d'allocation de puissance pour l'utilisateur secondaire accédant de manière opportuniste au spectre sous contraintes de performance de coupure pour tous les utilisateurs. En particulier, cette technique d'allocation de puissance n'utilise que l'information sur l'état des canaux des liens directs allant de l'émetteur secondaire vers les autres points du réseau. Finalement, considérant des modèles de canaux plus réalistes; après avoir montré l'existence d'une zone d'exclusion autour du récepteur primaire (zone où il n'y a aucun transmetteur secondaire, dans le but de protéger l'utilisateur primaire contre les fortes interférences), nous avons caractérisé l'effet du *shadowing* et du *path-loss* sur la zone d'exclusion du primaire.

Abstract

In this thesis, we address the problem of spectrum-sharing for wireless communication where multiple users attempt to access a common spectrum resource under mutual interference constraints. Our objective is to evaluate the gains of sharing by investigating different scenarios of spectrum access. Studying the Gaussian Interference Channel with interferences considered as noise, we found a geometrical description and several characteristics of the achievable rate region. Considering a more realistic scenario, with each user having a certain QoS, we found necessary and sufficient condition to be fulfilled for simultaneous communications over the two-user Gaussian Interference Channel. Furthermore, we proposed two lower bounds for a single-primary-user mean rate, depending on the secondary user power control scheme. Specially, we investigated an original power control policy, for a secondary user, under outage performance requirement for both users and partial knowledge of the channel state information. Finally, considering a spectrum-sharing with a licensee or primary user and several secondary or cognitive users, we showed the existence of an exclusive region around the primary receiver and we characterized the effects of shadowing and path-loss on this exclusive region (or *no-talk zone*).

Remerciements

Les travaux présentés dans ce mémoire ont été réalisés au sein du laboratoire RESA (RÉSeaux d'Accès) d'Orange Labs (France Telecom R&D) et du laboratoire ETIS[1] à l'ENSEA[2].

Je remercie solennellement et avec gratitude Monsieur Patrick TORTELIER d'Orange Labs et le Professeur Inbar FIJALKOW, de l'ENSEA, qui ont dirigé ces travaux avec enthousiasme et pédagogie. A côté de Patrick TORTELIER, J'ai appris à être patient dans la recherche, ainsi qu'à mieux m'organiser pour optimiser le rendement de mes efforts. Le Professeur Inbar FIJALKOW m'a aidé à améliorer ma démarche scientifique et à mieux synthétiser.

Je remercie le Prof. Mérouane DEBBAH, le Prof. Philippe GODLEWSKI, le Dr. David GESBERT, le Dr. Christophe LE MARTRET et le Dr. Berna SAYRAC d'avoir accepté de faire partie du jury de cette thèse.

Je remercie ma mère Korotoumou BAGAYOKO à qui je dédie ces modestes travaux. C'est grâce à son amour que je suis arrivé à fournir les efforts qui ont conduit aux résultats des travaux de cette thèse. Je remercie tout le reste de ma famille: mon père Zana BAGAYOKO, en particulier pour son exigence pour l'excellence, mes frères et mes soeurs que je chéris de tout mon coeur. J'ai une pensée particulièrement positive du soutien inestimable de la famille SANOGO, en particulier mon tonton Kalfa SANOGO du PNUD, ma tante Mme SANOGO Fatimata COULIBALY et leurs fils Kakotan SANOGO (pour tous les bons conseils que je garde encore au fond du tiroir) et Bakary Tagognon SANOGO.

Je remercie tous mes ami(e)s pour leur amitié sincère et chaleureuse qui m'a toujours permis de garder en vue mes objectifs, même pendant les moments les plus difficiles. Avec le Dr. Fousseynou BAH, Mr. Nouhoum Bouya TRAORE, Mlle Kadidia Kéïta, le Dr. Fatoumata Bintou SANTARA, Mlle Aïssata TRAORE et Mlle Diénèba POUDIOUGOU, je pouvais me relever à chaque échec.

Enfin, je remercie mes collègues d'Orange Labs et d'ETIS pour les discussions et les collaborations que j'ai eues avec eux durant les trois années de cette thèse.

[1] Équipes Traitement de l'Information et Systèmes

[2] École Nationale Supérieure de l'Électronique et de ses Applications

Contents

List of Figures v

Glossary ix

General Introduction 1

1 Introduction to Spectrum Sharing and Cognitive Radio 7
- 1.1 Fixed spectrum allocation and barriers to spectrum access . . . 7
  - 1.1.1 Command-and-control scheme . . . 8
  - 1.1.2 Spectrum Gridlock . . . 8
  - 1.1.3 Concluding Remarks . . . 9
- 1.2 Flexible spectrum usage based cognitive radio . . . 9
  - 1.2.1 Underlay spectrum-sharing . . . 11
  - 1.2.2 Overlay spectrum-sharing . . . 12
  - 1.2.3 Interweave spectrum-sharing . . . 13
  - 1.2.4 Concluding remarks . . . 15
- 1.3 Basic model of spectrum-sharing: the Gaussian Interference Channel . . . 16
  - 1.3.1 Definition and motivation . . . 17
  - 1.3.2 Capacity and achievable rate regions . . . 18
  - 1.3.3 Concluding remarks . . . 18
- 1.4 Conclusions . . . 19

2 Achievable rate region of the Gaussian Interference Channel 21
- 2.1 Introduction . . . 21
- 2.2 Achievable rate region for the 2-user GIC . . . 22
  - 2.2.1 Mathematical modelling . . . 22
  - 2.2.2 Geometrical description of the rates region . . . 23
  - 2.2.3 Numerical results and sum rate maximization . . . 25
- 2.3 Achievable rate region for the 3-user GIC . . . 27
  - 2.3.1 Mathematical modelling . . . 27
  - 2.3.2 Geometrical description of the SINR region . . . 29

2.3.3 Contour lines of the achievable rate region . . . 31
2.3.4 Maximum sum rate . . . 34
2.4 Conclusions . . . 37

3 Simultaneous outage performance of the 2-user Gaussian Interference Channel in fading environment 39
3.1 Introduction . . . 39
3.2 Problem formulation . . . 40
3.2.1 Signals model and assumptions . . . 40
3.2.2 Main goal . . . 41
3.2.3 Main results . . . 41
3.3 Mathematical description of simultaneous outage performance problem . . . 41
3.3.1 Distribution of the SINR variable . . . 42
3.3.2 Outage probability . . . 42
3.4 Set of possible power pairs . . . 43
3.5 Condition to ensure simultaneous outage performance . . . 44
3.5.1 Condition . . . 45
3.5.2 Numerical examples . . . 48
3.6 Linear approximation . . . 49
3.7 Conclusions . . . 50

4 Power control of spectrum-sharing in fading environment with partial channel state information 53
4.1 Problem formulation . . . 53
4.1.1 System and channel model . . . 54
4.1.2 Main goal . . . 54
4.1.2.1 Lower bounds for the primary user mean rate . . . 54
4.1.2.2 Secondary power control . . . 54
4.1.2.3 Channel and parameters estimation . . . 55
4.2 State of the art . . . 55
4.3 Lower bounds of the primary user mean rate . . . 56
4.3.1 Unconstrained spectrum-sharing . . . 57
4.3.2 Constrained spectrum-sharing . . . 58
4.3.2.1 Primary mean-rate loss constraint . . . 58
4.3.2.2 Interference constraints . . . 58
4.3.2.3 Lower bound . . . 59
4.4 Power control for spectrum secondary use . . . 60
4.4.1 Power control with mean-transmit-power constraint only . . . 60
4.4.1.1 Optimal power control . . . 60
4.4.1.2 A scheduling approximating the optimal power control . . . 60
4.4.1.3 Numerical examples . . . 61
4.4.2 Power control with outage performance requirement and direct links CSI . . . 62
4.4.2.1 Outage performance constraints . . . 62

4.4.2.2 Power control . . . 64
4.4.2.3 Mean transmit and mean interference power . . . 65
4.4.2.4 Overall outage probability . . . 66
4.4.2.5 Connection with TIFR transmission policy . . . 67
4.4.2.6 Numerical examples . . . 70
4.5 Conclusions . . . 75

5 Cognitive radio under path-loss in shadowing-fading environment 77
5.1 Problem formulation . . . 77
5.1.1 Channel models and impact on rate . . . 78
5.1.2 System model and main goal . . . 79
5.1.2.1 Primary *no-talk zone* . . . 79
5.1.2.2 System model . . . 79
5.1.2.3 Main Goal . . . 80
5.2 Distribution of the primary SINR . . . 82
5.3 Primary outage constraint . . . 83
5.3.1 Outage constraint in the worst case of interference . . . 84
5.3.2 Numerical examples . . . 86
5.4 Primary *no-talk zone* versus shadowing . . . 88
5.5 Conclusions . . . 91

Conclusions and perspectives 93

A Lower bounds of the primary mean rate 97
A.1 Lower bounds A.1 . . . 97
A.2 Lower bounds A.2 . . . 100

B Mean transmit power and mean interference power 101

Bibliography 104

List of Figures

1.1 RF spectrum allocation in France 8
1.2 Principle Elements of a cognitive radio, [5]. 10
1.3 Cognitive radio paradigms [12], [13]. 11
1.4 Underlay spectrum sharing corresponding to the Interference Temperature Concept of the FCC (from [13], [12]). 12
1.5 Illustration of spectrum opportunity: secondary transmitter Cr-Tx wishes to transmit to secondary receiver Cr-Rx, where Cr-Tx should watch for nearby primary receivers and Cr-Rx should watch for nearby primary transmitters, [60]. 15
1.6 "listen-before-talk"(LBT) spectrum opportunity detection: Cr-Tx detects spectrum opportunities by observing primary signals (the exposed transmitter Pr-Tx2 is a source of false alarms whereas the hidden transmitter Pr-Tx3 and the hidden receiver Pr-Rx1 are sources of miss detections), [60]. 16
1.7 The two-user Gaussian Interference Channel. 17

2.1 Illustration of the SINR region for the two-user GIC. 24
2.2 achievable rate region for $\mathcal{P}_1 = \mathcal{P}_2 = 4$, medium interference, $a_{12} = a_{21} = 0.2$; C_Σ is maximal when both users transmit at their maximum power. . . 25
2.3 achievable rate region for $\mathcal{P}_1 = \mathcal{P}_2 = 4$, strong interference, $a_{12} = a_{21} = 1.0$; C_Σ is maximum when only one user is transmitting at its maximum power. 26
2.4 Maximum sum rate point for the two-user Gaussian Interference Channel. . 27
2.5 The three-user Gaussian Interference Channel. 28
2.6 A Geometric representation of the constraints on S_3, when respectively $S_1 = 0$ and $S_2 = 0$. 30
2.7 Illustration of the SINR region for the three-user GIC 31
2.8 Contour lines of a three-user achievable rate region, $a_{i,j} = 0.2$ for all $i \neq j$. 34
2.9 Same parameters as Fig. 2.8, except $a_{23} = a_{32} = 1$ 35
2.10 Contour lines of the three-user achievable rate region of [30]. 36
2.11 Sum rate as a function of R_3. Same settings as for Fig. 2.10. 36

3.1 Curves of $\psi_1(P_1)$ and $\psi_2^{-1}(P_1)$. The curves meet in $P_{1,\alpha}$, then, there is a two-dimensional region $\mathcal{P}$ of (P_1, P_2) where the simultaneous outage performance is achievable. 45
3.2 Curves of $\psi_1(P_1)$ and $\psi_2^{-1}(P_1)$. The curves do not meet, then simultaneous outage performance is not achievable. 46
3.3 Linear approximation error: $\psi_1(P_1) - \psi_{1,\text{lin}}(P_1)$ and $\psi_2(P_2) - \psi_{2,\text{lin}}(P_2)$. . 50

4.1 Primary mean rate versus secondary mean power for different power control schemes from the secondary user: (a) optimal power control *water-filling*; (b) proposed scheduling approximating the optimal power control; (c) constant power control that provides the lower bound of the primary mean rate. $\bar{P}_1 = 1$, $\sigma^2 = 0.01$ and $\lambda_{11} = \lambda_{12} = \lambda_{22} = \lambda_{21} = 1$. 62
4.2 Secondary mean rate versus mean power for different power control schemes: (a) optimal power control *water-filling*; (b) proposed scheduling approximating the optimal power control; (c) constant power control that provides the lower bound of the primary mean rate. $\bar{P}_1 = 1$, $\sigma^2 = 0.01$ and $\lambda_{11} = \lambda_{12} = \lambda_{22} = \lambda_{21} = 1$. 63
4.3 Primary mean rate, $\mathbf{C}_1$, versus peak interference power Q_{peak} for different values of outage probability P_{out}. 71
4.4 Secondary mean rate, $\mathbf{C}_2$, versus peak interference power Q_{peak} for different values of outage probability P_{out}. 72
4.5 Primary mean rate $\mathbf{C}_1$ versus mean interference power $\mathbb{E}[p_2\,\hat{g}_{12}]$ for different values of outage probability P_{out}. 72
4.6 Mean transmit power, $\mathbb{E}[p_2]$, and mean interference power, $\mathbb{E}[p_2\,\hat{g}_{12}]$, versus peak interference power, Q_{peak}. $p_{2,\text{peak}} = 1$ and $\text{P}_{\text{out}} = 0.1$. 73
4.7 Outage probability, P_{out}, versus peak interference power, Q_{peak}, for different values of minimum received power, K, required for secondary service. . . . 73
4.8 Primary mean rate, $\mathbf{C}_1$, and secondary zero-outage capacity, $\mathbf{C}_{2,\text{out}}$, versus mean interference power, $\mathbb{E}[p_2\,\hat{g}_{12}]$, for $\text{P}_{\text{out}} = 0.1$. 74
4.9 Mean transmit power, $\mathbb{E}[p_2]$, versus mean interference power, $\mathbb{E}[p_2\,\hat{g}_{12}]$, for $\text{P}_{\text{out}} = 0.1$. 74

5.1 A single primary receiver Pr-Rx is outside the interference ranges of N cognitive users. We assume that there is a spectrum opportunity so that the N cognitive users can transmit without violating the interference constraints. Transmitter Cr-Tx_1 is supposed to be the closest to Pr-Rx. 80
5.2 The worst case of interference for primary receiver of Fig. 5.1 corresponds to the theoretical case where all the N secondary transmitters would be at the distance R_0 of Pr-Rx, where R_0 is the distance between Pr-Rx and the closest secondary transmitter. 81
5.3 Evolution of function $Q\left(\frac{a\,m_p - \log(\alpha\,(t+\sigma^2))}{a\,\nu_p}\right)$, $a\,m_p = 0$, $a\,\nu_p = 1$, $\sigma^2 = 0.01$ and $\alpha = 3$. 85
5.4 Probability density function of the random variable T, which is identically distributed with the sum interference variable I_{cr}. $a\,m_{I_{\text{cr}}} = 1$, $a\,\nu_{I_{\text{cr}}} = 1/10$. 87

5.5 Simulation settings 87
5.6 Outage probability versus radius of primary *no-talk zone* for different values of shadowing standard deviation. 88
5.7 Radius of primary *no-talk zone* and guard band versus standard deviation of secondary-links shadowing for different values of the upper bound of the outage probability. $P_p = 1$, $r_p = 1$, and $\eta = 4$. 90
5.8 Radius of primary *no-talk zone* and guard band versus standard deviation of secondary-links shadowing for different values of path-loss exponent η. $P_p = 1$, $r_p = 1$ and $p_{\text{up}} = 0.1$. 90

Glossary

CSI	Channel State Information.
CR	Cognitive Radio.
DL	Down Link.
GIC	Gaussian Interference Channel.
HSDPA	High Speed Downlink Packet Access.
LTE	Long Term Evolution.
MAC	Multiple Access Channel.
Mbps	Mega Bit per second.
MIMO	Multiple Input Multiple Output.
MISO	Multiple Input Simple Output.
PCLC	Primary-Capacity-Loss Constraint.
PR	Spectrum Primary User.
QoS	Quality of Service.
RF	Radio Frequency.
SDR	Software Defined Radio.
SINR	Signal to Interference plus Noise Ratio.
SNR	Signal to Noise Ratio.
TIFR	Truncated channel Inversion with Fixed Rate.
UL	Up Link.

General Introduction

Tremendous changes are occurring in wireless communications so that the mobile phone is rapidly turning into a sophisticated mobile device capable of most of the applications of PCs (Personal Computers). The market of smart phones with powerful processors, abundant memories and large screens has outpaced the rest of the mobile phone market for several years. Investigations show that the mobile data traffic footprint of a single mobile subscriber in 2015 could very conceivably be 450 times what it was in 2005 (10 years before), [7], and almost 66 percent of the world's mobile data traffic will be video by 2014, [6]. These changes come along with a strong demand in bandwidth and high data rates. For example, the data rates provided by the initial High Speed Downlink Packet Access (HSDPA) extension to 3G networks enable a user to access to Internet at speeds up to 1.8 Mbps. Enhancements in HSDPA modulation schemes increase this speed to greater than 10 Mbps. With the Long Term Evolution (LTE) technology, we are expecting a peak data rate of 100 Mbps DL/ 50 Mbps UL within 20 MHz bandwidth. With higher modulation and coding schemes, we are already close to the limit of what modulation and coding can bring to data rate enhancement. Then, there is a need of better frequency reuse and interference management.

Traditionally, licensing gave communications systems exclusive access to blocks of spectrum. It allows almost eliminating the danger of harmful interference but leaves the majority of the spectrum idle when and where the license holder is not active. A few bands were designated for unlicensed devices. Even if access to unlicensed spectrum is generally subject to few restrictions, we note limited transmit power constraint that keeps utilization low enough to limit mutual interference (although utilization and serious interference problems sometimes grow over time). However, with high demand for wireless products and services (especially bandwidth-greedy applications), there is motivation to support a greater density of wireless devices through adoption of new technology and policy, [10]. Very fortunately, emerging technology, including Cognitive Radio (CR) and Software-Defined-Radio (SDR), [1], are contributing to make this possible.

A Cognitive Radio uses sophisticated signal processing at the physical layer in order to adapt to changes in its environment, to its user's requirements and to the requirements of other radio users sharing the spectrum environment, [4]. So, Cognitive Radio could provide means to efficiently use the electromagnetic spectrum by autonomously detecting

and exploiting empty spectrum or by **sharing spectrum** with other users intelligently (by meeting given interference constraints for instance). Arising from the evolution of software radio, cognitive radio presents the possibility of numerous revolutionary applications.

However, there are two main obstacles to realizing a full Cognitive Radio. First, we have the challenge of making a truly cognitive device, or a machine with the ability to intelligently make decisions based on its own situational awareness. Second, we have the challenge of SDR technologies development to enable reconfigurability. It is expected that a single full Cognitive Radio device capable of operating in any frequency band up to 3GHz without the need for rigid front-end hardware (excluding the antenna) will not be available before 2030, [4]. For the meantime, at least, advanced investigations are taking place in the research to understand spectrum sharing and evaluate the gain of cognition. Specially, spectrum access strategy and power control to optimize given utility is a big challenge that may be illustrated with «*an analogy of crossing a multi-lane highway, each lane having different traffic load. The objective is to cross the highway as fast as possible subject to a risk constraint. Should we wait until all lanes are clear and dash through, or cross one lane at a time whenever an opportunity arises? What if our ability to detect traffic in multiple lanes varies with the number of lanes in question?*» [60].

Context and Objectives

We consider in this thesis the general problem of spectrum-sharing by allowing several users accessing a common frequency band while considering mutual interference as Gaussian additive noise at the reception. The Gaussian interference channel is considered as a basic model of spectrum sharing. Cognitive radio is considered to enhance the system performance by satisfying spectrum licensee user's requirements while having some performance for secondary users.

Our objective is to contribute to the works led within the framework of characterization and performance evaluation of spectrum-sharing networks. For this purpose, first, we aim to characterize the achievable performance of the Gaussian Interference Channel when mutual interference is treated as additive noise. Even known as suboptimal, considering interference as noise leads to a basic spectrum-sharing scenario that is important to understand before bringing cognition and sophisticated technics to enhance performance. Second, we aim to contribute to the cognitive networks topology design through quantitative study of the effects of wave propagation parameters on the topology. Finally, we investigate secondary power control constrained by both users requirements.

The main goal of the achievable rate set characterization for the Gaussian Interference Channel is to respond to the question: **How much throughput is it possible to achieve in spectrum-sharing, assuming channel gains are constant, using single user decoding ?** The users are not supposed to cooperate, so they do not know the message and codebook of each other. Furthermore, we suppose that the transmit power of each user is included between 0 (zero) and a maximum value. Due to mutual interference, own rates are function of the transmit powers of both users. We have to deal with these constraints to obtain an original geometrical description for the achievable rate region.

Besides, we address the following question, **is it possible, for at least two users, to simultaneously transmit over the same frequency band while achieving given outage performance for each user ?** We investigate the condition to enable such a spectrum sharing in a fading environment where outage performance guaranties for each user to have given minimum instantaneous rate at given occurrence.

Considering a basic spectrum-sharing between one primary user and one secondary user, we also address the question: **how harmful is the secondary transmission on the primary mean rate ?** The response to that question could provide a secondary power control scheme that leads to the lower bound of the primary mean rate for given spectrum access constraint. To address this question, we suppose that primary user is performing constant power control. Finally, in the concern to have a pattern of spectrum sharing that enable to guaranty for each user given outage performance while having only partial channel state information, in fading environment, we consider a primary user with constant power control and a secondary user with only partial channel state information. **Can the secondary user transmit, in the same time as the primary user, while meeting both outage performance constraints, having only direct links gains (channel from the secondary transmitter to the other points of the network) estimations ?** The response could provide an original opportunistic secondary power control which adapts well with the above definition of spectrum opportunity, because of QoS given (through outage performance) to both users.

When analyzing cognitive networks, we study the conditions for secondary or cognitive users to access the spectrum under opportunity condition only. Contrary to most of previous works, we assume that a spectrum is an opportunity not only when primary interference constraint is met (so primary reception quality should not be considerably affected by secondary transmission) but also when secondary interference constraint is met, as in [60]. In other words, both primary reception and secondary reception should be successful in term of QoS. Under this definition, wave propagation condition could impact on network topology: a spectrum may be an opportunity for given secondary user in area A for time t, but not for time $t+1$, due to shadowing for instance, even been in the same area A. So, we aim to contribute in searching a solution to the question **what is the impact of shadowing and path-loss on cognitive networks topology ?**

Outline of this thesis

The dissertation is organized in five chapters as follows.

In chapter 1, we give an introduction to cognitive radio and spectrum sharing. The goal of this chapter is to define and justify the underlying concepts of this thesis. In one hand, first, fixed spectrum allocation is presented with its disadvantages, then flexible spectrum sharing enabled by cognitive radio is explained. In the other hand, it is question of the Gaussian Interference Channel as a basic model of spectrum-haring. In particular, we define the Gaussian Interference Channel and give an overview of the investigations carried out on the capacity region of the two-user Gaussian Interference Channel.

In chapter 2, we present our works on the Gaussian Interference Channel. We give

a new geometrical description of the achievable rate region of the Gaussian Interference Channel when the interference is treated as Gaussian additive noise at the reception. We use this geometrical description to analyze different classes of interference and we give interpretation to known results on the sum rate maximization.

In chapter 3, for the two-user Gaussian Interference Channel with each user having an outage performance, we give an original, necessary and sufficient condition to enable simultaneous communication other a common spectrum resource. When the condition is fulfilled, we give analytical expressions to define the two dimensional region of transmit powers where given simultaneous outage performance is achievable.

The chapter 4 is devoted to the secondary user power control challenges in cognitive networks. We consider a basic network with one primary user and one secondary user, the interference been treated as noise. First, we look for lower bounds to the primary mean rate according to the channel state information available for the secondary user power control, and according to the type of constraint for spectrum sharing. So, we could compare primary mean rate, for different power control techniques, to its lower bounds. Specially, we will investigate an original power control, ensuring for each user given outage performance, and using only the channel state information for direct links from secondary transmitter to the other points of the network. Contrary to the optimal power control, derived in [57] and [58], and the non-cooperative games in [56], the goal of this power control is neither to achieve, in any case, maximum possible rate, nor to maximize *selfish* utilities. But the particularity is to ensure, at some occurrence predefined by the outage probability, at least given minimum instantaneous rates to the two users, while using only the direct links gains estimations.

In chapter 5, we consider a cognitive network with primary and secondary users. Using the definition of spectrum opportunity in [60], we demonstrate the existence of an exclusive region or *no-talk zone* around each primary user and we quantify the effects of shadowing and path-loss on a single primary *no-talk zone*. Analytical expressions of the radius of the primary *no-talk zone* in terms of shadowing standard deviation and path-loss exponent is investigated.

Contributions and Publications

We summarize below the main contributions of this work:

- In chapter 2, we propose a new characterization of the achievable rate region of the Gaussian Interference Channel when the interference is treated as noise. New analytical expressions are given to describe the achievable performance of the different users as well as their sum rate. Although it is known that this regime, where interference is treated as noise, leads to suboptimal performance, the knowledge of the *interference-noise* achievable rate region is useful to understand how to deal with interference without cognition and sophisticated technics.

- We find an original simple condition, in chapter 3, to allow simultaneous transmission for two users sharing the same frequency band, interference been treated as

Gaussian additive noise, with own outage performance, ensuring for each user to have a minimum necessary rate for given occurrence. Furthermore, this condition is clearly demonstrated to be necessary and sufficient.

- In Chapter 4, considering a basic spectrum-sharing between a primary and a secondary users, the interference been considered as noise and primary user performing a constant power control, we find new lower bounds for the primary user mean rate according to the power control scheme of the secondary user, depending on available channel state information and sharing constraints. We also propose an original secondary user power control appropriate for spectrum-sharing systems that carry out real-time delay-sensitive applications, e.g. voice and video.

- In chapter 5, we propose an original quantification of the effects of shadowing and path loss on a single primary-user *no-talk zone*, in the worst case of interference. We assume that the worst case of interference, for primary user, corresponds to the theoretical situation where all the secondary users are close to the boundaries of the *no-talk zone*. Although these results are intuitive, this work is the first one, in our knowledge, giving analytical quantification of shadowing and path-loss effects in cognitive networks.

At the present date, this thesis has led to the following publications:

Journal papers

1. P. Tortelier and A. Bagayoko, "On the achievable rate region of the Gaussian interference channel: the two and three-user cases," *Annals of Telecommunications*, October 2009, Online,
available: http://www.springerlink.com/content/p5524607963308m7.

2. A. Bagayoko, P. Tortelier and I. Fijalkow "Power control of spectrum-sharing in fading environment with partial channel state information," *IEEE transactions on Signal Processing, to appear.*

International Conferences

1. A. Bagayoko, P. Tortelier and I. Fijalkow "Impact of shadowing on the primary exclusive region in cognitive networks," *European Wireless 2010*, Lucca, Italy, April 2010.

2. A. Bagayoko, P. Tortelier and I. Fijalkow "Simultaneous outage performance in a spectrum-sharing fading environment," *IEEE SPAWC,* Marrakeck, Morocco, June 2010.

3. A. Bagayoko, P. Tortelier and I. Fijalkow "Spectrum-Sharing Power Control with Outage Performance Requirements and Direct Links CSI Only," *IEEE PIMRC,* Istanbul, Turkey, September 2010.

National Conferences

1. A. Bagayoko, P. Tortelier and I. Fijalkow "Allocation de puissance dans le partage du spectre avec une connaissance partielle des canaux," *Gretsi 2009,* Dijon, France, September 2009.

Chapter 1

Introduction to Spectrum Sharing and Cognitive Radio

The electromagnetic radio spectrum is a scarce natural resource, the use of which by telecommunication systems is licensed by governments. For a long time, spectrum management was based on rigid partitioning. The results are that most of the spectrum bands are vastly underutilized, even in urban environment, [46]. New technics are then investigating to make the spectrum usage more flexible.

The main goal of this chapter is to set and justify the problem that we will address in more details in the sequel. First, we present the long-term rigid spectrum management, named *Command-and-control*, and the barriers encountered by such a spectrum access. Then, we present and examine new spectrum-sharing methods based on cognitive radio. Finally, we give some concluding remarks.

1.1 Fixed spectrum allocation and barriers to spectrum access

Most of today's radio systems are not aware of their radio spectrum environment. In general, they operate in specific frequency bands using well defined spectrum access technologies. This static management of spectrum is commonly called command-and-control and leads to barriers to accessing the spectrum in various dimensions (space, time, polarization, frequency, power of signal transmission, interference...).

In this section, first we will present the current spectrum management scheme which has been traditionally adopted by most of the regulators around the globe. Second, we will talk about the barriers from this fixed spectrum allocation scheme. Finally, we give some conclusions.

1.1.1 Command-and-control scheme

Traditionally, interference protection is achieved through spectrum licensing policy, whereby wireless systems get exclusive access to spectrum [10]. The command and control scheme consists of a) dividing the spectrum into distinct bands, each defined over a range of frequencies; b) assigning specific communication uses to specific bands, and c) determining a licensee for each band, who is generally granted exclusive use of the band. Examples of licensed frequency bands today are the radio and television bands, cellular and satellite bands, and air traffic control bands. The main advantage of this approach is that the licensee completely controls its assigned spectrum, and can thus unilaterally manage interference between its users and hence their quality of service (QoS), [8]. Let us consider for instance the cellular spectrum licensing in France (Cf. Fig. 1.1). The GSM operates in channels located somewhere in 880-960 MHz and in 1710-1880 MHz and no other technology is allowed interfering with it. the UMTS bands are licensed in the same way (2000-2200 MHz). Similar situation exists in several countries in the world. While the command-and-control leads to almost eliminate the danger of harmful interference, it leaves the majority of the spectrum idle when and where the license-holder is not active [2]. In this way, spectral efficiency is not optimized.

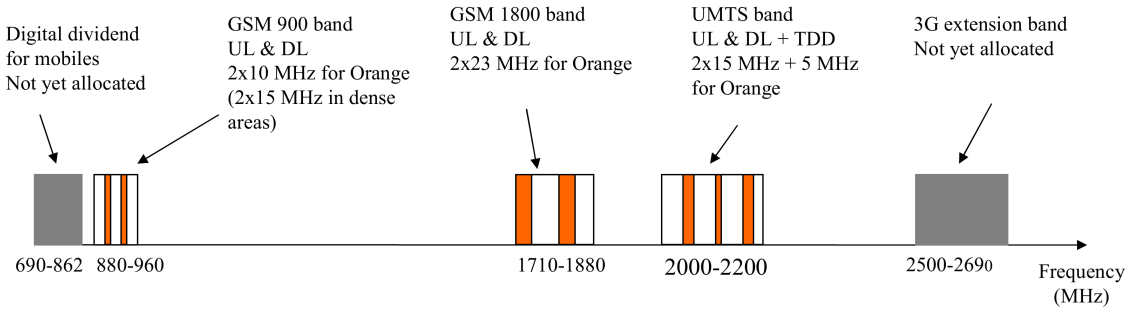

Figure 1.1: RF spectrum allocation in France

1.1.2 Spectrum Gridlock

Investigations show that the licensed spectrum is rarely utilized continuously across time and space [2]. The large spatial scope of the licenses (i.e. licenses are valid for very large regions) leaves the spectrum resource underused in areas where there is less need of the provided service. The same situation occurs in the time dimension. For example, in given areas, TV bands may be much more underused during rush hour than in night. However, in the current spectrum allocation, there is no way to *opportunistically* utilize the unused licensed bands commonly referred to as *white spaces*. Moreover, in current licensing regime, as specific services are mapped to fixed spectrum bands, if the providers of a particular service are under utilizing or not using the spectrum, no other services can be offered in that spectrum leaving it fallow (for example the analog broadcast TV bands are often showed to be unused) [3]. The license granularity is also pointed up as a barrier

to the spectrum usage. Actually, current cellular licenses are for large chunks of spectrum. There is no way for a provider to acquire smaller amounts of spectrum on small spatial and temporal scale [3]. Now, it is obvious that the traffic composition varies (from strict 8 Kbps voice to more bursty data traffic with significant throughputs). Then the amount of needed spectrum varies in time and space.

The current fixed spectrum allocation leads to several barriers to the spectrum usage. More sophisticated spectrum usage is needed to support the increase in user data rates and to support more heterogenous wireless applications.

1.1.3 Concluding Remarks

With the command-and-control management, all frequencies below 3 GHz have been allocated to specific uses [46]. By analyzing the spectrum scarcity as perceived today, it is found that this is largely due to inefficient frequency allocation rather than any physical shortage [35]. Investigations of spectrum utilization indicated that the spectrum is not fully used in space (geographic location) or time, [2], [3], [4], [5], [33], [34]. The command and control leads to a wasteful usage of spectrum which is a precious natural resource. It is necessary today to make the spectrum usage more flexible in order to support the increasing demand in user data rates and to counter the penury of available spectrum resources. New promising methods of spectrum usage based on cognitive radio may provide solutions.

1.2 Flexible spectrum usage based cognitive radio

Out of the spectrum shortage was born the idea of flexible spectrum access as recommended particularly by the 2002 report of the Federal Communications Commission (FCC)'s Spectrum Policy Task Force, [2]. Spectrum-sharing for unlicensed and licensed bands, dynamic spectrum access, together with cognitive radio have been proposed as promising solutions for improving the spectrum efficiency.

We can define cognitive radio as «*wireless communication system that intelligently utilizes any available side information about the a) activity, b) channel conditions, c) codebooks, or d) messages of other nodes with which it shares the spectrum,*» [8]. To make the spectrum-sharing more profitable (i.e. to protect the spectrum licensee against harmful interference while having some throughput for a secondary use) cognitive radio must collect and process information about its coexisting users within the spectrum. Then, advanced sensing and signal processing capabilities are required. When considering the regulatory aspects of cognitive radio, we can simplify its representation to just three principle elements (Cf. Fig. 1.2), [5]:

- *a software radio module which transmits and receives the wireless payload. The RF hardware within this module must be agile in order to utilize available spectrum. The inputs to this module are the user data with the required QoS. The module identifies suitable waveforms and passes this list of options on to the next module;*

- *a spectrum monitoring and options module which identifies suitable spectrum holes based on spectrum monitoring information. The output is a list of options, each one specifying a set of transmission parameters such as frequency, transmit power and waveform;*
- *a policy box module which evaluates the options, compares them with information on spectrum regulations, such as which spectrum is available for secondary usage and the relevant spectrum mask, and decides which is the most appropriate set of transmission parameters to use.*

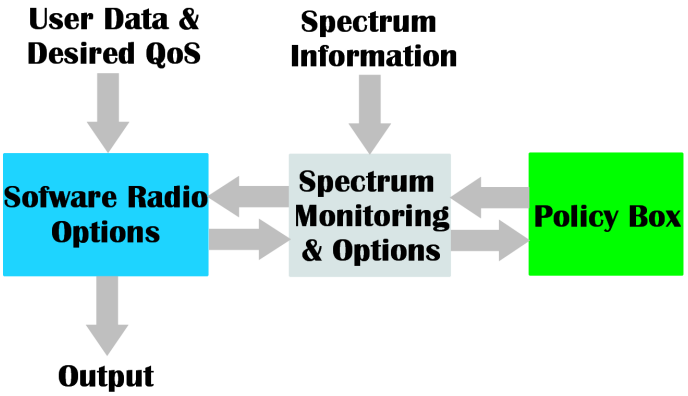

Figure 1.2: Principle Elements of a cognitive radio, [5].

Technological advances to support cognitive radio capabilities are either here today or on the horizon (see for instance [15] and references therein), and thus should not form a major barrier to the cognitive networks realization. The larger barrier is the willpower of regulatory bodies to allow significant changes in the way wireless spectrum is currently allocated to enable cognitive techniques, [8]. Cognitive radio is a rapidly developing technology area that should offer great benefits to all members of the radio community from regulators to users. Many profits are expected from spectrum sharing empowered by cognitive radio. Spectrum regulators will potentially benefit because of the spectrum efficiency gains achieved by sharing spectrum or using the spectrum opportunistically. The need for centralized (command-and-control style) spectrum management will be reduced. Automatic (seamless) spectrum management will also be possible with cognitive radio. For example, cognitive radios could be programmed to manage their own spectrum access using appropriate (software-based) regulatory policies, involving reduction in management costs. For service providers and spectrum owners, cognitive radio and spectrum-sharing will create opportunities for new service providers and existing service providers will be able to grow their businesses without being limited by the potential lack of spectrum. Cognitive radio users could benefit from improved QoS compared to fixed frequency radio users, because they can change frequency as required. Their intelligent signal processing capability will allow them adapting to their environment and support heterogeneous services. New markets should also emerge from cognitive technologies. [4] mentions four applications that

are more promising: *multimedia download with moderate data rates and near ubiquitous coverage, emergency communications with moderate data-rates and localized primary user coverage, broadband wireless networking with high data-rates and localized coverage, and multimedia wireless networking with high data-rate and localized coverage. A number of spectrum bands between ∼140MHz-11GHz were also highlighted where sharing could take place for each application.* However, there are significant regulatory, technological and application challenges that need to be addressed.

Based on the type of available network side information along with the regulatory constraints, cognitive radio systems seek to underlay, overlay or interweave their signals (or combine these technics) with those of existing users without significantly impacting their communication, [9].

In this section, we will present the ways a cognitive radio could share the spectrum with an existing licensee or noncognitive user.

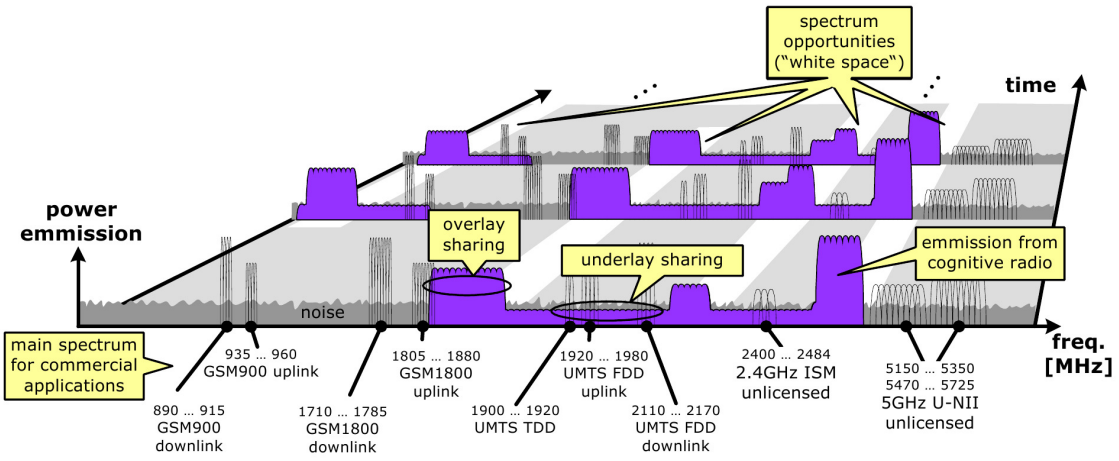

Figure 1.3: Cognitive radio paradigms [12], [13].

1.2.1 Underlay spectrum-sharing

The underlay sharing realizes a simultaneous uncoordinated usage of spectrum in the time and frequency domain. To allow the underlay spectrum-sharing, the cognitive radio is assuming to have knowledge of the interference caused by its transmitter to the receivers of noncognitive users. In this setting, the cognitive radio is often called *secondary user* and all of the complexity of sharing is borne by it. No change to the primary systems is needed, which are the legacy systems that are difficult to change. The secondary user cannot significantly interfere with the communication of the primary users. To protect primary or existing users, an interference constraint should specify at least two parameters $\{Q, \epsilon\}$. The first parameter Q is the maximum allowable interference power perceived by an active primary receiver; it specifies the noise floor. The second parameter ϵ is the maximum outage probability that the interference at an active primary receiver exceeds the noise floor Q, [60]. Actually, in the underlay paradigm, the cognitive user is mandated

to transmit in the common spectrum only if the interference generated at the primary receivers is below some acceptable threshold. In 2002, the FCC proposed *interference temperature* as the appropriate metric, [2], to estimate the harmfulness of the interference in a radio-frequency band. The recommendation is made with two key benefits in mind [11]:

- *The interference temperature at a receiving antenna must provide an accurate measure for the acceptable level of RF interference in the frequency band of interest; any transmission in that band is considered to be "harmful " if it would increase the noise floor above the interference-temperature limit.*

- *Given a particular frequency band in which the interference temperature is not exceeded, that band could be made available to unserviced users; the interference-temperature limit would then serve as a "cap "placed on potential RF energy that could be introduced into that band (Cf. Fig. 1.4).*

This metric was somewhat controversial in terms of how it could be known at the cognitive transmitter and whether it would provide sufficient protection for primary users with a cognitive underlay [8], [14].
The interference constraint for the cognitive users may be met by using multiple antennas to guide the cognitive signals away from the noncognitive receivers, or by using a wide bandwidth over which the cognitive signal can be spread below the noise floor (Cf. Fig. 1.3) as spread spectrum and ultra-wide-band (UWB) communications, [8], [10].

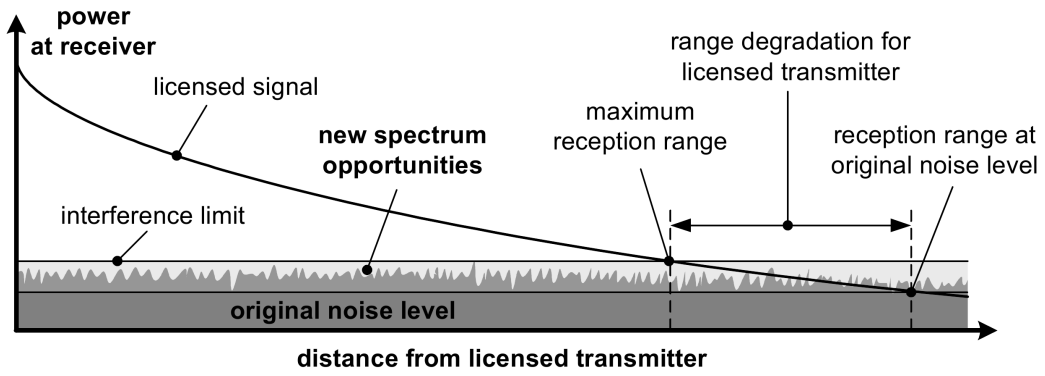

Figure 1.4: Underlay spectrum sharing corresponding to the Interference Temperature Concept of the FCC (from [13], [12]).

1.2.2 Overlay spectrum-sharing

The overlay approach is a form of cooperative transmission that requires more sophisticated protocols than the previous underlay sharing. It allows concurrent cognitive and noncognitive transmissions (Cf. Fig. 1.3) where the cognitive transmitter may now support the transmission of the noncognitive user. To allow the overlay sharing, the cognitive

transmitter is supposed to know the noncognitive user codebook and its message as well. This knowledge allows the cognitive transmitter applying several encoding schemes that will improve both its own rates and those of the noncognitive user [40]-[44]. The codebook information could be obtained, for example, if the noncognitive user follows a uniform standard for communication based on publicizing codebook [8]. Or it could broadcast its codebook periodically. The noncognitive user message is supposed to be known at the cognitive transmitter when the noncognitive user begins its transmission. However, in general, this is impractical for an initial transmission, but the assumption holds for a message retransmission where the cognitive user hears the first transmission and decodes it, while the intended receiver cannot decode the initial transmission due to fading or interference. Alternatively, the noncognitive user may send its message to the cognitive user (assumed to be close by) prior to its transmission [8]. Such information can be exploited in a variety of ways to either cancel or mitigate the interference seen at the cognitive and noncognitive receivers. On one hand, this information can be used to completely cancel the interference due to the noncognitive signal at the cognitive receiver by using sophisticated techniques, like dirty paper coding (DPC), [55]. On the other hand, the cognitive radio can use this knowledge and assign part of its power for its own communication and the remainder to assist (relay) the noncognitive transmissions. By setting carefully this power splitting, the decrease in the noncognitive user's SNR due to the interference caused by the part of the cognitive user's transmit power used for its own communication can be exactly offset by the increase in the noncognitive user SNR due to the assistance from cognitive relaying, [8].

1.2.3 Interweave spectrum-sharing

The interweave spectrum-sharing for a secondary (unlicensed user) consists of utilizing opportunistically the unused primary (licensed user) bands, commonly referred to as *white spaces* (Cf. Fig. 1.3). That was the original motivation for cognitive radio [1]. An interweave cognitive radio must be intelligent enough to periodically monitor the radio spectrum, detect occupancy in the different parts of the spectrum, and then opportunistically communicate over spectrum holes with minimal interference to the active users. Spectrum monitoring can be performed in several ways. Three main approaches are commonly discussing in the literature: the database registry, the beacon signals approach and the spectrum sensing. The first two approaches charge the primary system to provide secondary user with current spectrum usage information by either registering the relevant data (e.g., the primary system location and power as well as expected duration of usage) at a centralized database or broadcasting this information on regional beacons [16], [35]. Spectrum sensing relies on the secondary user to identify the spectrum holes by sensing the licensed bands.
Intuitively, *a channel is an opportunity to a pair of secondary transmitter-receiver if they can communicate successfully without violating the interference constraint*[1]. Then, the existence of a spectrum opportunity is determined by two conditions: the reception at the

[1]Here, "channel " is used in a general sense: it represents a signal dimension (time, frequency, code, etc.) that can be allocated to a particular user.

secondary receiver being successful and the transmission from the secondary transmitter being "harmless ", [60]. It is necessary to notice that this definition has significant implications for cognitive radio networks where primary and secondary users are geographically distributed and wireless transmissions are subject to path loss, shadowing and fading. In chapter 4 we provide an original quantitative characterization of the impact of path loss and shadowing on a cognitive radio network. Therefore, spectrum opportunity, for a secondary user, depends not only on the interference tolerance of primary users, but also on the interference tolerance of secondary user (so on primary users transmission power), [60]. In this way, even if no primary receiver is in the secondary interference range (area where secondary transmission must not interfere with primary receivers, solid circle in Fig. 1.5), the spectrum could not be an opportunity for secondary use. Actually, a channel is an opportunity for secondary use only if secondary transmission does not affect primary reception quality and secondary reception quality is not affected by primary transmission, [60]. For a simple illustration, consider the Fig. 1.5. The interference range of the secondary transmitter Cr-Tx is the circle [2] from Cr-Tx, of radius R_{cr}. The primary receivers Pr-Rx1 and Pr-Rx2 are in this range. So, secondary user must be able to detect any transmission between Pr-Tx1 and Pr-Rx1 as well as Pr-Tx2 and Pr-Rx2. It must cease transmission if there is an active primary receiver in its interference range, in order to not affect primary reception quality. The radius R_{cr} depends on the transmission power of Cr-Tx and the interference constraint Q. The protection zone of secondary users is defined by the circle from Cr-Rx, of radius R_{pr}. In the example of Fig. 1.5, if the interference tolerance of secondary user is not met (due to transmission from Pr-Tx1 and Pr-Tx2), the spectrum is not an opportunity for secondary use. Radius R_{pr} depends on the transmission power of primary users and the interference tolerance of Cr-Tx.

Building on the above definition, "perfect" spectrum opportunity detection is not an obvious problem, depending on the network activities information available for given secondary user. Consider for instance the common approach to spectrum opportunity detection, referred to as "listen-before-talk" (LBT). In this approach, there is no cooperation from primary users. The observations available to the secondary user for opportunity detection are the signals emitted from primary transmitters, Cf. Fig. 1.6. The secondary transmitter Cr-Tx infers the existence of spectrum opportunity from the absence of primary transmitters within its detection range R_D, where R_D depends, for instance, on the threshold of an energy detector. Even if we suppose a perfect detection of primary transmitters within secondary detection range R_D (Cr-Tx listens to primary signals with a perfect ear), there are three possible sources of detection errors: *hidden transmitters*, *hidden receivers* and *exposed transmitters*. A hidden transmitter is a primary transmitter that is located within distance R_{pr} of Cr-Rx but outside the detection range of Cr-Tx (node Pr-Tx3 in Fig. 1.6). A hidden receiver is a primary receiver that is located within the interference range R_{cr} of Cr-Tx but its corresponding primary transmitter is outside the detection range of Cr-Tx (node Pr-Rx1 in Fig. 1.6). An exposed transmitter is a

[2] The use of a circle to illustrate the interference region is immaterial. This definition applies to a general signal propagation and interference model by replacing the solid and dashed circles with interference footprints specifying the subset of primary receivers who are potential victims of secondary transmission and the subset of primary transmitters who can interfere with secondary reception, [60].

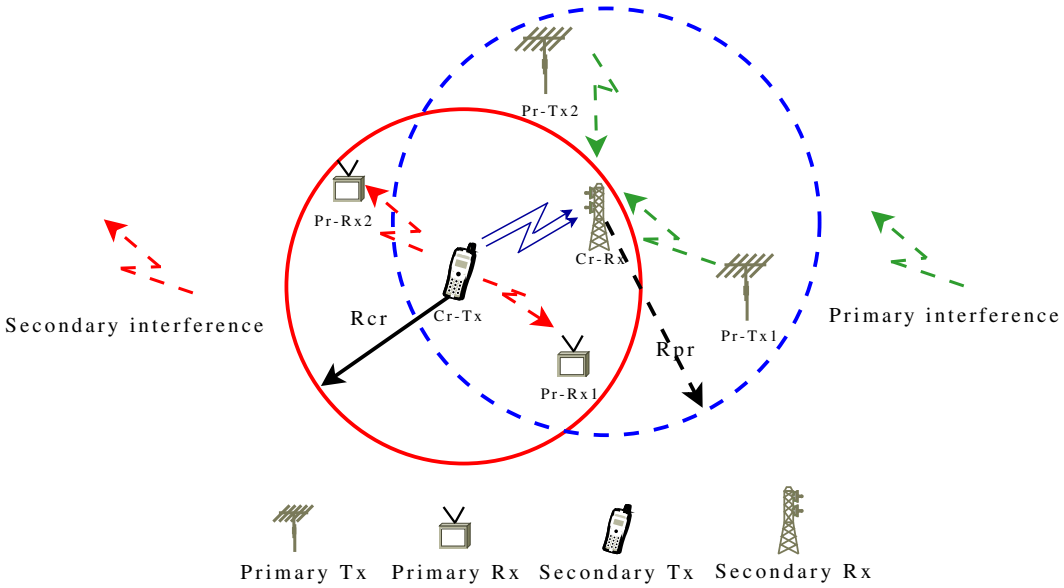

Figure 1.5: Illustration of spectrum opportunity: secondary transmitter Cr-Tx wishes to transmit to secondary receiver Cr-Rx, where Cr-Tx should watch for nearby primary receivers and Cr-Rx should watch for nearby primary transmitters, [60].

primary transmitter that is located within the detection range of Cr-Tx but transmits to a primary receiver outside the interference range, R_{cr}, of Cr-Tx (node Pr-Tx2 in Fig. 1.6).

Finally, "perfect" spectrum opportunity detection must take into account both the interference range R_{cr} around secondary transmitter and the secondary protection zone R_{pr} around secondary receiver.

1.2.4 Concluding remarks

In this thesis, we do not suppose that the cognitive transmitter knows the noncognitive user codebook and message. As a consequence, we investigate the underlay and interweave approaches of spectrum-sharing only. We propose, in [61], a new underlay spectrum-sharing power control with an original additional constraint, making the instantaneous sum rate to be always greater than the primary own rate when alone in the spectrum. According to the definition of spectrum opportunity of part 1.2.3, we propose in chapter 4 and [62] an original opportunistic power control, for one primary user and one secondary user, with the following modeling and requirements:

- we model the secondary interference range R_{cr} by given outage performance at the primary receiver: secondary user infers that no primary receiver is in its interference range R_{cr} when primary outage performance is achieved;

- we model the secondary protection zone R_{pr} by given outage performance at the secondary receiver: secondary user infers that no primary transmitter is in the pro-

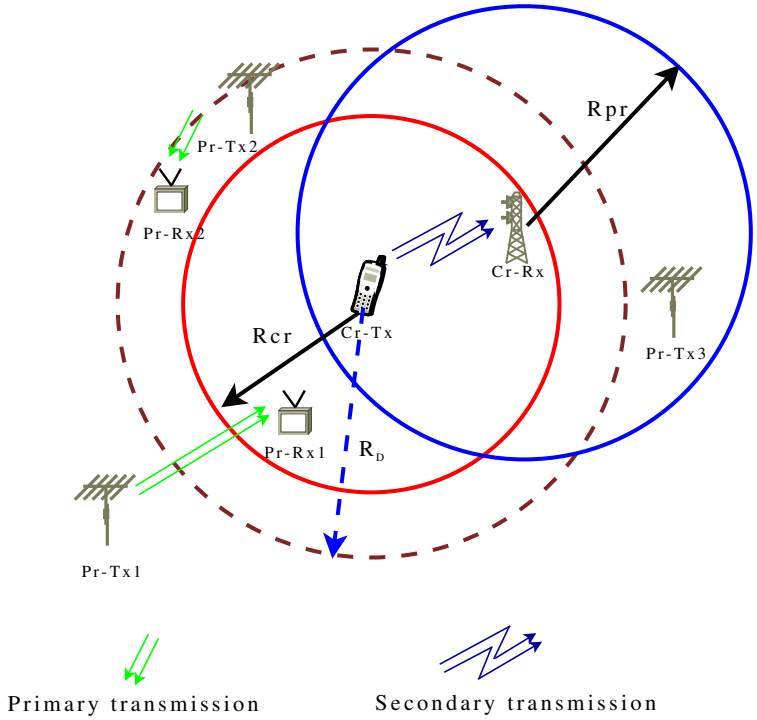

Figure 1.6: "listen-before-talk"(LBT) spectrum opportunity detection: Cr-Tx detects spectrum opportunities by observing primary signals (the exposed transmitter Pr-Tx2 is a source of false alarms whereas the hidden transmitter Pr-Tx3 and the hidden receiver Pr-Rx1 are sources of miss detections), [60].

tection zone of radius R_{pr} when secondary outage performance is achieved;

- to transmit over the common spectrum, the secondary user performs a power control such that both the outage performances are achieved. Furthermore, we consider a realistic case with partial knowledge of channel state information at the secondary receiver (only secondary user direct links gains are known at its receiver).

This power control takes into account both the underlay and interweave approaches of spectrum-sharing since secondary transmission is subject to some interference constraints and is off when one constraint is not fulfilled.

1.3 Basic model of spectrum-sharing: the Gaussian Interference Channel

With the penury of available spectrum resource, spectrum-sharing is more and more recommended in wireless communications. Cognitive Radio contributes to share the spectrum more intelligently in the ways presented in section 1.2. Before bringing cognition in

spectrum-sharing, it is important to study the performances achieved by a basic model of spectrum-sharing. In this section, we are interested in the interference channel, as a basic spectrum-sharing system, that should enable to understand how to cope with and exploit interference in spectrum-sharing networks.

1.3.1 Definition and motivation

The interference channel, [18], [19], consists of a network where multiple terminal pairs wish to communicate simultaneously in the presence of mutual interference. The users are not assumed to be cognitive (they do not monitor the activity or decode messages of other users). However, in general, it is assumed that all terminals know the channel gains and the codebooks of all the encoders. The two-user Gaussian Interference Channel (Cf. Fig. 1.7), consisting of two transmitter-receiver pairs, is the smallest interference network. Besides wireless communication, interference channel include many other types of communication such as digital subscriber lines (DSL) where there might be far-end cross-talk (FEXT) between two twisted pair cables in the same binder. Depending on the

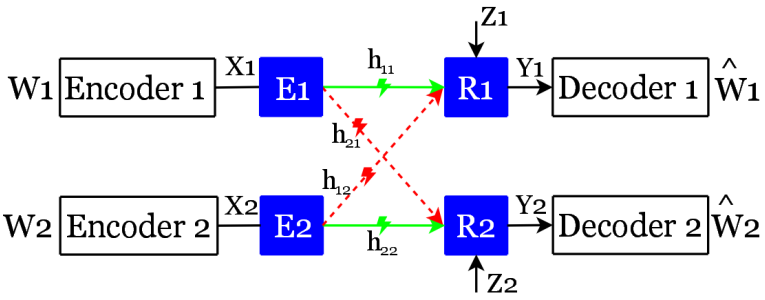

Figure 1.7: The two-user Gaussian Interference Channel.

level of interference at the receivers, different regimes can be distinguished, in particular the trivial no interference regime where the transverse links gains $|h_{12}|^2$ and $|h_{21}|^2$ are null; the degraded interference channel corresponding to $|h_{11}|^2 = |h_{22}|^2 = |h_{12}|^2 = |h_{21}|^2 = 0$; the strong interference regime where, in general (unit-variance noise at each receiver), $a_{12} \triangleq |h_{12}|^2/|h_{22}|^2$ and $a_{21} \triangleq |h_{21}|^2/|h_{11}|^2$ are greater or equal to 1; the moderate and weak interference regimes where $a_{12} < 1$ or/and $a_{21} < 1$; and the Z-interference regime where $a_{12} = 0$ or $a_{21} = 0$, [25].

The communication problem is to determine the highest rates that can simultaneously be achieved with arbitrarily small error probability at the desired receivers, i.e., to determine the capacity region. This performance can serve as a benchmark to evaluate the gains of cognition, [8]. Even for the two-user Gaussian Interference Channel, this problem has remained unsolved for more than 31 years, but as stated below, there has been a lot of progress in understanding communications in some interesting interference channels.

1.3.2 Capacity and achievable rate regions

Capacity region: the capacity region of the Interference channel of Fig. 1.7 is the set of all simultaneously achievable rate pairs (R_1, R_2) in the two interfering links. In information theory, capacity region analysis is typically performed in two steps:

- find a specific encoding and decoding scheme and evaluate its achievable rate region;
- determine an outer bound to the rate region that cannot be exceeded by any encoding scheme.

If the two bounds meet, then the capacity region is known and the proposed encoding scheme is said to be capacity achieving. It is also interesting to determine an inner bound to the rate region that is the closest possible to the outer bound. With outer and inner bounds, one can estimate how far the proposed rate region is from the capacity region.
For the Gaussian Interference Channel, when the interference is strong, the received interfering signal component carrying the unwanted message is strong enough so that this message can be decoded jointly with the desired one. This strategy is showed to be capacity achieving in strong interference regime and leads to the *interference-free* capacity region [17], [23]. Unfortunately, the capacity region of the Gaussian Interference Channel (even for two users) with moderate or weak interference is still not known. In these cases, interference is not strong enough to allow decoding of the unwanted message without reducing its rate, [8]. The best known achievable strategy is the Han-Kobayashi scheme [21], where each user splits its message into private and common parts, encoding them separately. Private information can be decoded only at own receiver and common information can be decoded at both receivers. By decoding the common information, part of the interference can be cancelled off and the remaining private information from the other user processed as noise. The Han-Kobayashi strategy allows arbitrary splits of each user's transmit power into the private and common information portions as well as time sharing between multiple such splits. Unfortunately, the optimization among such multiple possibilities is not well-understood to day, [27].

Achievable rate region: while the capacity region is more general and includes all achievable rates for all possible coding schemes, an achievable rate region is defined for given coding scheme. For the single user decoding, the achievable rate region is obviously an inner bound of the capacity region. However, it is important to characterize the achievable rate region in this case because it is realistic and does not require complex decoding. This basic coding scheme can be seen as a benchmark to understand how harmful can be the interference and how to deal with.

1.3.3 Concluding remarks

Interference channel is a benchmark to understand the spectrum sharing and the cognitive radio and to evaluate the resulting gain. Although there has been a lot of progress in understanding the capacity of such a system, the complete characterization of the capacity

region or the achievable performance is not yet entirely understood in the more general case.

When interference is considered as noise at the receivers, the resulting performance of the Gaussian Interference Channel forms a conservative lower bound of the complete achievable performance for the more general case. However, this assumption involving the single user decoding does not require sophisticated technics like rate splitting, dirty paper coding, interference suppression etc. It is then important to know the characterization of the achievable rate region in this coding scheme. We give an original characterization of the achievable rate region for the two and tree-user Gaussian Interference Channel when interference is considered as noise, in chapter 2. Geometrical interpretations are also given to some known results.

1.4 Conclusions

It has been widely shown that cognitive radio and spectrum-sharing approaches improve the utilization of the radio electromagnetic spectrum which is a precious natural resource. In spite of significant contributions to enable cognitive radio and spectrum-sharing, strong contributions are needed to test the potential impact of sharing and how networks really could co-exist in the same spectrum band. If successful, cognitive radio and spectrum sharing technologies could revolutionize the way spectrum is allocated worldwide as well as provide sufficient bandwidth to support the demand for higher quality and higher data rate wireless applications into the future. Many applications are constantly emerging as cognitive radio technologies develop. In this chapter, we have provided an overview of the different paradigms of cognitive radio and the spectrum-sharing understanding investigations via the Gaussian Interference Channel. We have placed the contributions of this thesis with regard to the Cognitive Radio and the Interference Channel.

Chapter 2

Achievable rate region of the Gaussian Interference Channel

In this chapter, we address the problem of computing the achievable rates for two (and three) users sharing the same frequency band without coordination and interfering with each other. It is primarily related to the field of cognitive radio studies as we look for the achievable increase in the spectrum use efficiency. It is also strongly related to the long-standing problem of the capacity region of a Gaussian interference channel because of the assumption of no user coordination and the assumption that all signals and interferences are Gaussian.

2.1 Introduction

Gaussian interference channel have received a lot of attention in the technical literature where the interference channel is generally addressed with information theoretic tools, see for instance [8], [18]-[25] and references therein. With the assumption of non-cooperating users (single user decoding) with power-limited Gaussian signals, the rate of each of them is given by the $\frac{1}{2} B \log_2(1 + \text{SINR})$ classical formula, where SINR is the signal-to-noise plus interference ratio at the receiver and B is the bandwidth. We aim to characterize the achievable rate region of the Gaussian Interference Channel with these assumptions, when the channels gains are constant. The difficulty we face is that the various SINR of the users are not independent; they are interrelated in a way involving the channel coefficients. Nevertheless, we can have some insight of the shape (the geometry) of the set of possible SINR, at least for the two and three-user Gaussian Interference Channel. We make use of this geometry to derive some new results: the achievable rate regions of the two and three-user Gaussian Interference Channel. Moreover, the way we will derive the three-user case can be generalized, and it should allow deriving the n-user SINR region provided we know the one corresponding to $(n-1)$ users. Then, we will give closed-form expressions of achievable rate regions of the two and three-user Gaussian Interference Channel when all interferences are considered as noise. Although it is known to be suboptimal, this

basic strategy is useful to evaluate the gain of sophisticated technics such as cooperation between users and interference suppression.

The remainder of this chapter is organized as follows: In Section 2.2, we derive the analytical expressions of the achievable rate region for the two-user Gaussian Interference Channel. This closed form expression allows us giving a geometric interpretation of a recently published result. The three-user Gaussian Interference Channel is then considered in Section 2.3, where we find the analytical expressions characterizing the SINR region for three users and give expressions of the contour lines of the three-dimensional achievable rate region. Finally, conclusions are given in Section 2.4.

2.2 Achievable rate region for the 2-user GIC

In this section, we provide a detailed geometrical description of the achievable rate region of the two-user Gaussian Interference Channel.

2.2.1 Mathematical modelling

We consider the Gaussian Interference Channel of figure 1.7 with two transmitters and two receivers. The output signals follow the equations:

$$\begin{aligned} Y_1 &= h_{11}\,X_1 + h_{12}\,X_2 + Z_1 \\ Y_2 &= h_{21}\,X_1 + h_{22}\,X_2 + Z_2. \end{aligned} \tag{2.1}$$

We shall assume that channel inputs X_1 and X_2 are power-limited real Gaussian processes such that $p_i = \mathbb{E}\left[X_i^2\right] \leq P_i$, and that there is no cooperation between users, so that interferences can be seen as Gaussian noise. The noises Z_1 and Z_2 are mutually independent Gaussian random variables, and independent from X_1 and X_2, with zero mean and same variance $\mathbb{E}\left[Z_i\right] = \sigma^2$. With these assumptions the two achievable rates of users 1 and 2, with normalized bandwidth, are:

$$\begin{aligned} \mathrm{C}_1 &= \frac{1}{2}\log_2\left(1 + \frac{g_{11}\,p_1}{\sigma^2 + g_{12}\,p_2}\right), \\ \mathrm{C}_2 &= \frac{1}{2}\log_2\left(1 + \frac{g_{22}\,p_2}{\sigma^2 + g_{21}\,p_1}\right), \end{aligned} \tag{2.2}$$

where $g_{ij} = |h_{ij}|^2$. With the change of variables $u_i = g_{ii}\,p_i/\sigma^2$, the above equations can be rewritten as:

$$\begin{aligned} \mathrm{C}_1 &= \frac{1}{2}\log_2\left(1 + S_1\right), \text{with} \quad S_1 = \frac{u_1}{1 + a_{12}u_2}. \\ \mathrm{C}_2 &= \frac{1}{2}\log_2\left(1 + S_2\right), \text{with} \quad S_2 = \frac{u_2}{1 + a_{21}u_1}, \end{aligned} \tag{2.3}$$

where $a_{12} = g_{12}/g_{22}$ and $a_{21} = g_{21}/g_{11}$. u_1, u_2 are the received SNR values when there is no interference and S_1, S_2 are the SINR values. The introduction of variables u_1, u_2 is similar to the introduction of the normalized channel in [19] to which the reader is referred. The relation between the SINR variables S_1, S_2 and the SNR values u_1, u_2 can be easily inverted to obtain the two following expressions:

$$\begin{aligned} u_1 &= \frac{S_1(1+S_2\,a_{12})}{1-a_{12}\,a_{21}\,S_1\,S_2} \\ u_2 &= \frac{S_2(1+S_1\,a_{21})}{1-a_{12}\,a_{21}\,S_1\,S_2}. \end{aligned} \tag{2.4}$$

Next, we give expressions to describe the achievable rate region of the two-user Gaussian Interference Channel.

2.2.2 Geometrical description of the rates region

In this part, we use the previous expressions to derive geometrical description of the achievable rate region of the two-user Gaussian Interference Channel.

Expressing the power constraints $0 \leq u_i \leq \mathcal{P}_i \triangleq g_{ii}P_i/\sigma^2$ allows us deriving corresponding constraints on the SINR variables, namely:

$$S_2 \leq \frac{1}{a_{12}\,a_{21}\,S_1} \tag{2.5}$$

$$S_1 \leq \phi_1(S_2) = \frac{\mathcal{P}_1}{1+a_{12}\,S_2(1+a_{21}\,\mathcal{P}_1)} \tag{2.6}$$

$$S_2 \leq \phi_2(S_1) = \frac{\mathcal{P}_2}{1+a_{21}\,S_1\,(1+a_{12}\,\mathcal{P}_2)}. \tag{2.7}$$

The SINR region is thus delimited by the curves defined by the equations 2.5-2.7. All variables being positive, the two functions $\phi_1(S_2)$ and $\phi_2(S_1)$ are respectively upper bounded by $(a_{12}\,a_{21}\,S_2)^{-1}$ and $(a_{12}\,a_{21}\,S_1)^{-1}$ so that the first inequality is redundant and is omitted in the sequel. The SINR region is then the intersection of the regions obeying, respectively, the constraints defined by ϕ_1, ϕ_2 :

$$\mathcal{D}' = \{0 \leq S_1 \leq \phi_1(S_2),\, S_2 \geq 0\} \cap \{0 \leq S_2 \leq \phi_2(S_1),\, S_1 \geq 0\} \tag{2.8}$$

We can also notice that $\phi_2(S_1)$ is simply obtained from $\phi_1(S_2)$ by the permutation $\{1,2\} \to \{2,1\}$, this result will be used later when considering the three-user case. The second inequality (2.6) above can be written in the equivalent form

$$S_2 \leq (\mathcal{P}_1 - S_1) / (a_{12}S_1(1+a_{21}\mathcal{P}_1))$$

so as to write the following analytic expression for the SINR region as a function of the

sole S_1 :

$$0 \leq S_2 \leq \min\left(\frac{\mathcal{P}_2}{1+a_{21}\,S_1\,(1+a_{12}\,\mathcal{P}_2)}, \frac{\mathcal{P}_1 - S_1}{a_{12}\,S_1\,(1+a_{21}\,\mathcal{P}_1)}\right). \tag{2.9}$$

We will use this expression to derive analytical bound to the capacity region of the interference channel.
The transformation $(u_1, u_2) \overset{\phi}{\to} (S_1, S_2)$ is a one to one correspondence of the region $\mathcal{D} = \{0 \leq u_1 \leq \mathcal{P}_1,\, 0 \leq u_2 \leq \mathcal{P}_2\}$ into the transformed region $\mathcal{D}'$, it leaves invariant the two points $(\mathcal{P}_1, 0)$ and $(0, \mathcal{P}_2)$. We have $\mathcal{D}' \subset \mathcal{D}$, because $S_i \leq u_i$. We can already notice that the more $\bar{P}_1$ and $\bar{P}_2$ increase the more the region $\mathcal{D}'$ is constrained by the curve with equation $S_2 = 1/(a_{12}\,a_{21}\,S_1)$ (Cf. Fig. 2.1) and its shape different from a rectangle.

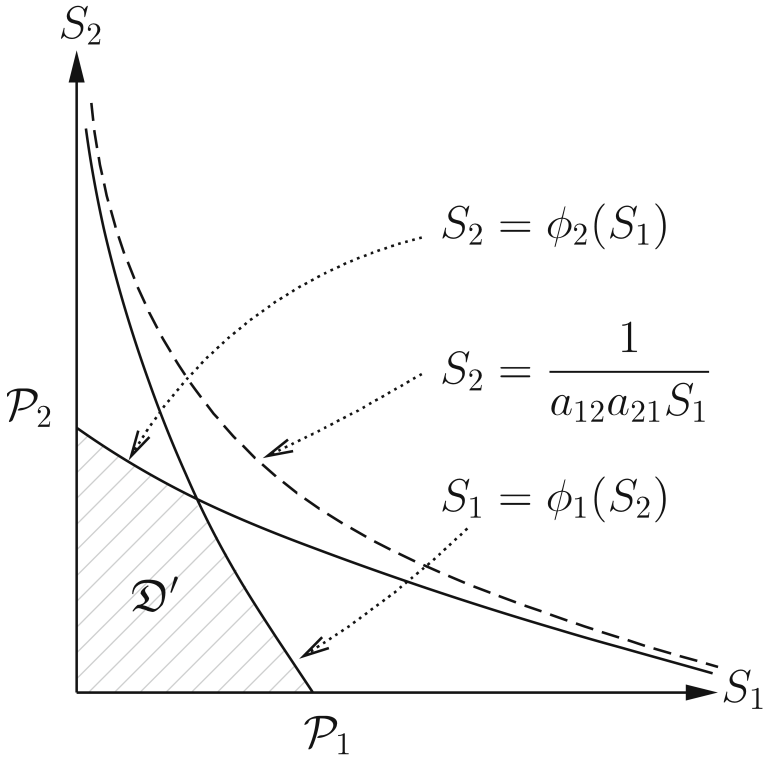

Figure 2.1: Illustration of the SINR region for the two-user GIC.

The last transform $S_i \to \log_2(1 + S_i)$, allows us giving an analytical expression of the achievable rate region boundary as a parametric curve rather than a simple function giving C_2 in terms of C_1:

$$\begin{aligned} 0 &\leq t \leq \mathcal{P}_1 \\ \mathrm{C}_1 &= \frac{1}{2}\log_2(1+t) \qquad (2.10) \\ \mathrm{C}_2 &= \frac{1}{2}\log_2(1+f(t))\,, \qquad (2.11) \end{aligned}$$

where f (t) is given by:

$$f(t) = \min\left(\frac{\mathcal{P}_2}{1 + a_{21}\, t\, (1 + a_{12}\, \mathcal{P}_2)}, \frac{\mathcal{P}_1 - t}{a_{12}\, t\, (1 + a_{21}\, \mathcal{P}_1)}\right). \tag{2.12}$$

It is easy to check that $f(0) = \mathcal{P}_2$ and $f(\mathcal{P}_1) = 0$, these are the two cases where all throughput is allocated to only one user. As a result of the parametrization 2.10-2.11, we obtain the following expression for the sum rate $\mathrm{C}_\Sigma \triangleq \mathrm{C}_1 + \mathrm{C}_2$:

$$\mathrm{C}_\Sigma = \frac{1}{2}\log_2(1+t) + \frac{1}{2}\log_2(1+f(t)). \tag{2.13}$$

Depending on the values of $\mathcal{P}_1$ and $\mathcal{P}_2$ and the coefficients of the normalized channel a_{12}, a_{21}, the achievable rate region and the sum rate will exhibit different behaviors as showed next in numerical examples for a symmetric case $a_{12} = a_{21}$.

2.2.3 Numerical results and sum rate maximization

Now, we shall study two typical examples: Fig. 2.2 corresponds to a medium interference case ($a_{12} = a_{21} = 0.2$), while Fig. 2.3 is a strong interference case ($a_{12} = a_{21} = 1.0$). When interference is low to medium, the maximum sum rate C_Σ^{max} is achieved when both users transmit with their maximum power $(u_1, u_2) = (\mathcal{P}_1, \mathcal{P}_2)$, and is greater than $\max(R_1^{max}, R_2^{max})$ where $R_i^{max} = \frac{1}{2}\log_2(1 + \mathcal{P}_i)$ is the maximum rate for user $i = 1, 2$ when alone in the channel. There is a global benefit to share the channel at the expense of individual rates. This is no longer true in a strong interference case, the maximum sum rate

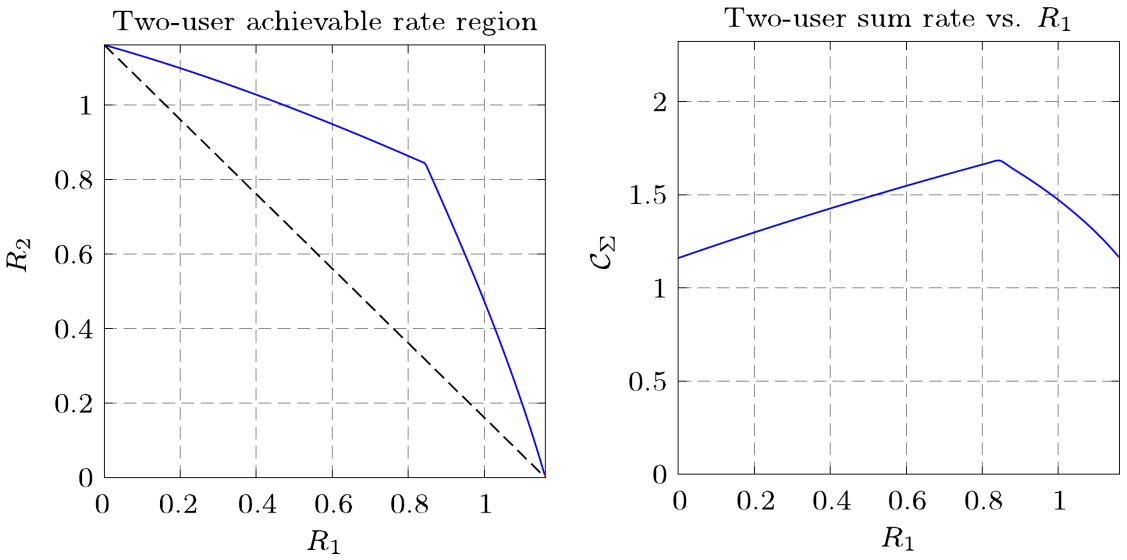

Figure 2.2: achievable rate region for $\mathcal{P}_1 = \mathcal{P}_2 = 4$, medium interference, $a_{12} = a_{21} = 0.2$; C_Σ is maximal when both users transmit at their maximum power.

is achieved when only one transmitter is active, more precisely: $\mathrm{C}_\Sigma^{max} = \max\left(R_1^{max}, R_2^{max}\right)$. It is not interesting to share the channel.

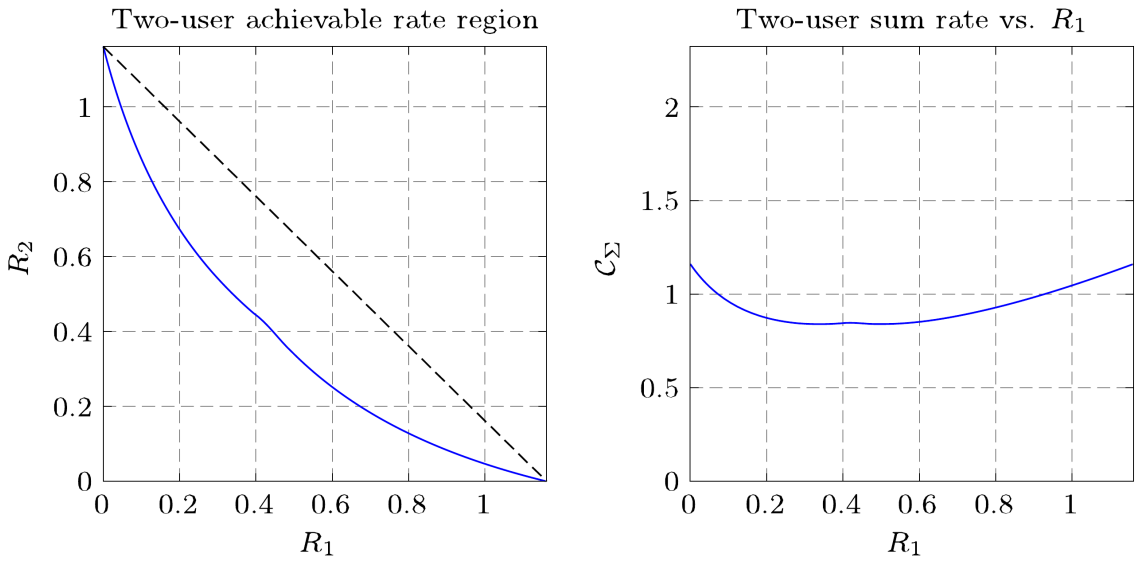

Figure 2.3: achievable rate region for $\mathcal{P}_1 = \mathcal{P}_2 = 4$, strong interference, $a_{12} = a_{21} = 1.0$; C_Σ is maximum when only one user is transmitting at its maximum power.

Actually, consider the sum rate C_Σ in terms of the two variables u_1, u_2 subject to the power constraints $u_i = \left(g_{ii}\, p_i/\sigma^2\right) \leq \mathcal{P}_i$:

$$\begin{aligned} \mathrm{C}_\Sigma &= C_1 + C_2 \\ &= \frac{1}{2}\log_2\left(1 + \frac{u_1}{1 + a_{12}\, u_2}\right) + \frac{1}{2}\log_2\left(1 + \frac{u_2}{1 + a_{21}\, u_1}\right) \end{aligned} \tag{2.14}$$

It is found in [26] that the power allocation $(u_1^*,\, u_2^*)$ to optimize C_Σ is one of the following couples: $(0,\, \mathcal{P}_2)$, $(\mathcal{P}_1,\, 0)$ or $(\mathcal{P}_1,\, \mathcal{P}_2)$. The same result is found in [28] using the geometric programming method. Let

$$R_1^* \triangleq \frac{1}{2}\log_2\left(1 + \frac{\mathcal{P}_1}{1 + a_{12}\, \mathcal{P}_2}\right) \tag{2.15}$$

$$R_2^* \triangleq \frac{1}{2}\log_2\left(1 + \frac{\mathcal{P}_2}{1 + a_{21}\, \mathcal{P}_1}\right), \tag{2.16}$$

$$\tag{2.17}$$

and $R^* = \max\left(R_1^{max}, R_2^{max}\right)$. The sum rate maximization can be stated as:

$$C_\Sigma^{max} = \begin{cases} R^*, & \text{if} \quad \left(R_1^* + R_2^*\right) \leq R^* \\ R_1^* + R_2^*, & \text{if} \quad \left(R_1^* + R_2^*\right) > R^* \end{cases} \tag{2.18}$$

Where C_{Σ}^{max} is the maximum sum rate. (2.18) can be illustrated geometrically by placing two different regions $\mathcal{A}$ and $\mathcal{B}$ (Cf. Fig. 2.4) such that they are separated by the straight line with equation $R_1 + R_2 = R^*$. $\mathcal{A}$ is the region above the separator straight line and $\mathcal{B}$ is the region below:

- if the corner point $M\,(R_1^*, R_2^*) \in \mathcal{A}$, then the optimal power allocation is $(\mathcal{P}_1,\, \mathcal{P}_2)$;
- if $M \in \mathcal{B}$, then the optimal power allocation is $(\mathcal{P}_1,\, 0)$ or $(0,\, \mathcal{P}_2)$.

Figure 2.4 illustrates a case where the corner point $M \in \mathcal{A}$ and $(R_1^* + R_2^*) > R^*$, therefore the maximum sum rate C_{Σ}^{max} is reached for the power allocation $(\mathcal{P}_1,\, \mathcal{P}_2)$.

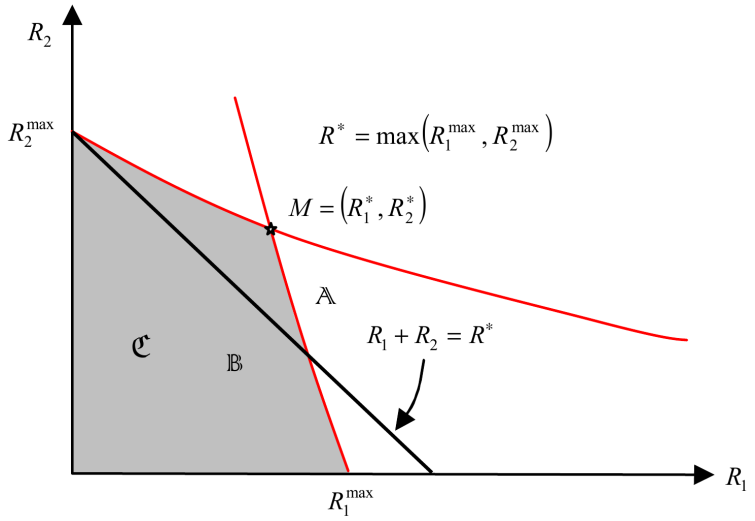

Figure 2.4: Maximum sum rate point for the two-user Gaussian Interference Channel.

2.3 Achievable rate region for the 3-user GIC

In this section, we aim to generalize the previous results to provide a geometrical description of the rates region for the three-user Gaussian Interference Channel. The method used should be generalizable to the n-user Gaussian Interference Channel ($n \geq 3$).

2.3.1 Mathematical modelling

When considering the three-user case, it is more convenient to write the relations between the SINR variables, S_1, S_2, S_3 and the SNR variables u_1, u_2, u_3 under the following form:

$$\begin{aligned} u_1 &= S_1\,(1 + a_{12}u_2 + a_{13}u_3) \\ u_2 &= S_2\,(1 + a_{21}u_1 + a_{23}u_3) \\ u_3 &= S_3\,(1 + a_{31}u_1 + a_{32}u_2) \end{aligned}$$

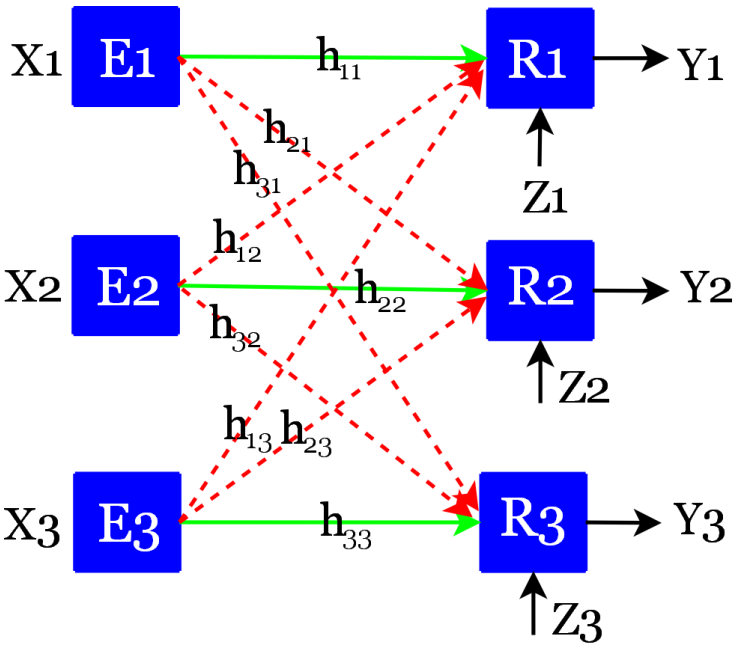

Figure 2.5: The three-user Gaussian Interference Channel.

which we rewrite as a linear system of variables (u_1, u_2, u_3):

$$\begin{pmatrix} 1 & -S_1 a_{12} & -S_1 a_{13} \\ -S_2 a_{21} & 1 & -S_2 a_{23} \\ -S_3 a_{31} & -S_3 a_{32} & 1 \end{pmatrix} \times \begin{pmatrix} u_1 \\ u_2 \\ u_3 \end{pmatrix} = \begin{pmatrix} S_1 \\ S_2 \\ S_3 \end{pmatrix} \tag{2.19}$$

This linear system could be inverted provided its 3×3 matrix, noted $\mathbf{A_3}$, is regular [29], [31], instead we make use of the structure of the above matrix in order to make apparent the matrix $\mathbf{A}_2$ associated to the two-user problem:

$$\mathbf{A_3} = \begin{pmatrix} \mathbf{A_2} & -\mathbf{a} \\ -S_3\, \mathbf{b^t} & 1 \end{pmatrix}$$

$$\mathbf{A_2} = \begin{pmatrix} 1 & -S_1\, a_{12} \\ -S_2 a_{21} & 1 \end{pmatrix}, \quad \mathbf{a} = \begin{pmatrix} S_1 a_{13} \\ S_2 a_{23} \end{pmatrix}, \quad \mathbf{b} = \begin{pmatrix} a_{31} \\ a_{32} \end{pmatrix}$$

The linear system (2.19) of unknowns (u_1, u_2, u_3) can now be written as:

$$\begin{cases} \mathbf{A_2} \begin{pmatrix} u_1 \\ u_2 \end{pmatrix} - \mathbf{a}\, u_3 = \begin{pmatrix} S_1 \\ S_2 \end{pmatrix} \\ -S_3\, \mathbf{b^t} \begin{pmatrix} u_1 \\ u_2 \end{pmatrix} + u_3 = S_3 \end{cases}$$

After some manipulations, and assuming that $\mathbf{A_2}$ is invertible we can express u_3 as:

$$u_3 = S_3 \times \frac{1 + \mathbf{b^t}\mathbf{A_2}^{-1}\begin{pmatrix} S_1 \\ S_2 \end{pmatrix}}{1 - S_3\, \mathbf{b^t}\mathbf{A_2}^{-1}\mathbf{a}}. \tag{2.20}$$

2.3.2 Geometrical description of the SINR region

Now, we use previous results to derive geometrical description of the SINR region of the three-user Gaussian Interference Channel.

From the constraint $u_3 \leqslant \mathcal{P}_3$, we have, after some manipulations, a constraint on S_3 as a function of S_1 and S_2:

$$S_3 \leqslant \phi_3\left(S_1, S_2\right) \triangleq \frac{\mathcal{P}_3}{1 + \left(a_{31}\, a_{32}\right)\mathbf{A_2}^{-1}\begin{bmatrix} S_1\left(1 + a_{13}\mathcal{P}_3\right) \\ S_2\left(1 + a_{23}\mathcal{P}_3\right) \end{bmatrix}} \tag{2.21}$$

We can develop the denominator of the right-hand-side of this inequality:

$$\begin{aligned} S_3 \leqslant \mathcal{P}_3\, &\left(1 - a_{12}\, a_{21}\, S_1 S_2\right) \\ &\times \Big(1 - a_{12}\, a_{21}\, S_1 S_2 + S_1\left(1 + a_{13}\mathcal{P}_3\right)\left(a_{31} + S_2 a_{32} a_{21}\right) + \\ &\qquad S_2\left(1 + a_{23}\mathcal{P}_3\right)\left(a_{32} + S_1 a_{31} a_{12}\right)\Big)^{-1} \end{aligned}$$

This is the equation of a surface in the three-dimensional space and it is worth noticing that when $S_1 = 0$ or $S_2 = 0$ the above upper bound becomes respectively equal to:

$$\begin{aligned} S_3 &\leqslant \frac{\mathcal{P}_3}{1 + a_{32} S_2 (1 + a_{23}\mathcal{P}_3)} \\ S_3 &\leqslant \frac{\mathcal{P}_3}{1 + a_{31} S_1 (1 + a_{13}\mathcal{P}_3)} \end{aligned}$$

in which we recognize the bounds already obtained for the two-user case when the two users are respectively $(2, 3)$ and $(1, 3)$. A geometric representation of the constraints on S_3, when respectively $S_1 = 0$ and $S_2 = 0$, is sketched in Fig. 2.6.

As we also want to derive analogous relations for S_1 and S_2, we can make use of the invariance of the structure of the linear system under any permutation of the indexes $\{1, 2, 3\}$. For instance, after the permutation $1 \leftrightarrow 3$, the linear system can be written as:

$$\begin{pmatrix} 1 & -S_3 a_{32} & -S_3 a_{31} \\ -S_2 a_{23} & 1 & -S_2 a_{21} \\ -S_1 a_{13} & -S_1 a_{12} & 1 \end{pmatrix} \times \begin{pmatrix} u_3 \\ u_2 \\ u_1 \end{pmatrix} = \begin{pmatrix} S_3 \\ S_2 \\ S_1 \end{pmatrix} \tag{2.22}$$

Solving with respect to the unknown $u_3' = u_1$ and taking into account the constraint on

u_1 lead to a constraint on S_1 as a function of S_2, S_3; likewise, after the permutation $1 \leftrightarrow 2$ which leads to a constraint on S_2 as a function of S_1, S_3. We shall denote these inequalities by $S_i \leqslant \phi_i(S_j, S_k)$ where $\{i, j, k\}$ is a permutation of the set $\{1, 2, 3\}$ and $\phi_i(S_j, S_k)$ is given by:

$$\begin{aligned}\phi_i(S_j, S_k) = \mathcal{P}_i \; & (1 - a_{jk}\, a_{kj}\, S_j S_k) \\ & \times \Big(1 - a_{jk}\, a_{kj}\, S_j S_k + S_j \left(1 + a_{ji}\mathcal{P}_i\right) \left(a_{ij} + S_k a_{ik}\, a_{kj}\right) + \\ & \qquad S_k \left(1 + a_{ki}\mathcal{P}_i\right) \left(a_{ik} + S_j a_{ij}\, a_{jk}\right)\Big)^{-1}\end{aligned}$$

With these notations the SINR region is the intersection of the three regions verifying respectively the three constraints:

$$\begin{aligned}\mathfrak{D}' &= \mathfrak{D}'_1 \cap \; \mathfrak{D}'_2 \cap \; \mathfrak{D}'_3 \\ \mathfrak{D}'_i &= \{0 \leqslant S_i \leqslant \phi_i(S_j, S_k),\; S_j, S_k \geqslant 0\}\,, \quad i = 1, 2, 3\end{aligned}$$

In the following Fig. 2.7, we give a sketch of $\mathfrak{D}'$ with the three sets of intersections on the

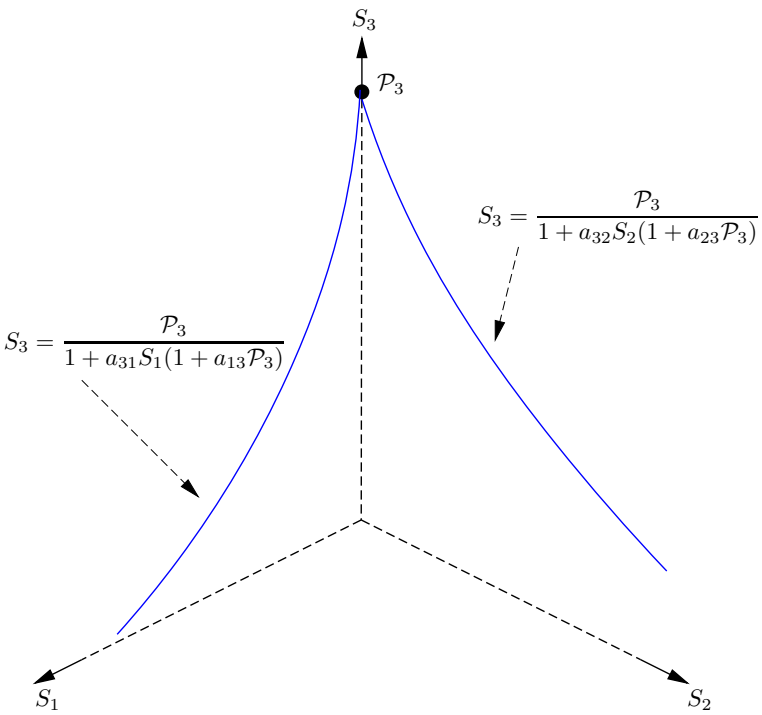

Figure 2.6: A Geometric representation of the constraints on S_3, when respectively $S_1 = 0$ and $S_2 = 0$.

faces of the positive orthant in dashed lines. On each face of the positive orthant we can recognize the SINR region of a two-user GIC.

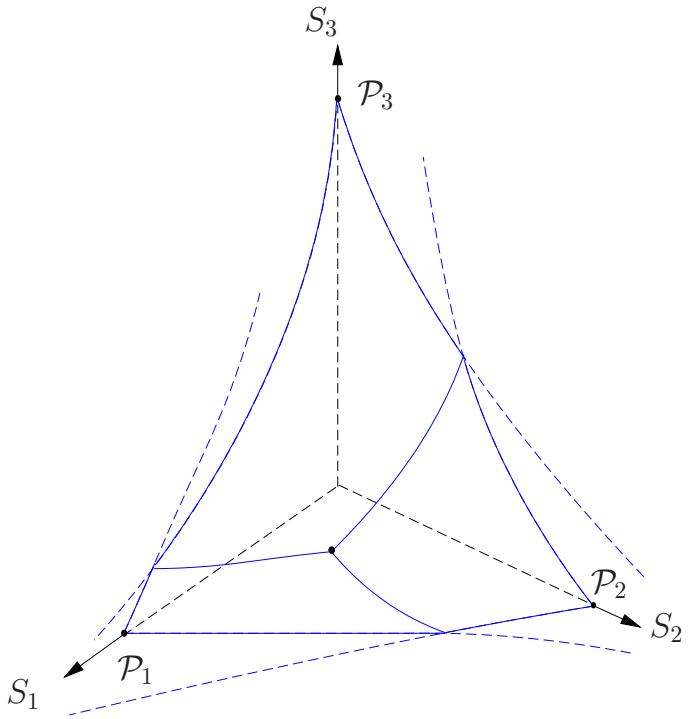

Figure 2.7: Illustration of the SINR region for the three-user GIC

2.3.3 Contour lines of the achievable rate region

We shall now give a two-dimensional description of this 3D SINR region; eliminating u_3 in the linear system leads to a system with unknowns u_1, u_2:

$$u_1\left(1-a_{13}a_{31}\,S_1\,S_3\right)=S_1\left(1+a_{13}S_3\right)+S_1\left(a_{12}+a_{13}a_{32}S_3\right)u_2$$
$$u_2\left(1-a_{23}a_{32}\,S_2\,S_3\right)=S_2\left(1+a_{23}S_3\right)+S_2\left(a_{21}+a_{23}a_{31}S_3\right)u_1$$

This system can be conveniently written in a form making apparent a two-user case with modified parameters:

$$u_1=S_1'\left(1+a_{12}'u_2\right)$$
$$u_2=S_2'\left(1+a_{21}'u_1\right),$$

where the modified parameters are given by:

$$S'_1 = \frac{S_1\,(1 + a_{13}S_3)}{1 - a_{13}a_{31}S_1S_3}, \qquad S'_2 = \frac{S_2\,(1 + a_{23}S_3)}{1 - a_{23}a_{32}S_2S_3}$$
$$a'_{12} = \frac{a_{12} + a_{13}a_{32}S_3}{1 + a_{13}S_3}, \qquad a'_{21} = \frac{a_{21} + a_{23}a_{31}S_3}{1 + a_{23}S_3}.$$

The relation between original and modified SINRs can easily be inverted; we already know the relation between S'_1 and S'_2, and can go back to original parameters S_1, S_2 applying the inverse transformation, with the result that for any value of S_3:

$$0 \leqslant S'_2 \leqslant \min\left(\frac{\mathcal{P}_2}{1 + a'_{21}S'_1\,(1 + a'_{12}\mathcal{P}_2)}, \frac{\mathcal{P}_1 - S'_1}{a'_{12}S'_1\,(1 + a'_{21}\mathcal{P}_1)}\right)$$
$$S_1 = \frac{S'_1}{1 + a_{13}S_3\,(1 + a_{31}S'_1)}$$
$$S_2 = \frac{S'_2}{1 + a_{23}S_3\,(1 + a_{32}S'_2)}.$$

Finally, we must take into account the constraint $u_3 \leqslant \mathcal{P}_3$. We can rewrite this constraint as a linear constraint on u_1, u_2:

$$a_{31}\,u_1 + a_{32}\,u_2 \leqslant \alpha \triangleq \frac{\mathcal{P}_3}{S_3} - 1.$$

Substituting the expressions of u_1, u_2 as functions of S'_1, S'_2 lead to the following inequality:

$$\frac{a_{31}\,S'_1\,(1 + a'_{12}S'_2) + a_{32}\,S'_2\,(1 + a'_{21}S'_1)}{1 - a'_{12}a'_{21}\,S'_1S'_2} \leqslant \alpha.$$

It is more convenient to rewrite this last inequality as a third bound on S'_2 as a function of S'_1:

$$S'_2 \leqslant \frac{\alpha - a_{31}S'_1}{a_{32} + (a_{31}a'_{12} + a_{32}a'_{21} + \alpha\,a'_{12}\,a'_{21})\,S'_1}.$$

This inequality tells us that $S'_1 \leqslant \alpha/a_{31}$ because S'_2 is non negative, we therefore have $S'_1 \leqslant \max(\mathcal{P}_1, \alpha/a_{31})$. It is now possible to plot the contour lines of the three-user achievable rate region; for a given rate R_3 of the third user, we determine the achievable region boundaries for users 1 and 2 thanks to Algorithm 1. We give two examples with $\mathcal{P}_1 = \mathcal{P}_2 = \mathcal{P}_3 = 4$. Fig. 2.9 has the same channel parameters as Fig. 2.8 except $a_{23} = a_{32} = 1$, that is to say user 2 and user 3 interfere each other more severely than with user 1. We can see that achievable rate of user 2 decreases more quickly as user 3 transmit with more power.

Algorithm 1 Contour lines of three-user achievable rate region

$\Gamma = \emptyset$ {the contour line at height R_3, initialized to empty list }
$S_3 = 2^{2R_3} - 1$
$\alpha = \mathcal{P}_3 / S_3 - 1$
$S_{\max} = \min\left(\mathcal{P}_1, \alpha / a_{31}\right)$

$$a'_{12} = \frac{a_{12} + a_{13} a_{32} S_3}{1 + a_{13} S_3}$$

$$a'_{21} = \frac{a_{21} + a_{23} a_{31} S_3}{1 + a_{23} S_3}$$

for $0 \leqslant S'_1 \leqslant S_{\max}$ **do**

$$u = \frac{\mathcal{P}_2}{1 + a'_{21} S'_1 \left(1 + a'_{12} \mathcal{P}_2\right)}$$

$$v = \frac{\mathcal{P}_1 - S'_1}{a'_{12} S'_1 \left(1 + a'_{21} \mathcal{P}_1\right)}$$

$$w = \frac{\alpha - a_{31} S'_1}{a_{32} + \left(a_{31} a'_{12} + a_{32} a'_{21} + \alpha\, a'_{12}\, a'_{21}\right) S'_1}$$

$S'_2 = \min(u, v, w)$

{inverse transform to (S_1, S_2)}

$$S_1 = \frac{S'_1}{1 + a_{13} S_3 \left(1 + a_{31} S'_1\right)}$$

$$S_2 = \frac{S'_2}{1 + a_{23} S_3 \left(1 + a_{32} S'_2\right)}$$

add point $\left(\frac{1}{2} \log_2\left(1 + S_1\right), \frac{1}{2} \log_2\left(1 + S_2\right)\right)$ to Γ

end for
return Γ

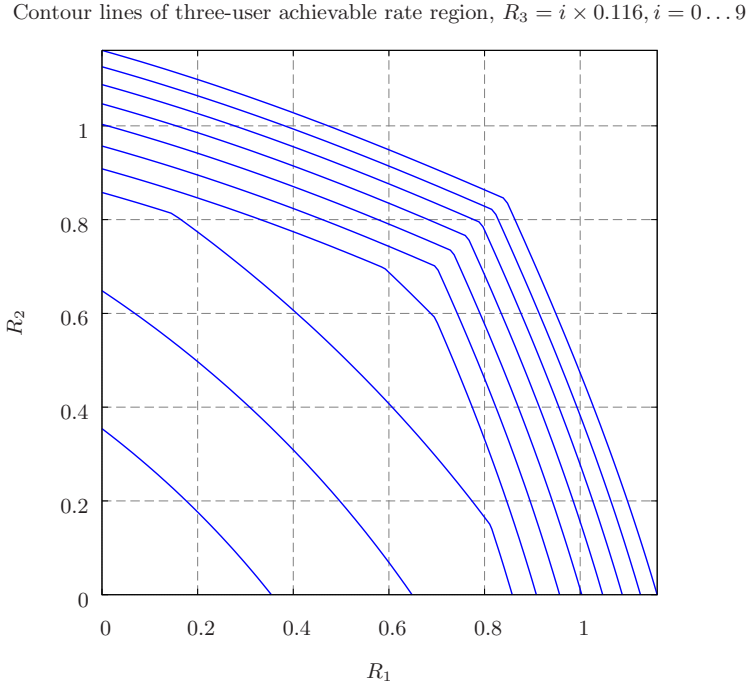

Figure 2.8: Contour lines of a three-user achievable rate region, $a_{i,j} = 0.2$ for all $i \neq j$

2.3.4 Maximum sum rate

It is showed (Section 2.2) that binary power control maximizes the sum rate of the two-user Gaussian Interference Channel. In this part, we address a more general case: the sum rate maximization of N-user case ($N \geq 3$). The question is to know whether the binary power control optimizes the sum rate for this general case.

Consider an example from [30] which is a generalization of [26] to a multi-cell case. The answer of *does the binary power control maximize the sum rate ?* is negative with a counter-example corresponding to a channel matrix given by:

$$G = 10^{-9} \times \begin{pmatrix} 0.0432 & 0.0106 & 0.0012 \\ 0.0004 & 0.2770 & 0.0043 \\ 0.0045 & 0.0137 & 0.1050 \end{pmatrix},$$

a maximum transmit power $P_{max} = 10^{-3}$ and a noise variance $\sigma^2 = 4.0039 \times 10^{-15}$, equal for the three users. Where the channel matrix is defined as:

$$G = \begin{pmatrix} g_{11} & g_{12} & g_{13} \\ g_{21} & g_{22} & g_{23} \\ g_{31} & g_{32} & g_{33} \end{pmatrix}.$$

After normalization, the parameters of the equivalent channel are $a_{ij} = g_{ij}/g_{jj}$ and $\mathcal{P}_i =$

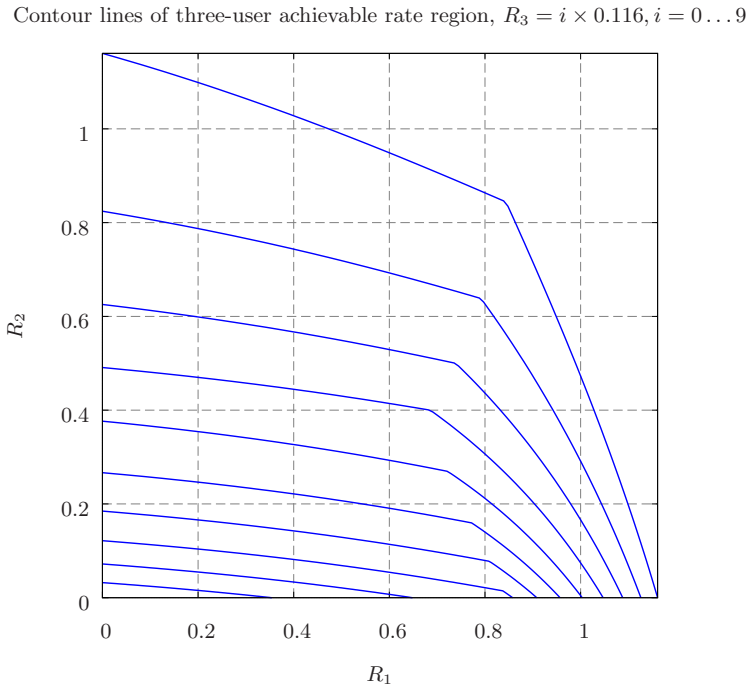

Figure 2.9: Same parameters as Fig. 2.8, except $a_{23} = a_{32} = 1$

$g_{ii} \times P_{max}/\sigma^2$, that is:

$$\mathbf{A} = \begin{pmatrix} 1 & 0.03826714801444 & 0.011428571428571 \\ 0.0092592592592593 & 1 & 0.040952380952381 \\ 0.10416666666667 & 0.049458483754513 & 1 \end{pmatrix}$$

$$\mathcal{P} = \begin{pmatrix} 10.78948025674967 \\ 69.18254701665876 \\ 26.22443117959989 \end{pmatrix}$$

Using Algorithm 1, we can compute the contour lines of the achievable rate region (Fig. 2.10) and the behavior of the sum rate $\mathcal{C}_\Sigma$ versus the rate R_3 of the third user (Fig. 2.11). Our result is in agreement with [30] within a factor 1/2 because we supposed real signals; indeed we obtain a maximum sum rate $\mathcal{C}_\Sigma = 4.72912$ slightly greater than the value 4.72775 obtained when three users transmit at their maximum power. We can notice the two values are very close, furthermore Fig. 2.11 shows that the maximum is very flat.

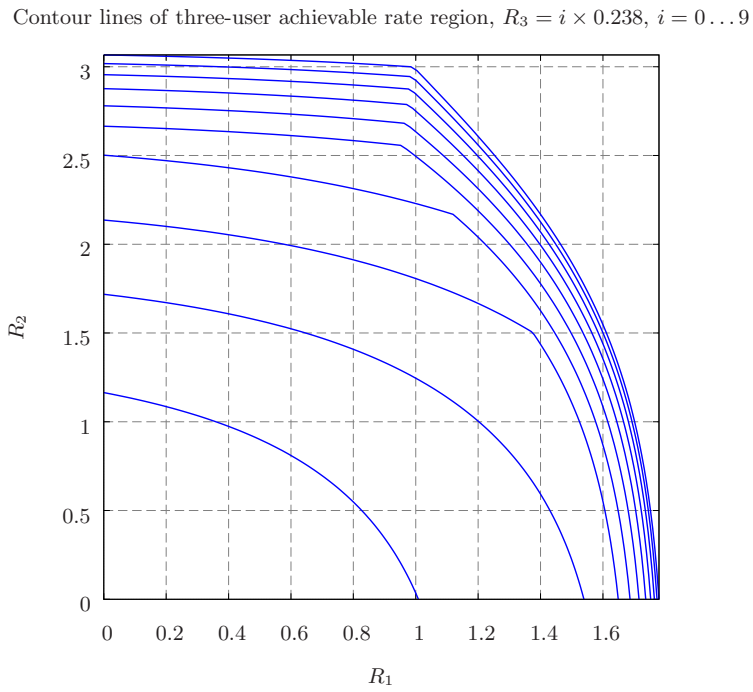

Figure 2.10: Contour lines of the three-user achievable rate region of [30].

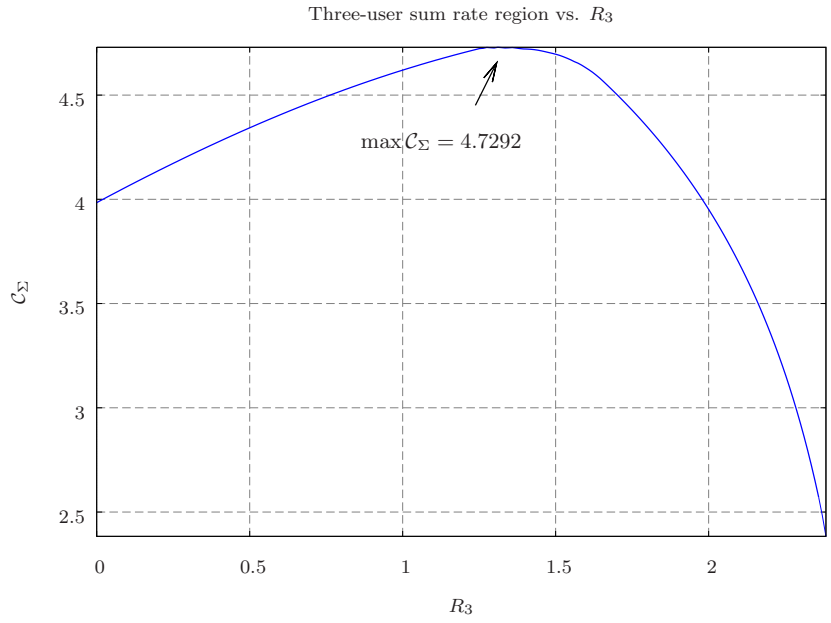

Figure 2.11: Sum rate as a function of R_3. Same settings as for Fig. 2.10.

2.4 Conclusions

In this chapter, we derived analytical expressions of the SINR region for the two and three-user Gaussian Interference Channel, considering the interference as noise. From these expressions, we obtained a geometrical description of the SINR region and an achievable rate region for the Gaussian Interference Channel. The way we derived the three-user achievable rate region is more general and it allows deriving the n-user achievable rate region provided we know the one corresponding to $(n-1)$ users. We gave some examples showing that there is room for more efficient use of the spectrum by sharing. Depending on the channels gains, the sum rate of two users sharing the same frequency band is greater than the maximum rate of one user alone, at the expense of a slight decrease of own rates.

At last, as our derivation of the achievable rate region does not involve any reciprocal knowledge of users messages, we can expect that any techniques assuming partial knowledge of each user's message will improve the achievable rates, that means the resulting rate region will contain our achievable region.

This contribution was published in the journal *Annals of Telecommunications*.

Chapter 3

Simultaneous outage performance of the 2-user Gaussian Interference Channel in fading environment

Previously, we investigated, in chapter 2, the achievable rate region of the Gaussian Interference Channel when interference is considered as noise and channels gains are constant. In this chapter, we consider the two-user Gaussian Interference Channel in a more realistic case when all users are achieving own outage performance. The question we face is: **is it possible, for at least two users, to simultaneously transmit over the same frequency band while achieving given own outage performance ?** We derive a practical condition to enable the spectrum-sharing under simultaneous outage performance. Furthermore, when the condition is fulfilled, we provide equations to define the two-dimensional region of allocated powers (P_1, P_2), for the two users, where a given simultaneous outage performance is achievable. Numerical examples are given to illustrate our results. The framework presented in this chapter covers more general settings and the results can be used to build power scheduling and sharing rules for licensed or unlicensed bands.

3.1 Introduction

We consider the Gaussian Interference Channel of figure 1.7 with each user having given outage performance. We do not consider a primary user having priority as in most of the works in spectrum-sharing and cognitive radio. In our study, all users have the same priority for spectrum access. We face the problem of simultaneous communication. Outage performance for user i is defined by a given minimum SINR γ_i required at the receiver i for successful transmission. Then an outage occurs at the receiver i when the SINR is lower than γ_i. We look for situations in spectrum-sharing where the users can simultaneously achieve their local outage performance. We aim to find a necessary and sufficient condition

to enable such a spectrum-sharing. Furthermore, when such a condition (if it exists) is fulfilled, we would like to give equations to define the two-dimensional region of allocated powers (P_1, P_2), for the two users, where a given simultaneous outage performance is achievable.

The remainder of this chapter is organized as follows. In the next section, we describe the signals model, our main assumptions, the problem we tackle and the main results. The problem of simultaneous outage performance is approached in sections 3.3 and 3.4. A novel condition to enable the spectrum-sharing, under simultaneous outage performance, is found is section 3.5. A linear approximation to simplify our expressions is given in section 3.6. Finally, conclusions are discussed in section 3.7.

3.2 Problem formulation

3.2.1 Signals model and assumptions

The fading channels are supposed to be flat. The channel power gains g_{ij} are assumed to be independent and identically distributed according to exponential distribution with parameters λ_{ij}, $i, j \in \{1, 2\}$, so, the probability density function, f_{ij}, of channel power gain g_{ij} can be expressed as:

$$f_{ij}(x) = \lambda_{ij} \exp\left(-\lambda_{ij}\, x\right), \quad x \geq 0. \tag{3.1}$$

Moreover the g_{ij} are supposed to be stationary, ergodic and mutually independent from the noise. The noise power spectral density (assumed to be the same for the two receivers) is denoted by σ^2 as previously.
We assume very simple receivers in which all undesired signals are processed as noise. Thus, with Gaussian signaling, the instantaneous rates (expressed in nats/s/Hz) of the first and the second users may be expressed as:

$$\mathrm{C}_1 = \log\left(1 + Z_1\right); \quad \mathrm{C}_2 = \log\left(1 + Z_2\right), \tag{3.2}$$

where the SINR Z_1 and Z_2 are defined, without considering coding and modulation, as:

$$Z_1 = \frac{P_1\, g_{11}}{\sigma^2 + P_2\, g_{12}}; \quad Z_2 = \frac{P_2\, g_{22}}{\sigma^2 + P_1\, g_{21}}.$$

P_1 and P_2 denote the first and the second users transmit powers. This assumption is somewhat pessimistic, and our results thus form a conservative lower bound. In practice, some form of multi-user detection allowing for interference suppression or mitigation may be used to enhance the rates achieved. We also assume the knowledge of outage SINR γ_1 and γ_2, maximum outage probabilities ϵ_1 and ϵ_2, and channels power gains parameters λ_{ij}, $i, j \in \{1, 2\}$ at the transmitters. For real channels, one can include path-loss to the means, $1/\lambda_{ij}$, of the channels power gains g_{ij}. Such information can be brought to the transmitters as follows. First, transmitter i, for $i \in \{1, 2\}$, sends a pilot signal of normalized power, then, receivers i and j ($j \neq i$) estimate simultaneously the values of λ_{ii} and λ_{ji}. Moreover,

one can imagine the existence of a *low rate control channel* that the receivers can use to feed back λ_{ii} and λ_{ji}, [36]. Finally, one can also imagine a coordination channel between transmitters that they can use to transmit to each other their own service-requiring γ_i and ϵ_i, as well as the inverse means λ_{ii} and λ_{ji} of local direct channels power gains.

3.2.2 Main goal

Our main goal is to respond to the question: what are the situations, in spectrum-sharing, where the users can simultaneously achieve local outage performances? Specifically, we aim to know the cases where the spectrum-sharing allows fulfilling simultaneously the following constraints:

$$\mathbf{Prob}\left(Z_1 \leq \gamma_1\right) \leq \epsilon_1 \tag{3.3}$$

$$\mathbf{Prob}\left(Z_2 \leq \gamma_2\right) \leq \epsilon_2 \tag{3.4}$$

where $\mathbf{Prob}(x)$ denotes the probability of event "x". The given outage SINR γ_1 and γ_2 are the minimum necessary SINR for the service of the two users. Furthermore, we look for the two-dimensional region of (P_1, P_2) where (3.3) and (3.4) are achieved simultaneously.

3.2.3 Main results

We will demonstrate that the simultaneous outage problem, that consists in fulfilling at the same time (3.3) and (3.4), has a solution only if the following condition holds:

$$\frac{(1-\epsilon_1)\,(1-\epsilon_2)}{\epsilon_1\,\epsilon_2} < \frac{\lambda_{12}\,\lambda_{21}}{\gamma_1\,\gamma_2\lambda_{11}\,\lambda_{22}}. \tag{3.5}$$

Otherwise, when the outage probabilities ϵ_1 and ϵ_2 do not verify (3.5), no power pair (P_1, P_2) can be allocated to share the spectrum under (3.3) and (3.4). It is interesting to note that the condition (3.5) depends on only the outage probabilities of both the users, the mean gains of all the links and the minimum SINR required for the services of the users. Furthermore, if the condition (3.5) is fulfilled, we give equations to define the two-dimensional region of (P_1, P_2) where given simultaneous outage performance is achievable.

3.3 Mathematical description of simultaneous outage performance problem

In this section, we formulate the problem of simultaneous outage performance. First, we study the distribution of the SINR variables, then we derive an outage probability for each user. At the end, we give a mathematical description of the problem.

3.3.1 Distribution of the SINR variable

In order to express the outage constraints (3.3) and (3.4), first we calculate the probability density function of the SINR for the two users.

To give the probability density function of the SINR variable, let $x = P_1\, g_{11}$, $y = \sigma^2 + P_2\, g_{12}$ and $z_1 = \frac{x}{y}$. Let variables X, Y and Z_1 be the random variables whose samples are respectively x, y and z_1. Since, the g_{ij} are exponentially distributed with parameters λ_{ij}, the random variable X is exponentially distributed with parameter $\frac{\lambda_{11}}{P_1}$, while the random variable Y has a *shifted-exponential distribution* with the following probability density function:

$$f_Y(y) = \begin{cases} \dfrac{\lambda_{12}}{P_2} \exp\left(\dfrac{\lambda_{12}}{P_2}\sigma^2\right) \exp\left(-\dfrac{\lambda_{12}}{P_2} y\right) & \text{if} \quad y \geq \sigma^2 \\ 0 & \text{if} \quad y < \sigma^2. \end{cases} \tag{3.6}$$

The ratio between the two independent random variables X and Y, is a random variable Z_1 with the following probability density function for $z_1 \geq 0$:

$$\begin{aligned} f_{Z_1}(z_1) &= \int_{\sigma^2}^{+\infty} y\, f_X(z_1\, y)\, f_Y(y)\, dy \\ &= \frac{\lambda_{11}}{P_1}\frac{\lambda_{12}}{P_2} \exp\left(\frac{\lambda_{12}}{P_2}\sigma^2\right) \int_{\sigma^2}^{+\infty} y \exp\left(-\left(\frac{\lambda_{11}}{P_1} z_1 + \frac{\lambda_{12}}{P_2}\right) y\right) dy. \end{aligned}$$

After an integration by parts, we obtain:

$$f_{Z_1}(z_1) = \begin{cases} \dfrac{1 + b + \dfrac{b}{a} z_1}{a\left(1 + \dfrac{1}{a} z_1\right)^2} \exp\left(-\dfrac{b}{a} z_1\right) & \text{if} \quad z_1 \geq 0 \\ 0 & \text{if} \quad z_1 < 0, \end{cases} \tag{3.7}$$

with $a = (P_1/\lambda_{11}) \times (\lambda_{12}/P_2)$ and $b = \sigma^2\ (\lambda_{12}/P_2)$.
The probability density function of user 2 is obtained from (3.7) by the indices permutation $\{1, 2\} \to \{2, 1\}$.

3.3.2 Outage probability

Using the probability density function (3.7), the outage probability of user 1 is obtained as:

$$\textbf{Prob}\,(Z_1 \leq \gamma_1) = \int_0^{\gamma_1} f_{Z_1}(z_1)\, dz_1 = 1 - \frac{\exp\left(-\sigma^2 \dfrac{\lambda_{11}}{P_1}\gamma_1\right)}{1 + \dfrac{\lambda_{11}}{\lambda_{12}}\dfrac{P_2}{P_1}\gamma_1}. \tag{3.8}$$

The outage probability of user 2 is obtained from (3.8) by the indices permutation $\{1,2\} \rightarrow \{2,1\}$. Then, the problem of simultaneous outage performance is expressed as:

$$\begin{cases} 1 - \dfrac{1}{1 + \dfrac{\lambda_{11}}{\lambda_{12}} \dfrac{P_2}{P_1} \gamma_1} \exp\left(-\sigma^2 \gamma_1 \dfrac{\lambda_{11}}{P_1}\right) & \leq \quad \epsilon_1 \\ 1 - \dfrac{1}{1 + \dfrac{\lambda_{22}}{\lambda_{21}} \dfrac{P_1}{P_2} \gamma_2} \exp\left(-\sigma^2 \gamma_2 \dfrac{\lambda_{22}}{P_2}\right) & \leq \quad \epsilon_2. \end{cases} \tag{3.9}$$

After some manipulations, we obtain:

$$\begin{cases} P_2 \quad \leq \quad \dfrac{\lambda_{12}}{\lambda_{11}\,\gamma_1} \left(\dfrac{\exp\left(-\sigma^2 \gamma_1 \dfrac{\lambda_{11}}{P_1}\right)}{1 - \epsilon_1} - 1 \right) P_1 \\ P_1 \quad \leq \quad \dfrac{\lambda_{21}}{\lambda_{22}\,\gamma_2} \left(\dfrac{\exp\left(-\sigma^2 \gamma_2 \dfrac{\lambda_{22}}{P_2}\right)}{1 - \epsilon_2} - 1 \right) P_2 \end{cases} \tag{3.10}$$

3.4 Set of possible power pairs

Now we characterize the set of possible pairs of power $(P_1,\, P_2)$ that verify the problem (3.10). The problem of simultaneous outage performance consists in seeking the set of pairs $(P_1,\, P_2)$ such that:

$$\begin{cases} P_2 \quad \leq \quad \psi_1\left(P_1\right) \\ P_1 \quad \leq \quad \psi_2\left(P_2\right), \end{cases} \tag{3.11}$$

where the functions ψ_1 and ψ_2 are defined as:

$$\begin{cases} \psi_1\left(P_1\right) \quad = \quad \dfrac{\lambda_{12}}{\lambda_{11}\,\gamma_1} \left(\dfrac{\exp\left(-\sigma^2 \gamma_1 \dfrac{\lambda_{11}}{P_1}\right)}{1 - \epsilon_1} - 1 \right) P_1 \\ \psi_2\left(P_2\right) \quad = \quad \dfrac{\lambda_{21}}{\lambda_{22}\,\gamma_2} \left(\dfrac{\exp\left(-\sigma^2 \gamma_2 \dfrac{\lambda_{22}}{P_2}\right)}{1 - \epsilon_2} - 1 \right) P_2. \end{cases} \tag{3.12}$$

The set of inequalities (3.11) shows that spectrum sharing under outage constraints (3.3) and (3.4) is possible only when the functions $\psi_1(P_1)$ and $\psi_2(P_2)$ are strictly positive:

$$\begin{cases} \psi_1(P_1) & > & 0 \\ \psi_2(P_2) & > & 0. \end{cases} \tag{3.13}$$

Using the expressions of (3.12), the conditions (3.13) imply:

$$\begin{cases} P_1 & > & P_{1,0} \triangleq -\dfrac{\sigma^2 \lambda_{11} \gamma_1}{\log(1-\epsilon_1)} \\ P_2 & > & P_{2,0} \triangleq -\dfrac{\sigma^2 \lambda_{22} \gamma_2}{\log(1-\epsilon_2)}. \end{cases} \tag{3.14}$$

The powers $P_{1,0}$ and $P_{2,0}$ verify:

$$\psi_1(P_{1,0}) = 0; \quad \psi_2(P_{2,0}) = 0. \tag{3.15}$$

For P_1 and P_2 verifying (3.14), that is, for $P_1 \in]P_{1,0}, +\infty[$ and $P_2 \in]P_{2,0}, +\infty[$, functions $\psi_1(P_1)$ and $\psi_2(P_2)$ are strictly increasing. Consequently, the inverse function $\psi_2^{-1}(P_1)$ is increasing in $]0, +\infty[$. The problem of simultaneous outage performance can be written as:

$$\psi_2^{-1}(P_1) \leq P_2 \leq \psi_1(P_1). \tag{3.16}$$

The set $\mathcal{P}$ of possible pairs (P_1, P_2) is as follows:

$$\mathcal{P} = \left\{ (P_1, P_2) \,/\, P_1 > P_{1,0},\, P_2 > P_{2,0},\, \psi_2^{-1}(P_1) \leq P_2 \leq \psi_1(P_1) \right\}. \tag{3.17}$$

Furthermore, since $\psi_2^{-1}(0) = P_{2,0} > 0$ (then $\psi_2^{-1}(P_{1,0}) > 0$) and $\psi_1(P_{1,0}) = 0$, we have:

$$\psi_2^{-1}(P_{1,0}) > \psi_1(P_{1,0}).$$

Therefore, the problem of simultaneous outage performance has a solution only if there exists $P_{1,\alpha} > P_{1,0}$ such as

$$\psi_2^{-1}(P_{1,\alpha}) = \psi_1(P_{1,\alpha}). \tag{3.18}$$

In other words, the curves of $\psi_2^{-1}(P_1)$ and $\psi_1(P_1)$ must meet in $P_{1,\alpha} \in]P_{1,0}, +\infty[$ (Cf. Fig. 3.1). Then, to ensure (3.3) and (3.4) are achieved simultaneously, power P_1 must verify $P_1 \geq P_{1,\alpha}$ and power P_2 must verify (3.16). If the curves of $\psi_2^{-1}(P_1)$ and $\psi_1(P_1)$ can not meet in $]P_{1,0}, +\infty[$ (Cf. Fig. 3.2), then problem of simultaneous outage performance has no solution. That is, there is no power pair (P_1, P_2) that can verify simultaneously (3.3) and (3.4).

3.5 Condition to ensure simultaneous outage performance

Previously, we proved that the set of power pairs (P_1, P_2) ensuring (3.3) and (3.4), is given by (3.17). Moreover, we showed that, to ensure the set $\mathcal{P}$ is not empty, the curves

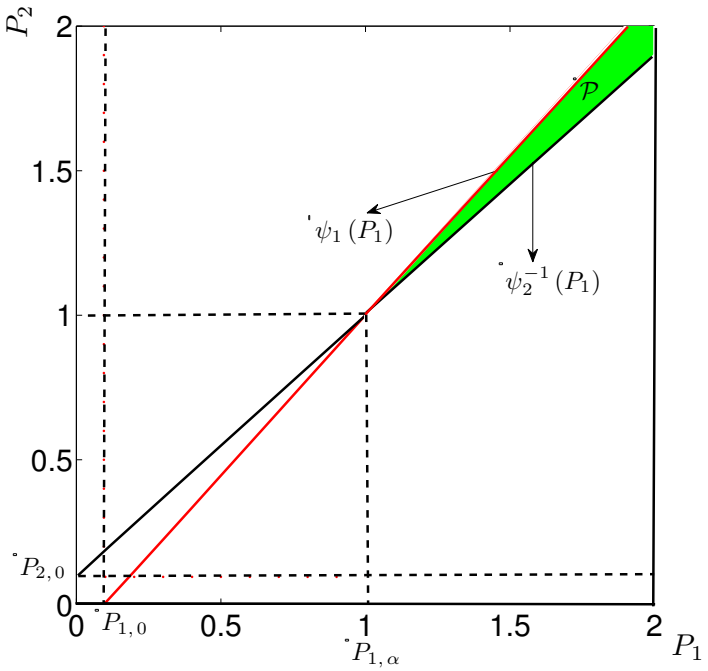

Figure 3.1: Curves of $\psi_1(P_1)$ and $\psi_2^{-1}(P_1)$. The curves meet in $P_{1,\alpha}$, then, there is a two-dimensional region $\mathcal{P}$ of (P_1, P_2) where the simultaneous outage performance is achievable.

of $\psi_2^{-1}(P_1)$ and $\psi_1(P_1)$ must meet to give solution to the problem (3.16). Now, we look for a condition that ensures existence of a solution to (3.11).

3.5.1 Condition

Thanks to (3.18), the curves of $\psi_2^{-1}(P_1)$ and $\psi_1(P_1)$ meet in $P_{1,\alpha} > P_{1,0}$ only if

$$P_{1,\alpha} = \psi_2(\psi_1(P_{1,\alpha})). \tag{3.19}$$

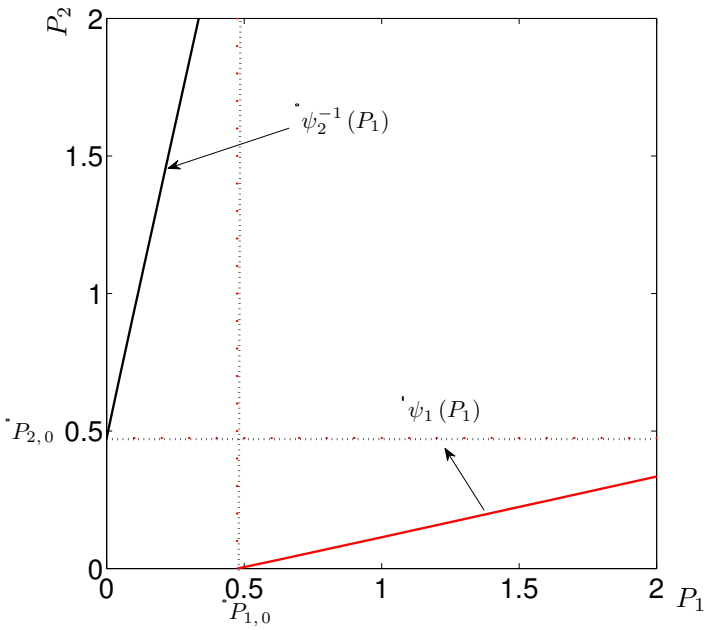

Figure 3.2: Curves of $\psi_1(P_1)$ and $\psi_2^{-1}(P_1)$. The curves do not meet, then simultaneous outage performance is not achievable.

Replacing $\psi_1(P_{1,\alpha})$ and $\psi_2(.)$ by theirs values and doing some manipulations, we show that $P_{1,\alpha}$ must verify the following equation:

$$\frac{\exp\left(-\dfrac{\sigma^2\,\gamma_2\,\lambda_{22}}{\dfrac{\lambda_{12}}{\gamma_1\,\lambda_{11}}\left(\dfrac{\exp\left(-\sigma^2\,\gamma_1\,\dfrac{\lambda_{11}}{P_{1,\alpha}}\right)}{1-\epsilon_1}-1\right)P_{1,\alpha}}\right)}{1+\dfrac{1}{\dfrac{\lambda_{12}\,\lambda_{21}}{\gamma_1\,\gamma_2\,\lambda_{11}\,\lambda_{22}}\left(\dfrac{\exp\left(-\sigma^2\,\gamma_1\,\dfrac{\lambda_{11}}{P_{1,\alpha}}\right)}{1-\epsilon_1}-1\right)}}=(1-\epsilon_2)\,. \tag{3.20}$$

This equation is equivalent to:

$$P_{1,\alpha} = \frac{-\sigma^2}{\left[\log(1-\epsilon_2) + \log\left(1 + \frac{1}{\lambda_{21}\,\chi(P_{1,\alpha})}\right)\right]\chi(P_{1,\alpha})}, \tag{3.21}$$

where

$$\chi(P_{1,\alpha}) = \frac{\lambda_{12}}{\gamma_1\,\gamma_2\lambda_{11}\,\lambda_{22}}\left(\frac{\exp\left(-\sigma^2\,\gamma_1\,\frac{\lambda_{11}}{P_{1,\alpha}}\right)}{1-\epsilon_1} - 1\right). \tag{3.22}$$

The function $\chi(P_{1,\alpha})$ is positive in $]P_{1,0}, +\infty[$. To have positive $P_{1,\alpha}$, the following inequality is necessary:

$$\log\left(1 + \frac{1}{\lambda_{21}\,\chi(P_{1,\alpha})}\right) < \log\left(\frac{1}{1-\epsilon_2}\right) \tag{3.23}$$

or equivalently

$$\chi(P_{1,\alpha}) > \frac{1}{\lambda_{21}}\left(\frac{1}{\epsilon_2} - 1\right). \tag{3.24}$$

Replacing $\chi(P_{1,\alpha})$ by its expression, inequality (3.24) becomes:

$$-\sigma^2\,\gamma_1\,\frac{\lambda_{11}}{P_{1,\alpha}} > \log(1-\epsilon_1) + \log\left(1 + \frac{\gamma_1\,\gamma_2\lambda_{11}\,\lambda_{22}}{\lambda_{12}\,\lambda_{21}}\left(\frac{1}{\epsilon_2} - 1\right)\right). \tag{3.25}$$

Since $P_{1,\alpha}$ must be positive, to fulfill the expression (3.25) the following condition holds:

$$\log(1-\epsilon_1) + \log\left(1 + \frac{\gamma_1\,\gamma_2\lambda_{11}\,\lambda_{22}}{\lambda_{12}\,\lambda_{21}}\left(\frac{1}{\epsilon_2} - 1\right)\right) < 0. \tag{3.26}$$

Finally, we derive from (3.26) the following necessary condition to ensure a solution to equation (3.20):

$$\frac{(1-\epsilon_1)\,(1-\epsilon_2)}{\epsilon_1\,\epsilon_2} < \frac{\lambda_{12}\,\lambda_{21}}{\gamma_1\,\gamma_2\lambda_{11}\,\lambda_{22}} \tag{3.27}$$

We can prove that the necessary condition (3.27) is also sufficient.

Proof. Suppose the condition (3.27) holds. First, let

$$f(P_1) = \frac{-\sigma^2}{\left[\log(1-\epsilon_2) + \log\left(1 + \frac{1}{\lambda_{21}\,\chi(P_1)}\right)\right]\chi(P_1)},$$

we must demonstrate that there exists $P_{1,\alpha} \in]P_{1,0}, +\infty[$ such that $P_{1,\alpha} = f(P_{1,\alpha})$.

Under the condition (3.27),

$$\log\left(1-\epsilon_2\right)+\log\left(1+\frac{1}{\lambda_{21}\,\chi\left(P_1\right)}\right)<0 \iff P_1>x_0,$$

with

$$x_0=-\frac{\sigma^2\,\lambda_{11}\,\gamma_1}{\log\left(1-\epsilon_1\right)+\log\left(1+\dfrac{\gamma_1\,\gamma_2\lambda_{11}\,\lambda_{22}}{\lambda_{12}\,\lambda_{21}}\left(\dfrac{1}{\epsilon_2}-1\right)\right)}>P_{1,0}.$$

We have:

$$\log\left(1-\epsilon_2\right)+\log\left(1+\frac{1}{\lambda_{21}\,\chi\left(x_0\right)}\right)=0.$$

Furthermore, as $x_0>P_{1,0}$, we have $\chi\left(x_0\right)>0$. Then,

$$\lim_{P_1\to x_0^+} f\left(P_1\right)=+\infty \tag{3.28}$$

where $P_1\to x_0^+$ means P_1 is tending to x_0 while $P_1>x_0$. Noting that

$$\lim_{P_1\to+\infty}\chi\left(P_1\right)=\frac{\lambda_{12}}{\gamma_1\,\gamma_2\lambda_{11}\,\lambda_{22}}\left(\frac{1}{1-\epsilon_1}-1\right),$$

we can give

$$\lim_{P_1\to+\infty} f\left(P_1\right)=\xi, \tag{3.29}$$

where the constant ξ is a negative number:

$$\xi=\frac{-\sigma^2}{\dfrac{\lambda_{12}}{\gamma_1\,\gamma_2\lambda_{11}\,\lambda_{22}}\left(\dfrac{1}{1-\epsilon_1}-1\right)\left(\log\left(1-\epsilon_2\right)+\log\left(1+\dfrac{1}{\dfrac{\lambda_{12}\,\lambda_{21}}{\gamma_1\,\gamma_2\lambda_{11}\,\lambda_{22}}\left(\dfrac{1}{1-\epsilon_1}-1\right)}\right)\right)} \tag{3.30}$$

The function f is decreasing in $]x_0,\,+\infty[$ with limit values (3.28) and (3.29). So, $\exists\, P_{1,\alpha}\in\,]x_0,\,+\infty[$ such that $P_{1,\alpha}=f\left(P_{1,\alpha}\right)$. □

3.5.2 Numerical examples

For numerical purpose, we set the channel parameters to $\lambda_{11}=\lambda_{22}=1$, $\lambda_{12}=\lambda_{21}=10$. The noise power is set to $\sigma^2=0.01$. We give the same outage probability to the two users: $\epsilon_1=\epsilon_2=0.1$.

Case where the simultaneous outage performance is achievable in Fig. 3.1, we set the outage SINR to $\gamma_1=\gamma_2=1$. So, Moreover, we showed that, to ensure the set

and $\psi_2^{-1}(P_1)$ meet and the simultaneous outage performance is achievable. The set of allocated (P_1, P_2) is described by a two-dimensional region $\mathcal{P}$.

Case where the simultaneous outage performance is not achievable in Fig. 3.2, we set the outage SINR to $\gamma_1 = \gamma_2 = 5$. So, $\frac{(1-\epsilon_1)(1-\epsilon_2)}{\epsilon_1 \epsilon_2} = 81 > \frac{\lambda_{12}\lambda_{21}}{\gamma_1 \gamma_2 \lambda_{11}\lambda_{22}} = 4$. The curves of $\psi_1(P_1)$ and $\psi_2^{-1}(P_1)$ do not meet and the simultaneous outage performance is not achievable. No power pair (P_1, P_2) can be allocated to the spectrum users to fulfill (3.3) and (3.4) simultaneously.

3.6 Linear approximation

When condition (3.27) holds, the powers (P_1, P_2), that can be allocated to the spectrum users, verify (3.16). Unfortunately, the expressions of (3.16) are not linear (in particular, we did not find a closed-form expression for $\psi_2^{-1}(P_1)$) and so do not provide practical way to choose allocated powers (P_1, P_2). However, $\psi_1(P_1)$ and $\psi_2^{-1}(P_1)$ look almost linear in examples such as in Fig. 3.1. In this section, we give practical results for weak values of outage SINR γ_1 and γ_2. First, let give the mean Signal-to-Noise Rations (SNR) defined by:

$$\mathbb{E}\left[\frac{P_1\, g_{11}}{\sigma^2}\right] = \frac{P_1}{\sigma^2\, \lambda_{11}}; \quad \mathbb{E}\left[\frac{P_2\, g_{22}}{\sigma^2}\right] = \frac{P_2}{\sigma^2\, \lambda_{22}}.$$

When the required outage SINR γ_1 and γ_2 are sufficiently weak:

$$\gamma_1 \ll \frac{P_1}{\sigma^2\, \lambda_{11}}; \quad \gamma_2 \ll \frac{P_2}{\sigma^2\, \lambda_{22}},$$

we can use Taylor series to approximate the exponential function: $\exp\left(-\sigma^2\, \gamma_1\, \frac{\lambda_{11}}{P_1}\right) \approx 1 - \sigma^2\, \gamma_1\, \frac{\lambda_{11}}{P_1}$ and $\exp\left(-\sigma^2\, \gamma_2\, \frac{\lambda_{22}}{P_2}\right) \approx 1 - \sigma^2\, \gamma_2\, \frac{\lambda_{22}}{P_2}$. Therefore, using expressions of (3.16), the allocating powers P_1 and P_2, verify:

$$\psi_{2,\,\mathrm{lin}}^{-1}(P_1) \leq P_2 \leq \psi_{1,\,\mathrm{lin}}(P_1)\,. \tag{3.31}$$

where the linear functions $\psi_{2,\,\mathrm{lin}}^{-1}(P_1)$ and $\psi_{1,\,\mathrm{lin}}(P_1)$ are defined as

$$\begin{aligned}
\psi_{2,\,\mathrm{lin}}^{-1}(P_1) &= \left(\frac{1}{\epsilon_2} - 1\right)\left[\frac{\gamma_2\, \lambda_{22}}{\lambda_{21}} P_1 + \frac{\sigma^2\, \gamma_2\, \lambda_{22}}{1 - \epsilon_2}\right] \\
\psi_{1,\,\mathrm{lin}}(P_1) &= \frac{\lambda_{12}}{\lambda_{11}\, \gamma_1}\left[\left(\frac{1}{1 - \epsilon_1} - 1\right) P_1 - \frac{\sigma^2\, \gamma_1\, \lambda_{11}}{1 - \epsilon_1}\right].
\end{aligned}$$

Expression (3.31) builds a linear and useful power control to ensure, simultaneously, given local outage performance to the users.

Numerical example: in figure 3.3, we plot the linear approximation error $\psi_1(P_1) - \psi_{1,\text{lin}}(P_1)$ and $\psi_2(P_2) - \psi_{2,\text{lin}}(P_2)$, for different values of P_1 or P_2, for the same setting as in Fig. 3.1. We have $\psi_1(x) - \psi_{1,\text{lin}}(x) = \psi_2(x) - \psi_{2,\text{lin}}(x)$ (symmetric interference channel).
As P_1 (or P_2) increases, the mean SNR increases and Taylor series approximation of the exponential function: $\exp\left(-\sigma^2 \gamma_1 \frac{\lambda_{11}}{P_1}\right) \approx 1 - \sigma^2 \gamma_1 \frac{\lambda_{11}}{P_1}$ and $\exp\left(-\sigma^2 \gamma_2 \frac{\lambda_{22}}{P_2}\right) \approx 1 - \sigma^2 \gamma_2 \frac{\lambda_{22}}{P_2}$ becomes more and more accurate. Consequently, allocated power (P_1, P_2) is fulfilling the expression (3.31) with increasing accuracy.

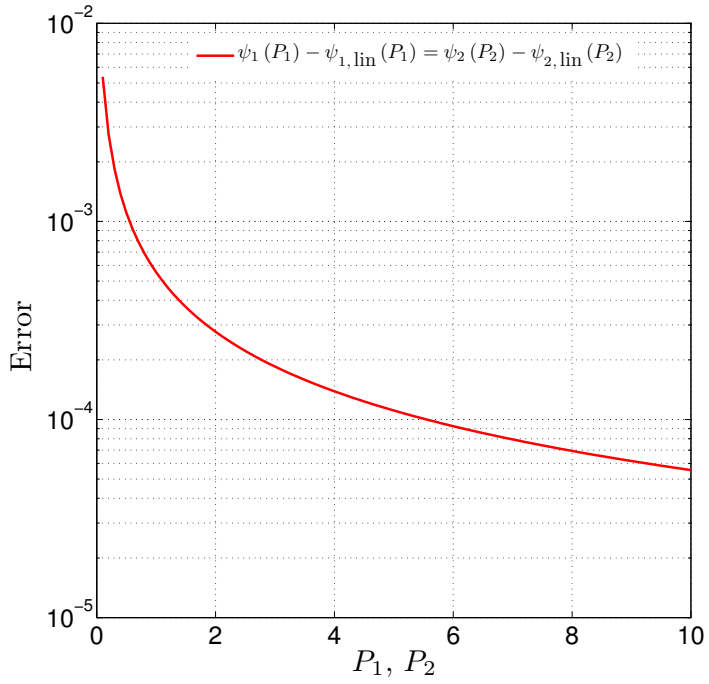

Figure 3.3: Linear approximation error: $\psi_1(P_1) - \psi_{1,\text{lin}}(P_1)$ and $\psi_2(P_2) - \psi_{2,\text{lin}}(P_2)$.

3.7 Conclusions

In this chapter, we considered two different users sharing the same frequency band, interfering with each other, under own outage performance requirement. We found an original and simple condition to enable such a spectrum-sharing based on the statistics of Rayleigh channel. Furthermore, this condition is shown to be necessary and sufficient. When it is fulfilled, we give equations to define the two-dimensional region of allocated powers (P_1, P_2), for the two users, where given simultaneous outage performance is achieved. Some numerical examples are given to illustrate our results. These results cover more general settings and can be extended to build power control schemes and sharing rules for licensed or unlicensed bands.

3.7 Conclusions

This contribution was published in the proceedings of the 11th *IEEE International Workshop on Signal Processing Advances in Wireless Communications (SPAWC 2010)*.

A perspective could be to generalize the simultaneous outage performance condition to more than 2 users.

Chapter 4

Power control of spectrum-sharing in fading environment with partial channel state information

In the previous chapters we have considered two users sharing the same frequency band with the same priority to access the spectrum. Now, we consider that there is a primary user which could be the spectrum license holder for instance. The other one is the secondary user whose access to the spectrum is subject to some constraints. The first question we face is **how harmful is the secondary transmission on the primary mean rate ?** We propose two lower bounds for the primary-user mean rate, according to the channel state information available for the secondary-user power control and to the type of constraint for spectrum access. Then, we investigate several power control policies and we compare the achievable primary-user mean rate with its lower bounds. Specially, assuming that the channel is an opportunity to the secondary user only if its transmission does not affect the primary reception quality and its (the secondary user) reception quality is not affected by the primary transmission, and considering the primary and the secondary reception qualities as outage performance, we propose a novel secondary-user power control policy, in a scenario that includes both underlay and interweave spectrum-sharing, for systems that carry out real-time delay-sensitive applications, e.g. voice and video. Moreover, considering that knowledge of primary user direct links gains estimations (estimation of g_{11} and g_{21}), at the secondary transmitter, requires sophisticated techniques, the proposed power control is built to use the secondary-user direct links gains estimations only (estimation of g_{22} and g_{12}).

4.1 Problem formulation

In this section, we present the system and channel model, introduce the problem and present our main goal.

4.1.1 System and channel model

We consider the network depicted in Fig. 1.7 with two users transmitting in the same frequency band and interfering with each other. The first user (PR) is assumed to be the licensee of the spectrum and is called primary user. The second user (CR) is the secondary user. We consider the same fading channels as in chapter 3. The estimations of g_{11}, g_{22}, g_{12} and g_{21} are respectively noted by $\hat{g}_{11}$, $\hat{g}_{22}$, $\hat{g}_{12}$ and $\hat{g}_{21}$. The mean rates are defined as $\mathbf{C}_1 \triangleq \mathbb{E}[\mathrm{C}_1]$ and $\mathbf{C}_2 \triangleq \mathbb{E}[\mathrm{C}_2]$, where $\mathbb{E}[x]$ denotes the mean of the random variable x.

4.1.2 Main goal

We consider a secondary user trying to access a licensed spectrum. We study the impact of its transmission on the reception quality of the primary user. In contrast, the primary user does not care about its interference to the secondary user. We aim to investigate lower bounds of the primary mean rate according to the CSI available for the secondary power control and to the type of constraint for spectrum access. We then compare these bounds to the primary achievable mean rates when the secondary user is performing different power control policies. In particular, we propose a novel power control policy, for the secondary user, when all pairs of transmitter-receiver are achieving real-time delay-sensitive applications.

For simplicity, in the sequel, we assume the primary user performs a constant power control. Therefore, we have $p_1 = \bar{P}_1$, where $\bar{P}_1$ denotes the mean transmit power of the primary user.

4.1.2.1 Lower bounds for the primary user mean rate

The lower bound for the primary user mean rate is investigated in two different spectrum-sharing scenarios:

- the first scenario is called *unconstrained spectrum-sharing*. It consists in a theoretical spectrum-sharing where the secondary user is subject to no constraint from the primary user other than the limited-mean-transmit-power constraint. A lower bound for the primary mean rate is derived when secondary user performs a $\{\hat{g}_{22}, \hat{g}_{21}\}$-dependent power control/scheduling,
- the other scenario is called *constrained spectrum-sharing*. Secondary transmission is subject to some interference constraints from the primary user. To meet the interference constraints, we assume that the secondary-to-primary link gain estimation is available at the secondary transmitter. A lower bound for the primary mean rate is derived in a more general case when secondary user performs a $\{\hat{g}_{22}, \hat{g}_{21}, \hat{g}_{12}\}$-dependent power control/scheduling.

4.1.2.2 Secondary power control

We investigate different power control schemes and compare the primary user achievable mean rate to its lower bounds. In particular, we propose an original secondary power control policy with the following requirements:

- the secondary user can only estimate the channel gains g_{22} (secondary-to-secondary link) and g_{12} (secondary-to-primary link),
- each spectrum user needs given outage performance to achieve its service.

More precisely, we ensure that the secondary transmission meets the following constraints:

$$\mathbf{Prob}_{g_{11},g_{21}}\left(\mathrm{C}_1 \leq \mathrm{C}_0\right) \leq \epsilon \tag{4.1}$$
$$\mathbf{Prob}_{g_{11},g_{21}}\left(\mathrm{C}_2 \leq \mathrm{C}'_0\right) \leq \epsilon', \tag{4.2}$$

where $\mathbf{Prob}_{g_{11},g_{21}}(x)$ denotes the probability of event "x" over the distributions of g_{11} and g_{21}. The given rates C_0 and C'_0 are the minimum necessary rates for the services of, respectively, the primary and the secondary users. In general, (4.1) and (4.2) ensure that primary and secondary instantaneous rates are greater than C_0 and C'_0 most of the time, the occurrence is determined by the maximum outage probabilities ϵ and ϵ'.

4.1.2.3 Channel and parameters estimation

The channels gains estimations $\hat{g}_{ij}$ and the means values $1/\lambda_{ij}$ can be brought to the transmitters thanks to the same protocol as in chapter 3. To perform the proposed power control, as shown farther, secondary user needs to know $\bar{P}_1$, λ_{11}, λ_{21}, ϵ, ϵ', C_0 and C'_0. We assume that $\bar{P}_1$, λ_{11}, ϵ and C_0 are sent to the secondary user via the coordination channel or by a *band manager* which mediates between the two parties.

The remainder of this chapter is organized as follows. In the next section, we state the art. We investigate two lower bounds for the primary user mean rate, in section 4.3. Power control for secondary user is considered in section 4.4. Finally, conclusions are discussed in section 4.5.

4.2 State of the art

Power control for spectrum-sharing users has been widely studied. In particular, [57] investigated the maximum ergodic capacity of a secondary user under joint peak and average interference power constraints at the primary receiver. The optimal power control derived in [57] to achieve the secondary maximum ergodic capacity is function of the CSI of the secondary user and of the link between the secondary transmitter and the primary receiver. However, this optimal power allocation does not take into account the interference from the primary user to the secondary user. Moreover, in non-outage states, the secondary's received power could be weak, providing bad quality to the secondary service. [58] presents a criterion to design the secondary transmit power control by introducing a *primary-capacity-loss constraint* (PCLC). This method is shown to be superior over the previous ones in terms of achievable ergodic capacities of both the primary and the secondary links. It protects the primary transmission by ensuring that the maximum ergodic capacity loss of the primary link, due to the secondary transmission, is no greater than some predefined value, [58]. However, to enable the *primary-capacity-loss constraint*-based power control, [58] assumes that not only the CSI of the secondary fading channel and the

fading channel from the secondary transmitter to the primary receiver (noted $g_{22} \triangleq |h_{22}|^2$ and $g_{12} \triangleq |h_{12}|^2$, Fig. 1.7) are known to the secondary transmitter, but also the CSI of the primary direct links (g_{11} and g_{21}). [60] qualitatively characterizes the impacts of the transmission power of a secondary user on the occurrence of spectrum opportunities and the reliability of opportunity detection. The probability of spectrum opportunity decreases exponentially with the transmission power of secondary users, where the exponential decay constant is given by the traffic load of primary users. So, secondary power control should take into account the definition of spectrum opportunity which is defined in [60] as: *a channel is an opportunity to a secondary user only if its transmission does not affect primary reception quality and its (secondary user) reception quality is not affected by primary transmission.* Therefore, the transmission power of a secondary user not only determines its communication range but also affects how often it sees spectrum opportunities. If secondary user should transmit with a high power to reach its intended receiver directly, it must wait for the opportunity that no primary receiver is active within its relatively large interference region, which happens less often. *If, on the other hand, it uses low power, it must rely on multi-hop relaying, and each hop must wait for its own opportunities to emerge.*

For concurrent spectrum-sharing (unlicensed spectrum-sharing or spectrum-sharing between several secondary users) where the goal may be to optimize selfish utilities or a centralized utility, game theory is used, see for instance [56] an the references therein. [56] investigates cooperative and non-cooperative scenarios of spectrum-sharing for unlicensed bands. The cooperative assumption may be realistic when the different systems are jointly designed with a common goal. They can be complying with some standard or regulation, or they can be as transmitter-receiver pairs of a single global system. Assuming a *selfish behavior* (non-cooperative scenarios) may be more realistic[1] when systems are competing with one another to gain access to the common medium.

Contrary to the optimal power control, derived in [57] and [58], and the non-cooperative games in [56], our goal is neither to achieve, in any case, maximum possible rate, nor to maximize *selfish* utilities. The power control derived in part 4.4.2 aims to ensure at some occurrence, predefined by the outage probabilities ϵ and ϵ', at least given minimum instantaneous rates to the two users, while using only the direct links gains estimations $\hat{g}_{22}$ and $\hat{g}_{12}$. That is not considered in the previous works such as [56], [57] and [58] and references therein. Furthermore, this power allocation allows the secondary user to transmit only if given outage performance is achievable simultaneously for both the users. As we will see, that adapts somewhat with the previous definition of spectrum opportunity.

4.3 Lower bounds of the primary user mean rate

In this section, we investigate two lower bounds for the primary user mean rate according to spectrum access constraints and available channel state information at the secondary user transmitter.

[1] *The systems are selfish in the sense that they only try to maximize their own utility [56].*

4.3.1 Unconstrained spectrum-sharing

In this part, we are interested in a scenario of spectrum-sharing where there is neither collaboration between the two users, nor interference or capacity loss constraint. We assume that

$$\mathbb{E}\left[p_2\right] \leq \bar{P}_2, \tag{4.3}$$

where $\bar{P}_2$ denotes the maximum mean transmit power of the secondary user.

Since the secondary user rate C_2 is function of g_{22} and g_{21} only, we assume that to achieve a desired rate, without interference constraint, the secondary user performs a power scheduling/control scheme such that the transmit power p_2 can be expressed as:

$$p_2 = \psi^{(1)}(\hat{g}_{22},\, \hat{g}_{21}), \tag{4.4}$$

thanks to appropriate techniques to estimate g_{22} and g_{21}. $\psi^{(1)}$ is a $\{\hat{g}_{22}, \hat{g}_{21}\}$-dependent function or operator. It includes all power control schemes which depend either on $\hat{g}_{22}$ only, or on $\hat{g}_{21}$ only, or both $\hat{g}_{22}$ and $\hat{g}_{21}$, and constant power control scheme. The primary mean rate can be expressed as:

$$\mathbf{C}_1 = \mathbb{E}\left[\log\left(1 + \frac{\dfrac{\bar{P}_1\, g_{11}}{g_{12}}}{\dfrac{\sigma^2}{g_{12}} + p_2}\right)\right].$$

Thanks to the independence of g_{11}, g_{12}, g_{22} and g_{21}, it follows that

$$\mathbf{C}_1 = \mathbb{E}_{g_{11},\, g_{12}}\left[\mathbb{E}_{\{g_{22},\, g_{21}\}/\{g_{11},\, g_{12}\}}\left[\log\left(1 + \frac{\dfrac{\bar{P}_1\, g_{11}}{g_{12}}}{\dfrac{\sigma^2}{g_{12}} + p_2}\right)\right]\right],$$

where $\mathbb{E}_{a,\,b}\left[x\right]$ denotes the expectation of the random variable x over the joint distribution of the random variables a and b, while $\mathbb{E}_{a/b}\left[x\right]$ denotes the expectation of the random variable x over the conditional distribution of a given b.
Moreover, we have:

$$\mathbb{E}_{\{g_{22},\, g_{21}\}/\{g_{11},\, g_{12}\}}\left[\log\left(1 + \frac{\dfrac{\bar{P}_1\, g_{11}}{g_{12}}}{\dfrac{\sigma^2}{g_{12}} + p_2}\right)\right] \geq \log\left(1 + \frac{\dfrac{\bar{P}_1\, g_{11}}{g_{12}}}{\dfrac{\sigma^2}{g_{12}} + \mathbb{E}\left[p_2\right]}\right) \geq \log\left(1 + \frac{\bar{P}_1\, g_{11}}{\sigma^2 + \bar{P}_2\, g_{12}}\right),$$

where the first inequality is due to Jensen inequality[2]. The second inequality is due to the

[2]Because of the convexity of the x-dependent function $\log\left(1 + \dfrac{A}{B + x}\right)$ with $A \geq 0$, $B \geq 0$ and $x \geq 0$.

power constraint (4.3). Finally, we obtain:

$$\mathbf{C}_1 \geq \mathbf{C}_{1,\min}^{(1)} \triangleq \mathbb{E}\left[\log\left(1+\frac{\bar{P}_1\, g_{11}}{\sigma^2+\bar{P}_2\, g_{12}}\right)\right].$$

The mean rate $\mathbf{C}_{1,\min}^{(1)}$ is achieved for a constant power control from the secondary user: $p_2 = \bar{P}_2$. Therefore, in this unconstrained spectrum-sharing, constant power control of the secondary user, $p_2 = \bar{P}_2$, achieves the lower bound of the primary mean rate. $\mathbf{C}_{1,\min}^{(1)}$ can be expressed (appendix A) as:

$$\mathbf{C}_{1,\min}^{(1)} = \frac{\bar{P}_1}{\bar{P}_1 - \frac{\lambda_{11}}{\lambda_{12}}\bar{P}_2}\left[\exp\left(\frac{\sigma^2\,\lambda_{11}}{\bar{P}_1}\right)\mathrm{E}_1\left(\frac{\sigma^2\,\lambda_{11}}{\bar{P}_1}\right) - \exp\left(\frac{\sigma^2\,\lambda_{12}}{\bar{P}_2}\right)\mathrm{E}_1\left(\frac{\sigma^2\,\lambda_{12}}{\bar{P}_2}\right)\right], \quad (4.5)$$

where the exponential integral function is defined as, [68],

$$\mathrm{E}_1(x) \triangleq \int_1^{+\infty} \frac{\exp(-x\,t)}{t}\,dt, \quad x \geq 0. \quad (4.6)$$

4.3.2 Constrained spectrum-sharing

Now we investigate a spectrum-sharing scenario where the secondary transmission is subject to some interference constraints in order to protect the primary user. In this case, estimating the secondary-to-primary link gain, g_{12}, may be crucial. In general, depending on the type of constraint, primary protection should require different CSI to the secondary transmitter.

4.3.2.1 Primary mean-rate loss constraint

This constraint is useful when improving the primary mean rate is in concern. It consists in setting a maximum loss of the primary mean rate:

$$\mathbf{C}_{1,\max} - \mathbf{C}_1 \leq \mathbf{C}_{1,\text{loss}}, \quad (4.7)$$

where $\mathbf{C}_{1,\max} \triangleq \mathbb{E}\left[\log\left(1+\frac{\bar{P}_1\, g_{11}}{\sigma^2}\right)\right]$ is the mean rate of the primary user without interfering signal. $\mathbf{C}_{1,\text{loss}}$ denotes the maximum mean-rate loss allowed by the primary user. Maximizing the secondary mean rate, subject to (4.7), may require primary link gain estimation $\hat{g}_{11}$, [58], that might demand sophisticated techniques. In the sequel, we do not use this constraint.

4.3.2.2 Interference constraints

The primary transmission can be also protected by using the dimensions time and space of the spectrum to manage the secondary user interference to the primary receiver. More general spatial spectrum-sharing problem is considered in [39]: given two different networks (for instance two MAC), to enable coexistence, we can regulate their transmission power,

such that a network may not create an interference that exceeds a prescribed level Q_I outside of a predefined zone. For the two-user spectrum-sharing problem, peak and average interference constraints, stated by (4.8) and (4.9), are commonly used to protect the primary transmission, [57] to [37], :

$$p_2\, g_{12} \leq Q_{\text{peak}} \tag{4.8}$$

$$\mathbb{E}\left[p_2\, g_{12}\right] \leq Q_{\text{avg}}, \tag{4.9}$$

where Q_{peak} denotes the instantaneous interference threshold and Q_{avg} the average interference threshold. Specially, performing a power control under the instantaneous interference constraint (4.8) requires the secondary-to-primary link gain estimation $\hat{g}_{12}$.

4.3.2.3 Lower bound

In order to protect the primary transmission, we assume that the secondary-to-primary link gain estimation $\hat{g}_{12}$ is available for secondary power control. Therefore, to achieve a desired rate under interference constraints, the secondary user performs a power scheduling/control scheme such that the transmit power p_2 can be expressed as:

$$p_2 = \psi^{(2)}(\hat{g}_{22},\, \hat{g}_{21},\, \hat{g}_{12}), \tag{4.10}$$

thanks to appropriate techniques to estimate g_{22}, g_{21} and g_{12}. $\psi^{(2)}$ is a $\{\hat{g}_{22},\, \hat{g}_{21},\, \hat{g}_{12}\}$-dependent function or operator. It includes all power control schemes that depend either on $\hat{g}_{22}$ only, or on $\hat{g}_{21}$ only, or on $\hat{g}_{12}$ only, or any combination of $\hat{g}_{22}$, $\hat{g}_{21}$, $\hat{g}_{12}$, and constant power control scheme. The primary mean rate verifies:

$$\begin{aligned}
\mathbf{C}_1 &= \mathbb{E}_{g_{11}}\left[\mathbb{E}_{\{g_{22},\, g_{21},\, g_{12}\}/g_{11}}\left[\log\left(1+\frac{\bar{P}_1\, g_{11}}{\sigma^2 + p_2\, g_{12}}\right)\right]\right] \\
&\geq \mathbb{E}_{g_{11}}\left[\log\left(1+\frac{\bar{P}_1\, g_{11}}{\sigma^2 + \mathbb{E}\left[p_2\, g_{12}\right]}\right)\right] \\
&\geq \mathbf{C}^{(2)}_{1,\min} \triangleq \mathbb{E}\left[\log\left(1+\frac{\bar{P}_1\, g_{11}}{\sigma^2 + Q_{\text{avg}}}\right)\right],
\end{aligned}$$

where the first inequality is due to Jensen. The second inequality is due to the mean interference power constraint (4.9). The lower bound $\mathbf{C}^{(2)}_{1,\min}$ can be expressed (appendix A) as[3]:

$$\mathbf{C}^{(2)}_{1,\min} = \exp\left(\frac{\lambda_{11}\left(\sigma^2 + Q_{\text{avg}}\right)}{\bar{P}_1}\right) \mathrm{E}_1\left(\frac{\lambda_{11}\left(\sigma^2 + Q_{\text{avg}}\right)}{\bar{P}_1}\right). \tag{4.11}$$

[3]This case includes obviously the unconstrained spectrum-sharing case, consequently $\mathbf{C}^{(1)}_{1,\min} \geq \mathbf{C}^{(2)}_{1,\min}$.

4.4 Power control for spectrum secondary use

In this section, we investigate secondary user power control and compare the achievable primary mean rate to its lower bounds found previously.

4.4.1 Power control with mean-transmit-power constraint only

We assume that there is only one constraint for secondary access to the spectrum: the mean transmit power constraint, stated by 4.3.

4.4.1.1 Optimal power control

The optimal power control maximizing the secondary mean rate $\mathbf{C}_2$, under the power constraint (4.3), is expressed by the well known *water filling* [67]:

$$p_2 = \left(\zeta - \frac{\sigma^2 + \bar{P}_1\, g_{21}}{g_{22}}\right)^+, \tag{4.12}$$

where the constant ζ is obtained such that the mean power constraint is met. $(.)^+$ denotes $\max(.,0)$. Let $w \triangleq \dfrac{g_{22}}{\sigma^2 + \bar{P}_1\, g_{21}}$, the constant ζ is obtained as:

$$\bar{P}_2 = \int_{\frac{1}{\zeta}}^{+\infty} \left(\zeta - \frac{1}{w}\right) f_W(w)\, dw, \tag{4.13}$$

where f_W is the probability density function of the random variable W with sample w. The probability density function of W is given by (appendix A):

$$f_W(w) = \begin{cases} \dfrac{1 + b + \dfrac{b}{a}w}{a\left(1 + \dfrac{1}{a}w\right)^2} \exp\left(-\dfrac{b}{a}w\right) & \text{if} \quad w \geq 0 \\ 0 & \text{if} \quad w < 0 \end{cases} \tag{4.14}$$

with $a = \dfrac{\lambda_{21}}{\bar{P}_1\, \lambda_{22}}$ and $b = \dfrac{\sigma^2\, \lambda_{21}}{\bar{P}_1}$.

4.4.1.2 A scheduling approximating the optimal power control

The difficulty of performing the optimal power allocation (4.12) is due to the uncertain knowledge of the information $w = \frac{g_{22}}{\sigma^2 + \bar{P}_1\, g_{21}}$. Using an adequate estimation technique, assume $\hat{w}$ is the estimated value of w. We can reduce the impact of estimation errors on

the power control (4.12) by using the following scheduling:

$$p_2 = \begin{cases} c & \text{if} \quad \hat{w} > \dfrac{1}{\zeta} \\ 0 & \text{if} \quad \hat{w} \leq \dfrac{1}{\zeta} \end{cases} \tag{4.15}$$

where the constant c is obtained such that

$$\mathbb{E}\left[p_2\right] = \bar{P}_2 = \int_{\frac{1}{\zeta}}^{+\infty} c\, f_W(w)\, dw,$$

thus, it can be expressed as:

$$c = \frac{\bar{P}_2}{\int_{\frac{1}{\zeta}}^{+\infty} f_W(w)\, dw}.$$

Using expression (4.14) of f_W, we obtain:

$$\int_{\frac{1}{\zeta}}^{+\infty} f_W(w)\, dw = \frac{\frac{\lambda_{21}}{\lambda_{22}}\bar{P}_1}{\frac{\lambda_{21}}{\lambda_{22}}\bar{P}_1 + \frac{1}{\zeta}} \exp\left(-\frac{\lambda_{22}\,\sigma^2}{\zeta}\right). \tag{4.16}$$

Therefore, constant c is expressed as:

$$c = \bar{P}_2 \left(1 + \frac{\lambda_{22}}{\lambda_{21}}\frac{1}{\zeta}\bar{P}_1\right) \exp\left(\frac{\lambda_{22}\,\sigma^2}{\zeta}\right). \tag{4.17}$$

In the scheduling (4.15), constant c does not depend on the channel realizations. Moreover, the *binary condition* $\hat{w} \lessgtr \frac{1}{\zeta}$ is less sensitive to the estimation errors. This relatively easy-done scheduling, for the secondary link, should achieve a primary mean rate close to the one achieved using the optimal *water-filling*.

4.4.1.3 Numerical examples

Both the theoretical optimal allocation (4.12) and the scheduling (4.15) are functions of the channels gains $\hat{g}_{22}$ and $\hat{g}_{12}$. So they have the form of (4.4). $\mathbf{C}^{(1)}_{1,\min}$ is a lower bound of such kinds of power control/scheduling. Now, we give numerical examples to compare the primary mean rates achieved, using (4.12) and (4.15), with the lower bound $\mathbf{C}^{(1)}_{1,\min}$. With the settings $\bar{P}_1 = 1$, $\sigma^2 = 0.01$ and $\lambda_{11} = \lambda_{12} = \lambda_{22} = \lambda_{21} = 1$, we obtain Fig. 4.1 and 4.2.

As it can be noticed in Fig. 4.1 and 4.2, the proposed scheduling (4.15) provides a performance that is very close to the optimal *water-filling*. Moreover, we can see the gap level between the lower bound $\mathbf{C}^{(1)}_{1,\min}$ and the considered power controls. The optimal power control at the secondary side does not cause the most harmful interference to the primary transmission, as we should imagine. On the contrary, for same mean power,

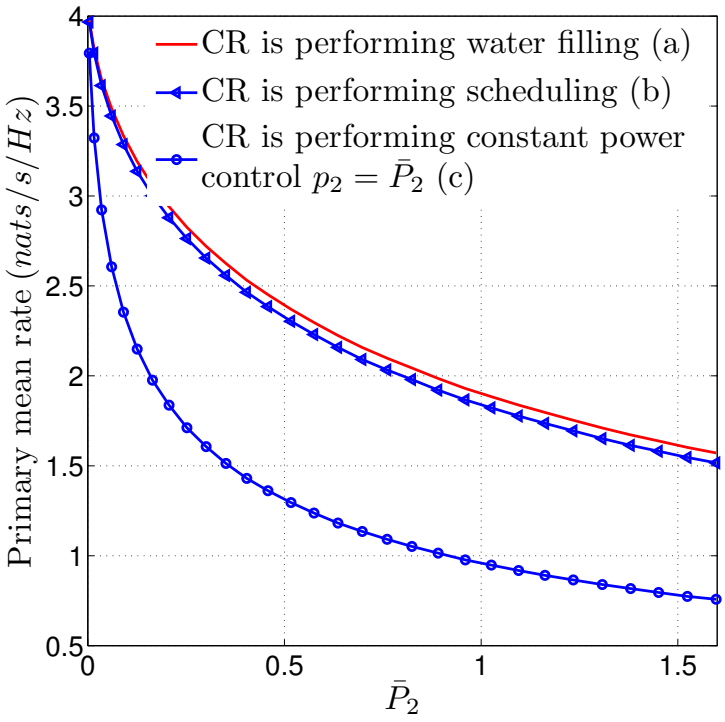

Figure 4.1: Primary mean rate versus secondary mean power for different power control schemes from the secondary user: (a) optimal power control *water-filling*; (b) proposed scheduling approximating the optimal power control; (c) constant power control that provides the lower bound of the primary mean rate. $\bar{P}_1 = 1$, $\sigma^2 = 0.01$ and $\lambda_{11} = \lambda_{12} = \lambda_{22} = \lambda_{21} = 1$.

$\bar{P}_1 = \bar{P}_2 = 1$ for instance, the optimal *water-filling* provides nearly 1 nat/s/Hz protection, to the primary user, more than the constant power control (Cf. Fig. 4.1). These results do not take into account the primary protection since there is no interference constraint.

4.4.2 Power control with outage performance requirement and direct links CSI

In this part, we propose a novel power control under the requirements (4.1) and (4.2). We assume that the secondary user can estimate the secondary-to-secondary and the secondary-to-primary links gains only. That is, only $\hat{g}_{22}$ and $\hat{g}_{12}$ are available for the secondary user power control.

4.4.2.1 Outage performance constraints

The primary and secondary outage constraints are modeled by (4.1) and (4.2). By replacing C_1 and C_2 by theirs formulas, events "$C_1 \leq C_0$" and "$C_2 \leq C_0'$" can be expressed,

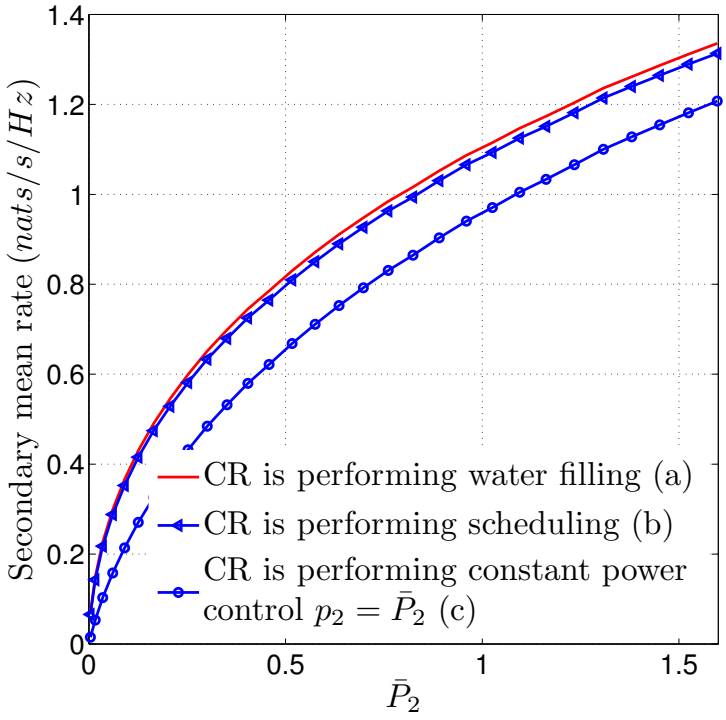

Figure 4.2: Secondary mean rate versus mean power for different power control schemes: (a) optimal power control *water-filling*; (b) proposed scheduling approximating the optimal power control; (c) constant power control that provides the lower bound of the primary mean rate. $\bar{P}_1 = 1$, $\sigma^2 = 0.01$ and $\lambda_{11} = \lambda_{12} = \lambda_{22} = \lambda_{21} = 1$.

respectively, as:

$$\mathrm{C}_1 \leq \mathrm{C}_0 \quad \Rightarrow \quad g_{11} \leq \frac{\alpha_0 \, \left(\sigma^2 + p_2 \, \hat{g}_{12}\right)}{\bar{P}_1}, \tag{4.18}$$

$$\mathrm{C}_2 \leq \mathrm{C}'_0 \quad \Rightarrow \quad g_{21} \geq \frac{1}{\bar{P}_1} \left(\frac{p_2 \, \hat{g}_{22}}{\alpha'_0} - \sigma^2 \right), \tag{4.19}$$

with $\alpha_0 = \exp\left(\mathrm{C}_0\right) - 1$ and $\alpha'_0 = \exp\left(\mathrm{C}'_0\right) - 1$. The outage probabilities become:

$$\begin{aligned} \mathbf{Prob}_{g_{11},\, g_{21}} \left(\mathrm{C}_1 \leq \mathrm{C}_0\right) &= \int_0^{\gamma} \lambda_{11} \, \exp\left(-\lambda_{11} \, x\right) \, dx \\ &= 1 - \exp\left(-\lambda_{11} \, \gamma\right), \end{aligned} \tag{4.20}$$

where $\gamma = \frac{\alpha_0 \left(\sigma^2 + p_2\, \hat{g}_{12}\right)}{\bar{P}_1}$, and

$$\begin{aligned} \mathbf{Prob}_{g_{11},\, g_{21}} \left(\mathrm{C}_2 \leq \mathrm{C}_0'\right) &= \int_{\gamma'}^{+\infty} \lambda_{21}\, \exp\left(-\lambda_{21}\, x\right)\, dx \\ &= \exp\left(-\lambda_{21}\, \gamma'\right), \end{aligned} \tag{4.21}$$

with $\gamma' = \frac{1}{\bar{P}_1}\left(\frac{p_2\, \hat{g}_{22}}{\alpha_0'} - \sigma^2\right)$. Then, outage constraints (4.1) and (4.2) can be expressed, respectively, as:

$$1 - \exp\left(-\lambda_{11}\, \frac{\alpha_0\, \left(\sigma^2 + p_2\, \hat{g}_{12}\right)}{\bar{P}_1}\right) \leq \epsilon, \tag{4.22}$$

$$\exp\left(-\frac{\lambda_{21}}{\bar{P}_1}\left(\frac{p_2\, \hat{g}_{22}}{\alpha_0'} - \sigma^2\right)\right) \leq \epsilon'. \tag{4.23}$$

After some manipulations, expressions (4.22) and (4.23) become

$$p_2\, \hat{g}_{12} \leq Q_{\text{peak}}, \tag{4.24}$$

$$p_2\, \hat{g}_{22} \geq K. \tag{4.25}$$

Where the peak interference threshold is defined as:

$$Q_{\text{peak}} = \frac{\bar{P}_1}{\lambda_{11}\, \alpha_0} \log\left(\frac{1}{1-\epsilon}\right) - \sigma^2, \tag{4.26}$$

and the minimum received power K as:

$$K = \alpha_0' \left(\sigma^2 - \frac{\bar{P}_1}{\lambda_{21}} \log\left(\epsilon'\right)\right). \tag{4.27}$$

Therefore, the primary outage constraint (4.1) consists in forcing the instantaneous interference $p_2\, \hat{g}_{12}$, from the secondary user, to be lower than a threshold Q_{peak}, while secondary outage constraint (4.2) consists in forcing the secondary instantaneous received power $p_2 \hat{g}_{22}$ to be greater than a threshold K. For a given network and system, the peak interference threshold Q_{peak} is determined by the primary minimum required rate C_0, the outage probability ϵ and the mean transmit power $\bar{P}_1$. Specially, Q_{peak} is proportional to $\bar{P}_1$ and log-increasing in ϵ. Otherwise, when the outage probability ϵ' increases, the secondary service quality is low, and thus, the threshold K decreases.

4.4.2.2 Power control

Previously, we found the constraints (4.24) and (4.25) to ensure given outage performance to both the primary and the secondary users. In this respect, transmit power p_2 of the

secondary user must fulfill the set of inequalities

$$\begin{cases} p_2\,\hat{g}_{12} & \leq & Q_{\text{peak}} \\ p_2\,\hat{g}_{22} & \geq & K \end{cases} \tag{4.28}$$

We verify the compatibility of both the equations in (4.28):

- if $\left(\frac{\hat{g}_{22}}{\hat{g}_{12}} \geq \frac{K}{Q_{\text{peak}}}\right)$, then[4] power p_2 can be greater than the minimum required $\mathrm{p}_{2,\min} \triangleq \frac{K}{\hat{g}_{22}}$. But to meet the interference constraint, power p_2 must always fulfill $p_2\,\hat{g}_{12} \leq Q_{\text{peak}}$. So, the cognitive user can opportunistically communicate with $p_2 = \frac{Q_{\text{peak}}}{\hat{g}_{12}}$;
- if $\left(\frac{\hat{g}_{22}}{\hat{g}_{12}} < \frac{K}{Q_{\text{peak}}}\right)$, then the minimum power $\mathrm{p}_{2,\min}$ can not meet the interference constraint. Consequently, we set $p_2 = 0$ (CR transmission is off).

However, the maximum transmit power $\frac{Q_{\text{peak}}}{\hat{g}_{12}}$ can be infinitely high (when $\hat{g}_{12}$ is very low), while in real system instantaneous transmit power is limited. To alleviate this problem, we set the practical constraint $p_2 \leq p_{2,\text{peak}}$. Finally, we propose the following original power control policy:

$$p_2 = \begin{cases} p_{2,\text{peak}} & \text{if} \quad \dfrac{\hat{g}_{22}}{\hat{g}_{12}} \geq \dfrac{K}{Q_{\text{peak}}} \quad \text{and} \quad p_{2,\text{peak}} \leq \dfrac{Q_{\text{peak}}}{\hat{g}_{12}} \\ \dfrac{Q_{\text{peak}}}{\hat{g}_{12}} & \text{if} \quad \dfrac{\hat{g}_{22}}{\hat{g}_{12}} \geq \dfrac{K}{Q_{\text{peak}}} \quad \text{and} \quad p_{2,\text{peak}} > \dfrac{Q_{\text{peak}}}{\hat{g}_{12}} \\ 0 & \text{if} \quad \dfrac{\hat{g}_{22}}{\hat{g}_{12}} < \dfrac{K}{Q_{\text{peak}}} \end{cases} \tag{4.29}$$

Where $p_{2,\text{peak}}$ is the secondary-user maximum transmit power. Contrary to the optimal power control, derived in [57] and [58], and the non-cooperative games in [56], the goal of the allocation strategy (4.29) is neither to achieve, in any case, maximum possible rate, nor to maximize *selfish* utilities. But the particularity of (4.29) is to ensure, at some occurrence predefined by the outage probabilities ϵ and ϵ', at least given minimum instantaneous rates to the two users, while using only the direct links gains estimations $\hat{g}_{22}$ and $\hat{g}_{12}$ (that is not considered in the previous works such as [57], [58] and [56]). It is then more appropriate for spectrum-sharing systems that carry out real-time delay-sensitive applications, e.g. voice and video.

Now, we will study some typical parameters of this power control.

4.4.2.3 Mean transmit and mean interference power

In this part, we study the evolution of the mean transmit power and the mean received interference power, according to the parameters K, $p_{2,\text{peak}}$ and Q_{peak}, which are imposed by the desired performance of the network, and according to the parameters λ_{11}, λ_{22}, λ_{12} and λ_{21}, which are imposed by the channel fades.

[4] When $p_2 = \mathrm{p}_{2,\min} \triangleq \frac{K}{\hat{g}_{22}}$, then $p_2\,\hat{g}_{12} \leq Q_{\text{peak}} \Leftrightarrow \frac{\hat{g}_{22}}{\hat{g}_{12}} \geq \frac{K}{Q_{\text{peak}}}$

Let $x = \hat{g}_{12}$ and $y = \hat{g}_{22}$. The mean transmit power can be expressed as:

$$\begin{aligned}\mathbb{E}[p_2] &= \int_0^{\frac{Q_{\text{peak}}}{p_{2,\text{peak}}}} \int_{\frac{K}{Q_{\text{peak}}}\,x}^{+\infty} \lambda_{22}\,\lambda_{12}\,p_{2,\text{peak}}\,\exp(-\lambda_{22}\,y)\,\exp(-\lambda_{12}\,x)\,dx\,dy \\ &+ \int_{\frac{Q_{\text{peak}}}{p_{2,\text{peak}}}}^{+\infty} \int_{\frac{K}{Q_{\text{peak}}}\,x}^{+\infty} \lambda_{22}\,\lambda_{12}\,\frac{Q_{\text{peak}}}{x}\,\exp(-\lambda_{22}\,y)\,\exp(-\lambda_{12}\,x)\,dx\,dy.\end{aligned}$$

After some manipulations (Cf. appendix B), we obtain:

$$\mathbb{E}[p_2] = \frac{p_{2,\text{peak}}}{1+\frac{\lambda_{22}}{\lambda_{12}}\frac{K}{Q_{\text{peak}}}}\left[1-\exp\left(-\frac{\lambda_{22}\,K+\lambda_{12}\,Q_{\text{peak}}}{p_{2,\text{peak}}}\right)\right] + \lambda_{12}\,Q_{\text{peak}}\,\mathrm{E}_1\left(\frac{\lambda_{22}\,K+\lambda_{12}\,Q_{\text{peak}}}{p_{2,\text{peak}}}\right) \quad (4.30)$$

The mean received interference power is obtained similarly as follows:

$$\begin{aligned}\mathbb{E}[p_2\,\hat{g}_{12}] &= \int_0^{\frac{Q_{\text{peak}}}{p_{2,\text{peak}}}} \int_{\frac{K}{Q_{\text{peak}}}\,x}^{+\infty} \lambda_{22}\,\lambda_{12}\,x\,p_{2,\text{peak}}\,\exp(-\lambda_{22}\,y)\,\exp(-\lambda_{12}\,x)\,dx\,dy \\ &+ \int_{\frac{Q_{\text{peak}}}{p_{2,\text{peak}}}}^{+\infty} \int_{\frac{K}{Q_{\text{peak}}}\,x}^{+\infty} \lambda_{22}\,\lambda_{12}\,Q_{\text{peak}}\,\exp(-\lambda_{22}\,y)\,\exp(-\lambda_{12}\,x)\,dx\,dy. \quad (4.31)\end{aligned}$$

After some manipulations (Cf. appendix B), it can be expressed as:

$$\mathbb{E}[p_2\,\hat{g}_{12}] = \frac{p_{2,\text{peak}}/\lambda_{12}}{\left(1+\frac{\lambda_{22}}{\lambda_{12}}\,\frac{K}{Q_{\text{peak}}}\right)^2}\left[1-\exp\left(-\frac{\lambda_{22}\,K+\lambda_{12}\,Q_{\text{peak}}}{p_{2,\text{peak}}}\right)\right]. \quad (4.32)$$

Therefore, the mean transmit power $\mathbb{E}[p_2]$ and the mean interference power $\mathbb{E}[p_2\,\hat{g}_{12}]$ are connected via the following equation:

$$\mathbb{E}[p_2] = \lambda_{12}\,Q_{\text{peak}}\left[\left(1+\frac{\lambda_{22}}{\lambda_{12}}\,\frac{K}{Q_{\text{peak}}}\right)\frac{\mathbb{E}[p_2\,\hat{g}_{12}]}{Q_{\text{peak}}} + \mathrm{E}_1\left(\frac{\lambda_{22}\,K+\lambda_{12}\,Q_{\text{peak}}}{p_{2,\text{peak}}}\right)\right]. \quad (4.33)$$

In practical situations, we assume $\lambda_{12} \geq 1$. Therefore, from (4.33), the mean transmit power is greater than the mean interference power, especially when $\mathrm{E}_1\left(\frac{\lambda_{22}\,K+\lambda_{12}\,Q_{\text{peak}}}{p_{2,\text{peak}}}\right)$ is high or equivalently when $\frac{\lambda_{22}\,K+\lambda_{12}\,Q_{\text{peak}}}{p_{2,\text{peak}}}$ is low. As we can see below with numerical examples, this situation is profitable because the challenge in spectrum-sharing and cognitive networks is to achieve better services to the secondary user while minimizing the interference towards the licensee-primary user.

4.4.2.4 Overall outage probability

Previously, the strategy for the power control (4.29) is stated by firstly setting $\mathbf{Prob}_{g_{11},\,g_{21}}(\mathrm{C}_2 \leq \mathrm{C}_0') = \epsilon'$ or equivalently $p_2 = \mathrm{p}_{2,\min}$. Then, to transmit if $\mathbf{Prob}_{g_{11},\,g_{21}}(\mathrm{C}_1 \leq \mathrm{C}_0) \leq \epsilon$. The overall

outage probability of (4.29) can be expressed as:

$$\mathrm{P}_{\text{out}} = \mathbf{Prob}\left(\mathbf{Prob}_{g_{11},\,g_{21}}\left(\mathrm{C}_1 \leq \mathrm{C}_0\right) > \epsilon \,/\, \mathbf{Prob}_{g_{11},\,g_{21}}\left(\mathrm{C}_2 \leq \mathrm{C}_0'\right) = \epsilon'\right). \tag{4.34}$$

Let $x = \hat{g}_{12}$, $y = \hat{g}_{22}$, $z = y/x$ and $z_0 = K/Q_{\text{peak}}$. From (4.29), the outage probability P_{out} is obtained as follows:

$$\mathrm{P}_{\text{out}} \;=\; \mathbf{Prob}\left(z \,<\, z_0\right) = \int_0^{z_0} f_Z(z)\, dz,$$

where f_Z is the probability density function of the ratio $\hat{g}_{22}/\hat{g}_{12}$. The ratio of two independent exponential random variables $\hat{g}_{22}$ and $\hat{g}_{12}$, with parameters λ_{22} and λ_{12}, is a random variable Z with the following probability density function:

$$\begin{aligned} f_Z(z) &= \int_0^{+\infty} x\, f_Y(z\,x)\, f_X(x)\, dx \\ &= \lambda_{22}\,\lambda_{12} \int_0^{+\infty} x\, \exp\left(-\left(\lambda_{22}\, z + \lambda_{12}\right)\, x\right)\, dx \\ &= \frac{\left(\lambda_{12}/\lambda_{22}\right)}{\left(z + \dfrac{\lambda_{12}}{\lambda_{22}}\right)^2} \end{aligned} \tag{4.35}$$

The outage probability is then expressed as:

$$\mathrm{P}_{\text{out}} \;=\; \int_0^{z_0} \frac{\left(\lambda_{12}/\lambda_{22}\right)}{\left(z + \dfrac{\lambda_{12}}{\lambda_{22}}\right)^2} dz = 1 - \frac{\left(\lambda_{12}/\lambda_{22}\right)}{\dfrac{\lambda_{12}}{\lambda_{22}} + z_0}.$$

Finally, we obtain:

$$\mathrm{P}_{\text{out}} = \frac{K}{K + \frac{\lambda_{12}}{\lambda_{22}} Q_{\text{peak}}}. \tag{4.36}$$

The outage occurrence depends on the thresholds K and Q_{peak} that model the quality requirements of the services for the two users. The cut-off value z_0 of the ratio $\hat{g}_{22}/\hat{g}_{12}$ is function of the outage probability and of the channel parameters λ_{22} and λ_{12}: $z_0 = \dfrac{\lambda_{12}}{\lambda_{22}} \dfrac{\mathrm{P}_{\text{out}}}{1 - \mathrm{P}_{\text{out}}}$.

4.4.2.5 Connection with TIFR transmission policy

Now, we investigate a special case where the primary-to-secondary link is sufficiently attenuated to neglect the primary interference $\bar{P}_1\, g_{21}$ to the secondary user. Such a situation occurs for instance when the secondary receiver is located outside an *exclusive region* around the primary transmitter, [46], [48]. In this case, we can define a delay-limited capacity (also referred to as zero-outage capacity) which represents the constant-rate that is achievable in all fading states [57]. Assuming the secondary user transmits with the

minimum required power $\mathrm{p}_{2,\min}$ in non-outage states, to fulfill the set of constraints (4.28) we propose:

$$p_2 = \begin{cases} \dfrac{K}{\hat{g}_{22}} & \text{if} \quad z \geq z_0 \\ 0 & \text{if} \quad z < z_0. \end{cases} \tag{4.37}$$

The adaptive transmission technique (4.37) is called *truncated channel inversion with fixed rate* (TIFR), [57], [53]. Since the secondary user transmits $\mathrm{p}_{2,\min}$ in non-outage events, then, power transmission policy (4.37) is a variant of (4.29) in which primary user receives always the weakest instantaneous interference. This case is interesting because it protects, the best, primary user. We derive the mean transmit power of (4.37) as follows:

$$\begin{aligned} \mathbb{E}\left[p_2\right] &= \int_0^{+\infty} \int_0^{\frac{y}{z_0}} \lambda_{12}\, \lambda_{22}\, \frac{K}{y} \exp\left(-\lambda_{12}\, x\right) \exp\left(-\lambda_{22}\, y\right)\, dx\, dy \\ &= \int_0^{+\infty} \lambda_{22}\, \frac{K}{y} \exp\left(-\lambda_{22}\, y\right) \left(\int_0^{\frac{y}{z_0}} \lambda_{12}\, \exp\left(-\lambda_{12}\, x\right)\, dx \right) dy. \end{aligned} \tag{4.38}$$

Since

$$\int_0^{\frac{y}{z_0}} \lambda_{12}\, \exp\left(-\lambda_{12}\, x\right)\, dx = 1 - \exp\left(-\lambda_{12}\, \frac{y}{z_0}\right),$$

we have

$$\mathbb{E}\left[p_2\right] = \int_0^{+\infty} \lambda_{22}\, \frac{K}{y} \exp\left(-\lambda_{22}\, y\right)\, dy - \int_0^{+\infty} \lambda_{22}\, \frac{K}{y} \exp\left(-\left(\lambda_{22} + \frac{\lambda_{12}}{z_0}\right) y\right) dy \tag{4.39}$$

The first integral can be calculated as:

$$\int_0^{+\infty} \lambda_{22}\, \frac{K}{y} \exp\left(-\lambda_{22}\, y\right)\, dy = \lambda_{22}\, K \left[\lim_{y \longrightarrow 0} \mathrm{E}_1\left(\lambda_{22}\, y\right) - \lim_{y \longrightarrow +\infty} \mathrm{E}_1\left(\lambda_{22}\, y\right) \right] \tag{4.40}$$

The exponential integral function verifies, [68]:

$$\lim_{y \longrightarrow +\infty} \mathrm{E}_1\left(\lambda_{22}\, y\right) = 0.$$

So, we obtain the following expression for the first integral in (4.39):

$$\int_0^{+\infty} \lambda_{22}\, \frac{K}{y} \exp\left(-\lambda_{22}\, y\right)\, dy = \lambda_{22}\, K \lim_{y \longrightarrow 0} \mathrm{E}_1\left(\lambda_{22}\, y\right).$$

The second integral has the same form as the first one. Then,

$$\mathbb{E}\left[p_2\right] = \lim_{y \longrightarrow 0} \left[\mathrm{E}_1\left(\lambda_{22}\, y\right) - \mathrm{E}_1\left(y \left(\lambda_{22} + \frac{\lambda_{12}}{z_0} \right) \right) \right] \lambda_{22}\, K.$$

The exponential integral function $\mathrm{E}_1(.)$ can be approximated around zero, [68], as

$$\mathrm{E}_1(y) \approx -\gamma - \log(y), \tag{4.41}$$

where γ is the Euler-Mascheroni constant: $\gamma = 0.57721....$ Using this closed-form approximation, we obtain a closed-form expression of $\mathbb{E}[p_2]$ as follows:

$$\mathbb{E}[p_2] \approx \lambda_{22} K \log\left(1 + \frac{\lambda_{12}}{\lambda_{22}} \frac{1}{z_0}\right). \tag{4.42}$$

Therefore, for given mean transmit power $\mathbb{E}[p_2]$, we can determine the constant received power K as follows:

$$K = \frac{\mathbb{E}[p_2]}{\lambda_{22} \log\left(1 + \frac{\lambda_{12}}{\lambda_{22}} \frac{1}{z_0}\right)}. \tag{4.43}$$

The mean interference power for (4.37) is derived as:

$$\begin{aligned}
\mathbb{E}[p_2\, \hat{g}_{12}] &= \int_{z_0}^{+\infty} \frac{K}{z} f_z(z)\, dz \\
&= \int_{z_0}^{+\infty} \frac{K}{z} \frac{(\lambda_{12}/\lambda_{22})}{\left(z + \frac{\lambda_{12}}{\lambda_{22}}\right)^2} dz \\
&= K \left[\frac{\lambda_{22}}{\lambda_{12}} \log\left(1 + \frac{\lambda_{12}}{\lambda_{22}} \frac{1}{z_0}\right) - \frac{1}{z_0 + \frac{\lambda_{12}}{\lambda_{22}}}\right].
\end{aligned} \tag{4.44}$$

We can express $\mathbb{E}[p_2\, \hat{g}_{12}]$ in terms of P_{out} as:

$$\mathbb{E}[p_2\, \hat{g}_{12}] = \frac{\lambda_{22}}{\lambda_{12}} \left(\mathrm{P}_{\text{out}} - 1 - \log\left(\mathrm{P}_{\text{out}}\right)\right) K. \tag{4.45}$$

The zero-outage capacity $\mathbf{C}_{2,\text{out}}$ is expressed as:

$$\mathbf{C}_{2,\text{out}} = (1 - \mathrm{P}_{\text{out}}) \log\left(1 + \frac{K}{\sigma^2}\right). \tag{4.46}$$

This capacity is obviously increasing with the mean interference power and the increasing speed is function of P_{out}.

4.4.2.6 Numerical examples

Now we give some numerical examples in order to evaluate some achievable performances of (4.29). We set $\bar{P}_1 = 1$ and $\sigma^2 = 0.01$. The channel is set as: $\lambda_{11} = \lambda_{22} = 1$, $\lambda_{21} = 5$ (in the part 4.4.2.6, we will neglect the primary-to-secondary link, so λ_{21} is not used there) and $\lambda_{12} = 10$. That is, we choose to attenuate the secondary-to-primary link in order to avoid very strong interference. Some authors, e.g. [46], [48], [52], advocate to set an *exclusive region* around the primary receiver. No secondary operation is possible inside this range. So we can consider that the choice of $\lambda_{12} = 10$ (the value of the channel gain $\hat{g}_{12}$ is then $\frac{1}{\lambda_{12}} = 0.1$) is due to the fact that the secondary transmitter is located outside the primary *exclusive region*.

Mean rates In Fig. 4.3 and 4.4, we plot respectively the primary mean rate and the secondary mean rate, versus the peak interference threshold Q_{peak} for different values of the outage probability P_{out}. We set $p_{2,\text{peak}} = 1$. As the peak interference threshold increases, the secondary mean rate increases too, and consequently the primary mean rate decreases. For higher Q_{peak}, the cut-off value z_0 is weak and $p_{2,\text{peak}}$ is more likely to be lower than $\frac{Q_{\text{peak}}}{g_{12}}$. Consequently, $p_2 = p_{2,\text{peak}}$ in most of the channel fades. Therefore, primary mean rate is tending to $\mathbb{E}\left[\log\left(1 + \frac{\bar{P}_1 g_{11}}{\sigma^2 + p_{2,\text{peak}}\, g_{12}}\right)\right]$ and secondary mean rate is tending to $\mathbb{E}\left[\log\left(1 + \frac{p_{2,\text{peak}}\, g_{22}}{\sigma^2 + \bar{P}_1\, g_{21}}\right)\right]$. For given Q_{peak}, secondary mean rate $\mathbf{C}_2$ decreases with P_{out} while primary mean rate $\mathbf{C}_1$ increases.
In Fig. 4.5, we compare the primary mean rate $\mathbf{C}_1$ with the lower bound $\mathbf{C}_{1,\min}^{(2)}$. For given P_{out}, when Q_{avg} increases, Q_{peak} increases to[5]. Therefore, we have high occurrence of events $p_{2,\text{peak}} \leq \frac{Q_{\text{peak}}}{g_{12}}$ and $p_2 = p_{2,\text{peak}}$. As a consequence, primary mean rate is more and more greater than the lower bound $\mathbf{C}_{1,\min}^{(2)}$.

Mean transmit and interference powers In Fig. 4.6, we compare the mean transmit power $\mathbb{E}[p_2]$ and the mean interference power $\mathbb{E}[p_2\, \hat{g}_{12}]$ in order to evaluate the ratio between the achievable service for the secondary user and the protection level of the primary user. The mean transmit power $\mathbb{E}[p_2]$ is very high (ratio>9) compared to the mean received interference power $\mathbb{E}[p_2\, \hat{g}_{12}]$. Moreover, $\mathbb{E}[p_2]$ increases more speedily than $\mathbb{E}[p_2\, \hat{g}_{12}]$. Then, we note that the secondary user can achieve important information without causing important interference to the primary user.

Outage probability In Fig. 4.7, we plot the outage probability, P_{out}, versus the peak interference power Q_{peak} for different values of the minimum received power K. As predicted, when the primary user is less demanding (Q_{peak} is increasing), the outage probability is

[5] From (4.32), it follows that $Q_{\text{peak}} = -\frac{p_{2,\text{peak}}}{\lambda_{22}\, z_0 + \lambda_{12}} \log\left(1 - \frac{\mathbb{E}[p_2\, \hat{g}_{12}]\left(1 + \frac{\lambda_{22}}{\lambda_{12}}\, z_0\right)^2}{p_{2,\text{peak}}/\lambda_{12}}\right)$. In realistic situations, we have $Q_{\text{peak}} \geq \mathbb{E}[p_2\, \hat{g}_{12}]$ and $\mathbb{E}[p_2\, \hat{g}_{12}] \leq \frac{p_{2,\text{peak}}/\lambda_{12}}{\left(1 + \frac{\lambda_{22}}{\lambda_{12}}\, z_0\right)^2}$.

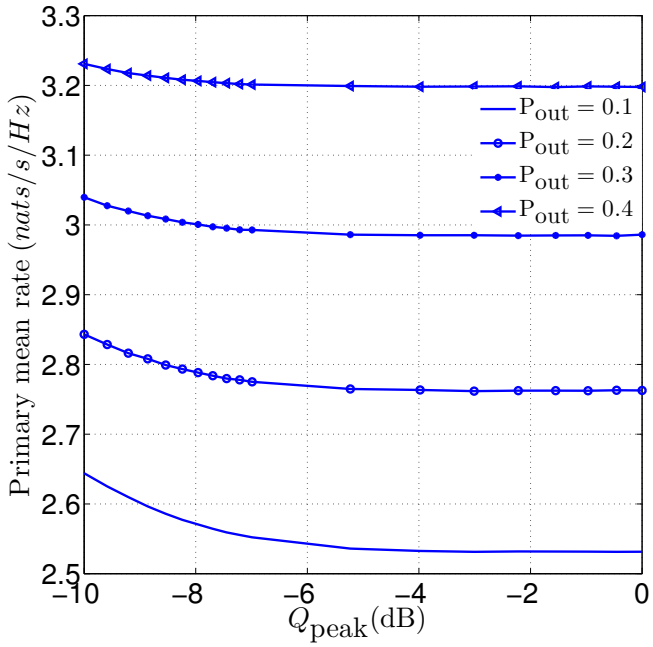

Figure 4.3: Primary mean rate, $\mathbf{C}_1$, versus peak interference power Q_{peak} for different values of outage probability P_{out}.

decreasing. Otherwise, for given Q_{peak}, the more the secondary user is less demanding (K is decreasing), the more it can transmit frequently over the common spectrum (P_{out} is decreasing). In particular, we note that for greater values of Q_{peak}, the outage probability is less sensitive to the variations of K, therefore the secondary service quality requirement is less impacting on the outage occurrence.

TIFR transmission policy In Fig. 4.8, we plot the evolution of the primary mean rate $\mathbf{C}_1$ and the secondary zero-outage capacity $\mathbf{C}_{2,\text{out}}$ versus $\mathbb{E}\left[p_2\,\hat{g}_{12}\right]$ for $\mathrm{P}_{\text{out}} = 0.1$. Because secondary user transmits with the minimum required power $\mathrm{p}_{2,\min}$ in non-outage states, primary mean rate $\mathbf{C}_1$ decreases slowly with the mean interference power $\mathbb{E}\left[p_2\,\hat{g}_{12}\right]$, while $\mathbf{C}_{2,\text{out}}$ increases speedily because the primary interference is neglected. Moreover, Fig. 4.9 shows that little mean power is required to achieve $\mathbf{C}_{2,\text{out}}$.

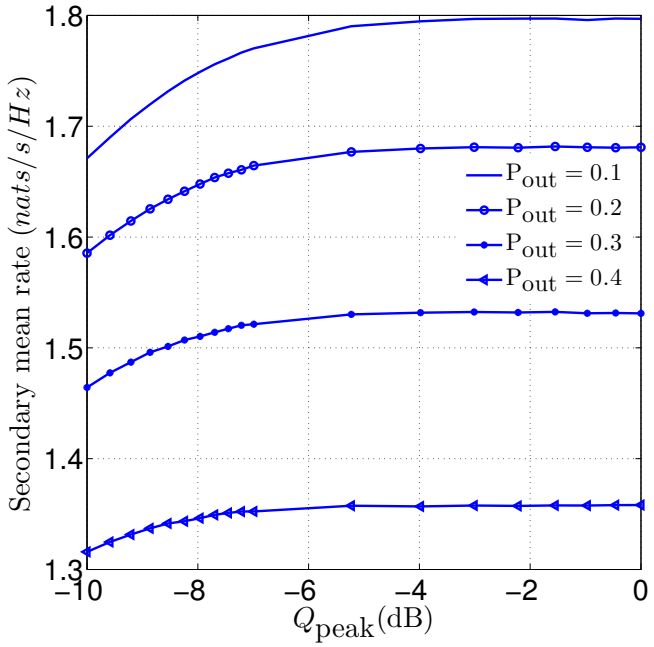

Figure 4.4: Secondary mean rate, $\mathbf{C}_2$, versus peak interference power Q_{peak} for different values of outage probability P_{out}.

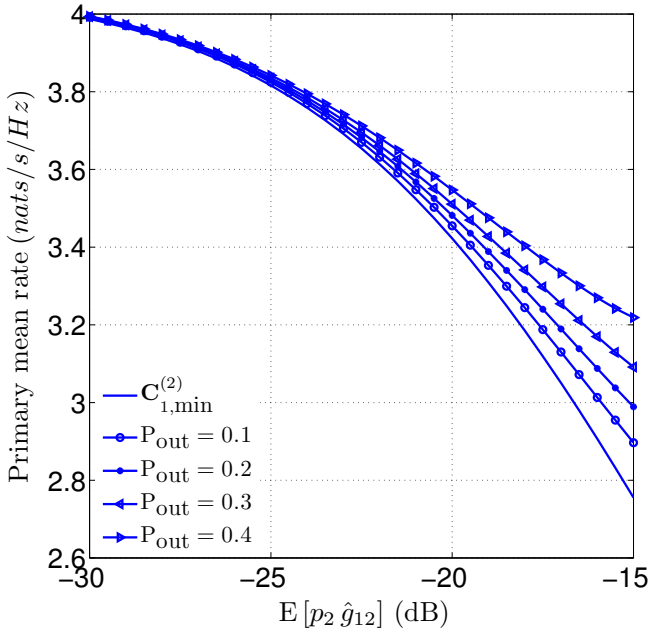

Figure 4.5: Primary mean rate $\mathbf{C}_1$ versus mean interference power $\mathbb{E}\left[p_2\,\hat{g}_{12}\right]$ for different values of outage probability P_{out}.

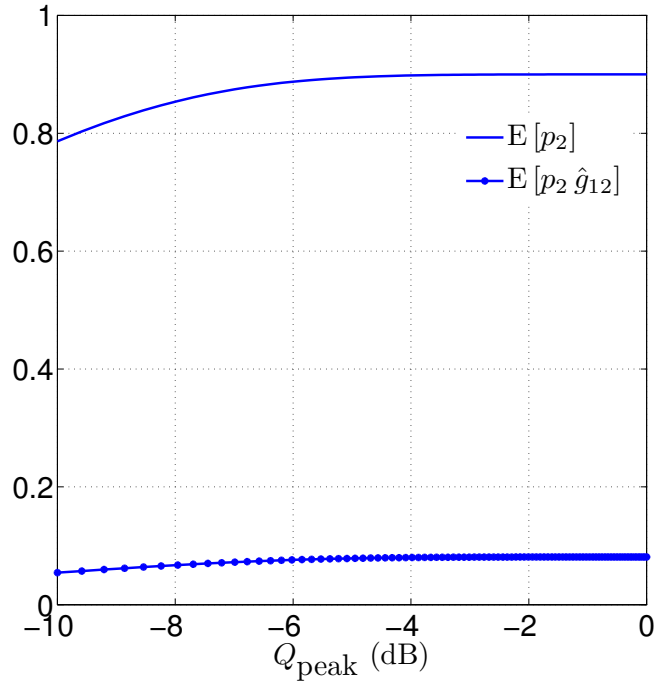

Figure 4.6: Mean transmit power, $\mathbb{E}\,[p_2]$, and mean interference power, $\mathbb{E}\,[p_2\,\hat{g}_{12}]$, versus peak interference power, Q_{peak}. $p_{2,\mathrm{peak}} = 1$ and $\mathrm{P}_{\mathrm{out}} = 0.1$.

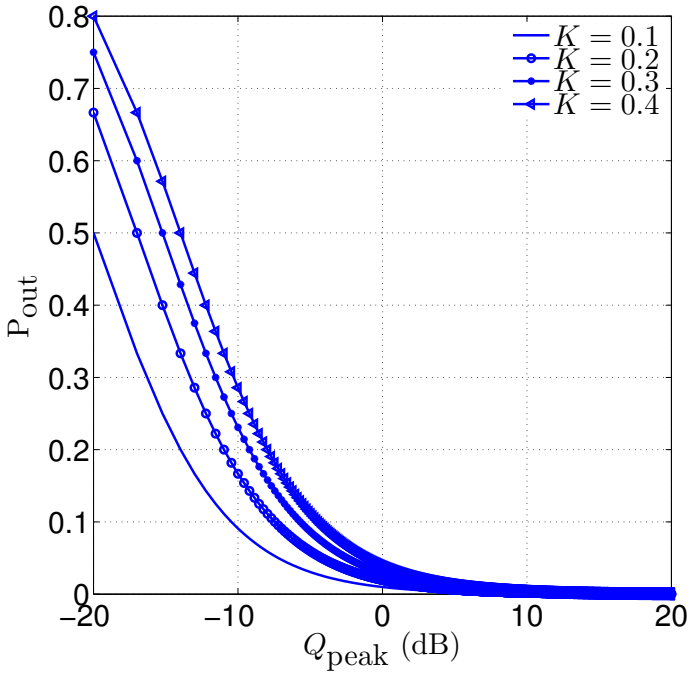

Figure 4.7: Outage probability, $\mathrm{P}_{\mathrm{out}}$, versus peak interference power, Q_{peak}, for different values of minimum received power, K, required for secondary service.

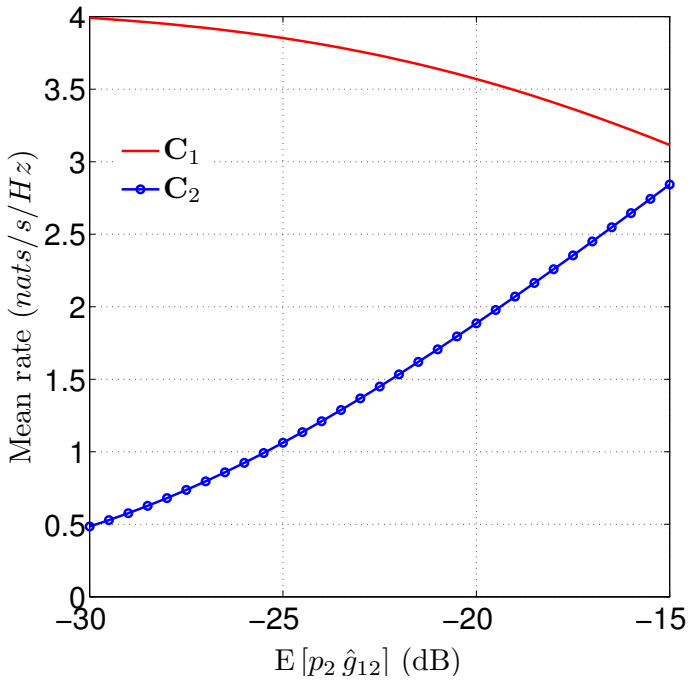

Figure 4.8: Primary mean rate, $\mathbf{C}_1$, and secondary zero-outage capacity, $\mathbf{C}_{2,\text{out}}$, versus mean interference power, $\mathbb{E}\,[p_2\,\hat{g}_{12}]$, for $\mathrm{P}_{\text{out}} = 0.1$.

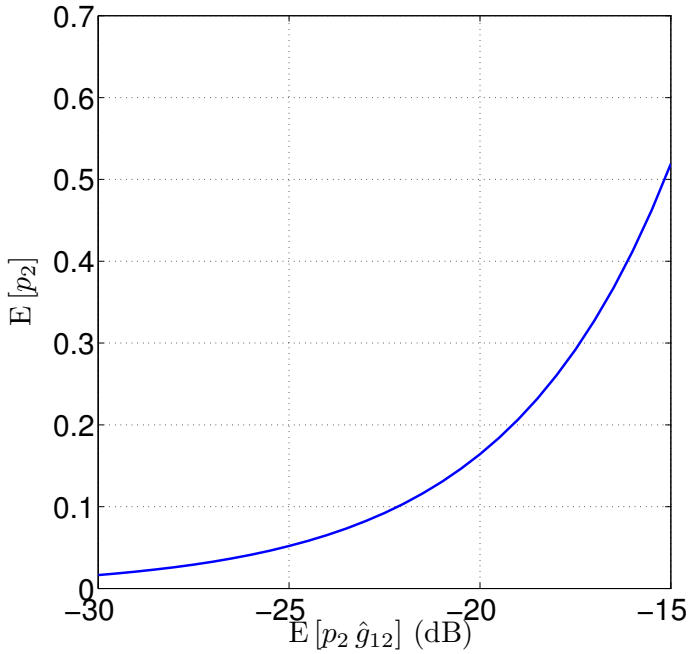

Figure 4.9: Mean transmit power, $\mathbb{E}\,[p_2]$, versus mean interference power, $\mathbb{E}\,[p_2\,\hat{g}_{12}]$, for $\mathrm{P}_{\text{out}} = 0.1$.

4.5 Conclusions

In this chapter, we considered the problem of spectrum-secondary-user power control policy in single-antenna flat-fading channels. The secondary user shares the spectrum with an existing spectrum-licensee or primary user. We proposed two lower bounds, for the primary mean rate, depending on the secondary-user power control scheme. Then, we compared the primary achievable mean rate to these lower bounds when the secondary user is performing several power control schemes. Specially, we proposed an original secondary-user power control for systems that carry out real-time delay-sensitive applications, e.g. voice and video, where it is crucial to guarantee, for given occurrence, predefined minimum instantaneous rates for both the users. This power control uses only the estimations of the secondary direct links (secondary-to-secondary and secondary-to-primary) gains. As a consequence, we did not use complex signal processing to estimate the primary direct links gains. Several numerical examples are given to illustrate the performance of this power control which adapts somewhat with the previous definition of spectrum opportunity.

This contribution has been accepted for publication in the *IEEE transactions on Signal Processing*. Part of this contribution has also been presented in the 21st *Annual IEEE International Symposium on Personal, Indoor and Mobile Radio Communications (PIMRC 2010)*.

Chapter 5

Cognitive radio under path-loss in shadowing-fading environment

In the previous chapters, we have considered theoretical channel without taking into account the impacts of the environment on the wave propagation. Now, we consider a more realistic fading environment by taking into account the shadowing effect and the path-loss. We use the spatial dimension of spectrum-sharing to allow the re-use of a radio frequency spectrum, first licensed to a primary user, by several secondary or cognitive users, while providing an outage performance to the primary user. After showing the existence of a *no-talk zone* (where, there is no secondary transmitter, in order to protect the primary transmission against strong interference) around the primary receiver, we study the effects of shadowing and path-loss on the primary *no-talk zone* when its service is protected by an outage constraint making the its rate to be greater, most of the time, than a minimal necessary rate C_0 .

The remainder of this chapter is organized as follows. In the next section we describe the system and signals model, our main assumptions and the problem we tackle. In order to express the outage probability, we give the probability density function of primary-user SINR, in section 5.2. The primary outage constraint is derived and analyzed, in section 5.3. Using the results of the outage probability, we study the shadowing impact on the primary *no-talk zone* in section 5.4. Finally, conclusions are discussed in section 5.5

5.1 Problem formulation

We consider a single primary user sharing the spectrum with several secondary users. We first describe the channel models and resulting impact on the rate, then we describe the system and give the main goal of our investigation.

5.1.1 Channel models and impact on rate

As we have to study the shadowing impact, we assume the fading is due only to shadowing from obstacles affecting the wave propagation. Moreover, we consider a log-normal model for the shadowing [50]. Let P_i be the transmitted signal of a cognitive user i. The signal I_i received by primary user as interference can be written as:

$$I_i = P_i\, G\left(r_i\right)\, 10^{\frac{\xi_i}{10}}. \tag{5.1}$$

where $G\left(r_i\right)$ is the deterministic propagation path-loss that depends on the distance r_i, from the cognitive transmitter to the primary receiver. The term $10^{\frac{\xi_i}{10}}$ represents the shadowing effect. It characterizes the random variations of the received signal power around the mean value $P_i\, G\left(r_i\right)$. The random variable ξ_i is normally distributed with mean 0 and standard deviation ν_i: $\xi_i \sim \mathcal{N}\left(0, \nu_i^2\right)$, $i = 1, ..., N$. We assume that the logarithmic path-loss $G_{\mathrm{dB}}\left(r_i\right) = -10\, \log_{10} G\left(r_i\right)$ follows the *exponent model* [50] defined by:

$$G_{\mathrm{dB}}\left(r_i\right) = G_{\mathrm{dB}}\left(r_0\right) + 10\, \eta\, \log_{10} \frac{r_i}{r_0}, \tag{5.2}$$

where the term $G_{\mathrm{dB}}\left(r_0\right)$ is the path-loss at a *reference distance* r_0, while η is the path-loss exponent which depends on different characteristics and especially on type of environment, e.g. urban (where $\eta \approx 3 - 4$) or country, and on the antenna height. We have, [50]:

$$G_{\mathrm{dB}}\left(r_0\right) = 20\, \log_{10} \frac{4\, \pi\, f\, r_0}{c} \tag{5.3}$$

where f is the center frequency of the spectrum band and c is the light speed. We take an unit reference distance ($r_0 = 1$), then path-loss can be written as follows:

$$G\left(r_i\right) = G_0\, r_i^{-\eta} \tag{5.4}$$

with $G_0 = (c/4\pi f)^2$. Therefore the term $I_i = P_i\, G_0\, r_i^{-\eta} 10^{\frac{\xi_p}{10}}$ represents the received interference power at the distance r_i from the cognitive user i. Similarly, the primary received signal (the desired signal) is $P_p\, G_0\, r_p^{-\eta}\, 10^{\frac{\xi_p}{10}}$, where P_p is the primary transmitted signal and r_p is the distance between the primary transmitter and its receiver. The primary-link shadowing is characterized by $\xi_p \sim \mathcal{N}\left(0,\, \nu_p^2\right)$. We assume very simple receivers in which all undesired signals are processed as noise (they perform a single user detection, we do not assume any cooperation between primary and secondary users). Thus, with Gaussian signalling, the rate of the primary user may be expressed as

$$\mathrm{C_{pr}} = \log_2 \left(1 + \frac{P_p\, G_0\, r_p^{-\eta}\, 10^{\frac{\xi_p}{10}}}{\sigma^2 + I_{\mathrm{cr}}}\right) \tag{5.5}$$

where I_{cr} is the sum received interference from cognitive transmitters whose total number is set to N:

$$I_{\text{cr}} \triangleq \sum_{i=1}^{N} I_i. \tag{5.6}$$

This assumption is somewhat pessimistic and therefore our results form a conservative lower bound. In practice, some form of multi-user detection allowing for interference suppression or mitigation may be used to enhance the rates achieved [48].

5.1.2 System model and main goal

Now, we show the existence of a *no-talk zone* around the primary receiver and we formulate the problem we will tackle in the sequel.

5.1.2.1 Primary *no-talk zone*

We have defined a spectrum opportunity for a pair of secondary transmitter-receiver, in chapter 1, as a situation where the reception at the secondary receiver should be successful and the transmission from the secondary transmitter should be "harmless". Then, for simple illustration (Cf. Fig. 1.5) two interference regions have been defined: the interference range of secondary users where there should be no primary receiver, and the secondary protection zone where there should be no primary transmitter.

Consider a spectrum is an opportunity for N secondary users distributed randomly, and one primary receiver Pr-Rx. Then, Pr-Rx is outside the interference ranges of the N secondary transmitters as illustrated in figure 5.1. Assume Cr-Tx1 is the closest secondary receiver to Pr-Rx. The worst case of interference for primary receiver Pr-Rx corresponds to the theoretical scenario where all the N secondary transmitters would be at the distance R_0 of Pr-Rx, where R_0 is the distance between Pr-Rx and Cr-Tx1 (Cf. Fig. 5.2). So, there is an exclusive region or *no-talk zone* around the primary receiver Pr-Rx. Inside the primary *no-talk zone*, there is no secondary transmitter in order to guarantee an acceptable level of interference to the primary receiver. In the most general scenario, the exact location of the primary receiver is unknown to the cognitive transmitters (as in TV broadcast scenario for example) [48], then the latter place a guard band of width ϵ_P surrounding the *no-talk zone*. [48] proposed bounds on the primary exclusive region radius R_0 and the guard band ϵ_p to guarantee an outage performance to the primary user.

5.1.2.2 System model

According to the previous remarks on the existence of an exclusive region around the primary receiver, we consider the cognitive network depicted in figure 5.2 with a primary receiver Pr-Tx and N secondary transmitters. The primary receiver is located in the center of a circle of radius R_0 which we call primary *no-talk zone*. In this region no secondary operation is possible to ensure that there is no harmful interference to the primary user's operation in the band. Surrounding the *no-talk zone* is a guard band of width ϵ_p. Close to the *no-talk zone* and the guard band, N cognitive transmitters are distributed randomly.

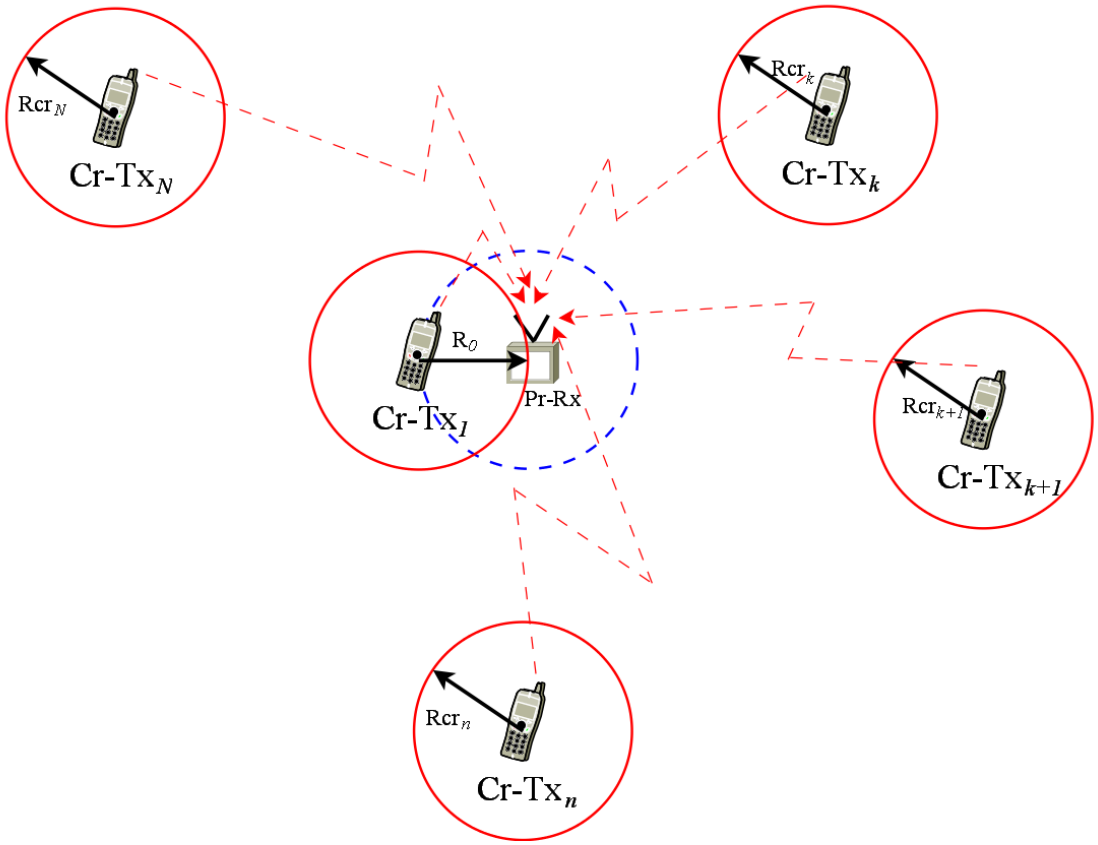

Figure 5.1: A single primary receiver Pr-Rx is outside the interference ranges of N cognitive users. We assume that there is a spectrum opportunity so that the N cognitive users can transmit without violating the interference constraints. Transmitter Cr-Tx$_1$ is supposed to be the closest to Pr-Rx.

A guard band is imposed because, in the most general scenario, the exact location of the primary receiver is unknown to the cognitive transmitters. Thus for cognitive transmitters to meet the interference constraint, they must lie outside the circle of radius $R_0 + \epsilon_p$.

5.1.2.3 Main Goal

In a real network, the power received at any point of a system depends on the local environment (terrain, buildings, trees). Based on this remark, the shadowing has been introduced in [49], where an analytical study of its impact on the outage probability in cellular radio networks is given. Moreover, in cognitive radio, the primary user may be providing socially important services, or it might simply be legacy system that is unable to change. Therefore, we must impose some constraints that guarantee given performance for the primary user in the presence of cognitive users. We model such constraints by an

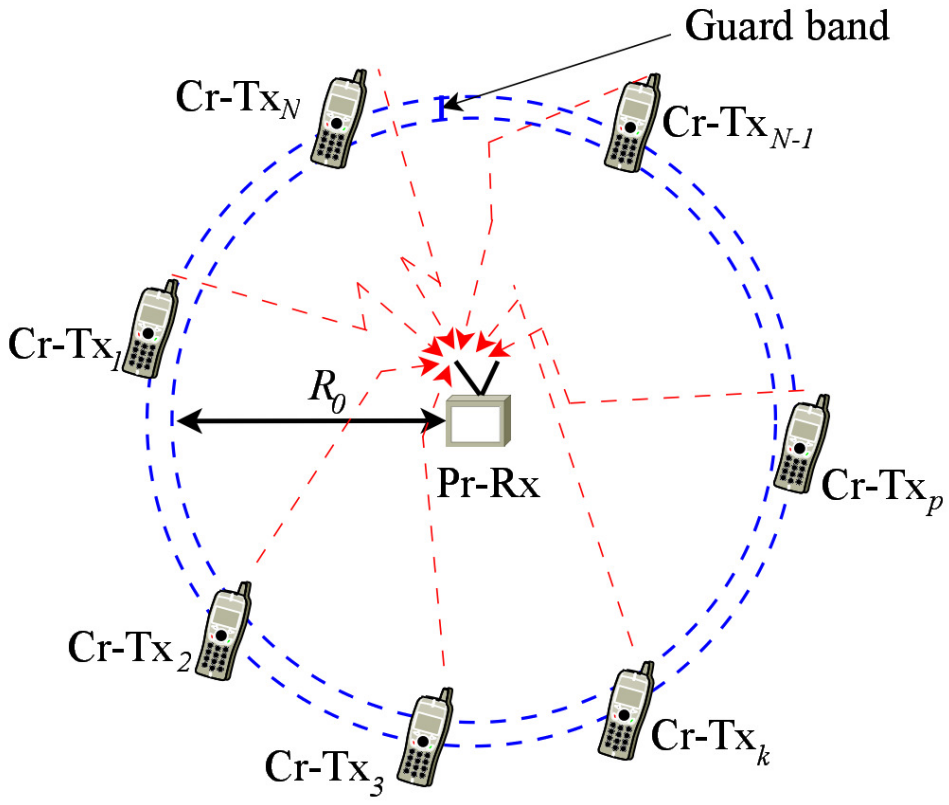

Figure 5.2: The worst case of interference for primary receiver of Fig. 5.1 corresponds to the theoretical case where all the N secondary transmitters would be at the distance R_0 of Pr-Rx, where R_0 is the distance between Pr-Rx and the closest secondary transmitter.

outage rate C_0 for given outage probability P_e, as follows:

$$\mathbf{Pr}\left(\mathrm{C_{pr}} \leq \mathrm{C}_0\right) \leq P_e \tag{5.7}$$

where C_0 is the minimal rate required for the primary service. In the worst case of interference, we set $\mathbf{Pr}\left(\mathrm{C_{pr}} \leq \mathrm{C}_0\right) = P_e$. We assume that such a scenario occurs when all the secondary users are located in the boundaries of the guard band. Thus, the probability P_e is not only function of the shadowing, but also function of radius $R_0 + \epsilon_p$ of the primary *no-talk zone* and the guard band. For a given probability P_e, that depends on the quality of service of the primary user, we may be able to express the radius $R_0 + \epsilon_p$ in terms of the shadowing and path-loss. Then, we can study the impact of the shadowing and path-loss on the primary *no-talk zone*.

5.2 Distribution of the primary SINR

Now, in order to express the outage probability $\mathbf{Pr}\left(\mathrm{C_{pr}} \leq \mathrm{C}_0\right)$, we study the distribution of the primary Signal-to-Noise Ration (SINR).

Let $z_{\mathrm{sh}} \triangleq \frac{x_{\mathrm{sh}}}{y_{\mathrm{sh}}}$ be the primary SINR, where the primary received signal $x_{\mathrm{sh}} \triangleq P_p\, G_0\, r_p^{-\eta}\, 10^{\frac{\xi_p}{10}}$ is a sample of a random variable X_{sh}. The interference plus noise $y_{\mathrm{sh}} \triangleq I_{\mathrm{cr}} + \sigma^2$ is a sample of a random variable Y_{sh}.
Since $\xi_p \sim \mathcal{N}(0, \nu_p)$, the random variable X_{sh} is lognormally distributed. It is characterized by the mean $a\, m_p$ and the standard deviation $a\, \nu_p$ of its natural logarithm ($\log X_{\mathrm{sh}}$ is normally distributed): $a \triangleq \frac{\log(10)}{10}$ and $m_p \triangleq \frac{1}{a} \log\left(P_p\, G_0\, r_p^{-\eta}\right)$. We note $X_{\mathrm{sh}} \sim \text{Log-}\mathcal{N}\left(a\, m_p, a^2 \nu_p^2\right)$. The probability density function of X_{sh} can be expressed as, [66]:

$$f_{X_{\mathrm{sh}}}(x_{\mathrm{sh}}) = \frac{1}{a\, \nu_p\, x_{\mathrm{sh}}\, \sqrt{2\pi}} \exp\left(-\frac{\left(\log(x_{\mathrm{sh}}) - a\, m_p\right)^2}{2\, a^2 \nu_p^2}\right), \quad x_{\mathrm{sh}} > 0 \tag{5.8}$$

The sum interference I_{cr} is a sum of N independant lognormal random variables $I_i \sim \text{Log-}\mathcal{N}\left(a\, m_i,\, a^2\, \nu_i^2\right)$, with $m_i \triangleq \frac{1}{a} \log\left(P_i\, G_0\, r_i^{-\eta}\right)$, $i = 1, ..., N$. Such a sum can be approximated by another lognormal distribution [49], [65]: $I_{\mathrm{cr}} \sim \text{Log-}\mathcal{N}\left(a\, m_{I_{\mathrm{cr}}},\, a^2\, \nu_{I_{\mathrm{cr}}}^2\right)$. Using the Fenton-Wilkinson [65] method, the mean $a\, m_{I_{\mathrm{cr}}}$ and the standard deviation $a\, \nu_{I_{\mathrm{cr}}}$ of the logarithm of I_{cr} can be written as

$$m_{I_{\mathrm{cr}}} = \frac{1}{a}\left[\log\left(\sum_{i=1}^{N} e^{a\, m_i + \frac{a^2\, \nu_i^2}{2}}\right) - \frac{a^2\, \nu_{I_{\mathrm{cr}}}^2}{2}\right] \tag{5.9}$$

$$a^2\, \nu_{I_{\mathrm{cr}}}^2 = \log\left(\frac{\sum_{i=1}^{N} e^{2\, a\, m_i + a^2\, \nu_i^2}\left(e^{a^2\, \nu_i^2} - 1\right)}{\left(\sum_{i=1}^{N} e^{a\, m_i + \frac{a^2\, \nu_i^2}{2}}\right)^2} + 1\right). \tag{5.10}$$

Considering identical shadowing standard deviation for each secondary link, $\nu_i = \nu_0$, $i = 1, ..., N$, and considering all the secondary transmitters are at the same distance from the primary receiver, that is $r_i = r$, $i = 1, ..., N$, we have:

$$m_{I_{\mathrm{cr}}} = \frac{1}{a}\left[\log\left(G_0\, r^{-\eta} \sum_{i=1}^{N} P_i\right) + \frac{a^2\, \nu_0^2}{2} - \frac{a^2\, \nu_{I_{\mathrm{cr}}}^2}{2}\right] \tag{5.11}$$

$$a^2\, \nu_{I_{\mathrm{cr}}}^2 = \log\left[\left(e^{a^2\, \nu_0^2} - 1\right) \frac{\sum_{i=1}^{N} P_i^2}{\left(\sum_{i=1}^{N} P_i\right)^2} + 1\right]. \tag{5.12}$$

The interference plus noise variable Y_{sh} is then a *shifted lognormal* random variable with

the following probability density function:

$$f_{Y_{\rm sh}}(y_{\rm sh}) = \frac{1}{a\,\nu_{I_{\rm cr}}\,(y_{\rm sh}-\sigma^2)\,\sqrt{2\pi}} \exp\left(-\frac{\left(\log(y_{\rm sh}-\sigma^2)-a\,m_{I_{\rm cr}}\right)^2}{2\,a^2\,\nu_{I_{\rm cr}}^2}\right), \quad y_{\rm sh} > \sigma^2. \tag{5.13}$$

We can now express the probability density function of the SINR variable $Z_{\rm sh} = \frac{X_{\rm sh}}{Y_{\rm sh}}$ as:

$$f_{Z_{\rm sh}}(z_{\rm sh}) = \int_{\sigma^2}^{+\infty} y_{\rm sh}\, f_{X_{\rm sh}}(z_{\rm sh}\, y_{\rm sh})\, f_{Y_{\rm sh}}(y_{\rm sh})\, dy_{\rm sh}, \quad z_{\rm sh} > 0. \tag{5.14}$$

We did not find a closed-form expression for $f_{Z_{\rm sh}}(z_{\rm sh})$. However, using (5.14), we derive in the next section some analysis on its cumulative function $\mathbf{Pr}\,(Z_{\rm sh} \leq \alpha) \triangleq \int_0^{\alpha} f_{Z_{\rm sh}}(z_{\rm sh})\, dz_{\rm sh}$, with $\alpha \geq 0$.

5.3 Primary outage constraint

In this section, we analyze the primary outage constraint (5.7) by using previous results on the primary user SINR.

The primary outage constraint (5.7) can be expressed in terms of the SINR variable $z_{\rm sh}$ by using the fact that:

$$\mathbf{Pr}\,(\mathrm{C_{pr}} \leq \mathrm{C_0}) = \mathbf{Pr}\,(Z_{\rm sh} \leq \alpha) \tag{5.15}$$

where $\alpha = 2^{\mathrm{C_0}} - 1$. The constraint (5.7) is then equivalent to:

$$\mathbf{Pr}\,(Z_{\rm sh} \leq \alpha) \leq P_e. \tag{5.16}$$

Now, using the probability density function of $Z_{\rm sh}$ in (5.14), we get

$$\mathbf{Pr}\,(Z_{\rm sh} \leq \alpha) = \int_{\sigma^2}^{+\infty} \left(\int_0^{\alpha} y_{\rm sh}\, f_{X_{\rm sh}}(z_{\rm sh}\, y_{\rm sh})\, dz_{\rm sh} \right) f_{Y_{\rm sh}}(y_{\rm sh})\, dy_{\rm sh} \tag{5.17}$$

with

$$\begin{aligned} \int_0^{\alpha} y_{\rm sh}\, f_{X_{\rm sh}}(z_{\rm sh}\, y_{\rm sh})\, dz_{\rm sh} &= \int_0^{\alpha} \frac{1}{a\,\nu_p\, z_{\rm sh}\,\sqrt{2\pi}} \exp\left(-\frac{\left(\log(z_{\rm sh}\, y_{\rm sh})-a\,m_p\right)^2}{2\,a^2\,\nu_p^2}\right) dz_{\rm sh} \\ &= Q\left(\frac{a\,m_p - \log(\alpha\, y_{\rm sh})}{a\,\nu_p}\right) \end{aligned} \tag{5.18}$$

where the Q-function is defined as

$$Q(x) \triangleq \int_x^{+\infty} \frac{1}{\sqrt{2\pi}} \exp\left(-\frac{t^2}{2}\right) dt. \tag{5.19}$$

Finally we express the probability $\mathbf{Pr}\left(Z_{\text{sh}} \leq \alpha\right)$ as follows:

$$\begin{aligned}\mathbf{Pr}\left(Z_{\text{sh}} \leq \alpha\right) &= \int_0^{+\infty} \frac{1}{a\,\nu_{I_{\text{cr}}}\,t\,\sqrt{2\pi}}\,Q\left(\frac{a\,m_p - \log\left(\alpha\left(t+\sigma^2\right)\right)}{a\,\nu_p}\right) \\ &\times \exp\left(-\frac{\left(\log t - a\,m_{I_{\text{cr}}}\right)^2}{2\,a^2\,\nu_{I_{\text{cr}}}^2}\right)\,dt \qquad (5.20)\\ &= \mathbb{E}_T\left[Q\left(\frac{a\,m_p - \log\left(\alpha\left(T+\sigma^2\right)\right)}{a\,\nu_p}\right)\right]. \qquad (5.21)\end{aligned}$$

Therefore, the probability of event "$Z_{\text{sh}} \leq \alpha$", with $\alpha \geq 0$, is the expectation of the function $Q\left(\frac{a\,m_p - \log\left(\alpha\left(T+\sigma^2\right)\right)}{a\,\nu_p}\right)$, where $T \sim \text{Log-}\mathcal{N}\left(a\,m_{I_{\text{cr}}},\, a^2\,\nu_{I_{\text{cr}}}^2\right)$ is a random variable identically distributed with the sum interference variable I_{cr}.

5.3.1 Outage constraint in the worst case of interference

Since the cognitive transmitters are distributed randomly outside the primary *no-talk zone* and the guard band, the worst case of interference occurs when all the cognitive transmitters are located on the boundaries of the guard band. In this case, $\mathbf{Pr}\left(Z_{\text{sh}} \leq \alpha\right)$ is maximal, so we set:

$$\mathbf{Pr}\left(Z_{\text{sh}} \leq \alpha\right) = P_e, \quad \text{for} \quad r_i = R_0 + \epsilon_p, \quad i = 1, ..., N \qquad (5.22)$$

In the sequel, we set $r = R_0 + \epsilon_p$. Therefore, when $r_i = r$, $i = 1, ..., N$, we have

$$\begin{aligned}P_e &= \int_0^{+\infty} \frac{1}{a\,\nu_{I_{\text{cr}}}\,t\,\sqrt{2\pi}}\,Q\left(\frac{a\,m_p - \log\left(\alpha\left(t+\sigma^2\right)\right)}{a\,\nu_p}\right) \\ &\times \exp\left(-\frac{\left(\log t - a\,m_{I_{\text{cr}}}\right)^2}{2\,a^2\,\nu_{I_{\text{cr}}}^2}\right)\,dt, \qquad (5.23)\end{aligned}$$

where $m_{I_{\text{cr}}}$ is a r-dependent function given by (5.11). The outage probability P_e is function of the radius r, the shadowing standard deviations ν_p and ν_0, as well as of the parameters of the distribution of random variable T.

An Approximation of the outage probability: in order to give an approximation to P_e, we will give some analysis on the evolution of the function $t \longmapsto Q\left(\frac{a\,m_p - \log\left(\alpha\left(t+\sigma^2\right)\right)}{a\,\nu_p}\right)$ and on the distribution of the random variable T.

The Q-function: the function $t \longmapsto Q\left(\frac{a\,m_p - \log\left(\alpha\left(t+\sigma^2\right)\right)}{a\,\nu_p}\right)$ is increasing with t. A numerical example is given in Fig. 5.3, where we set $a\,m_p = 0$, $a\,\nu_p = 1$ and $\alpha = 3$ (that is $\text{C}_0 = 2\,bits/Hertz$). As a special feature, the function $t \longmapsto Q\left(\frac{a\,m_p - \log\left(\alpha\left(t+\sigma^2\right)\right)}{a\,\nu_p}\right)$ is very

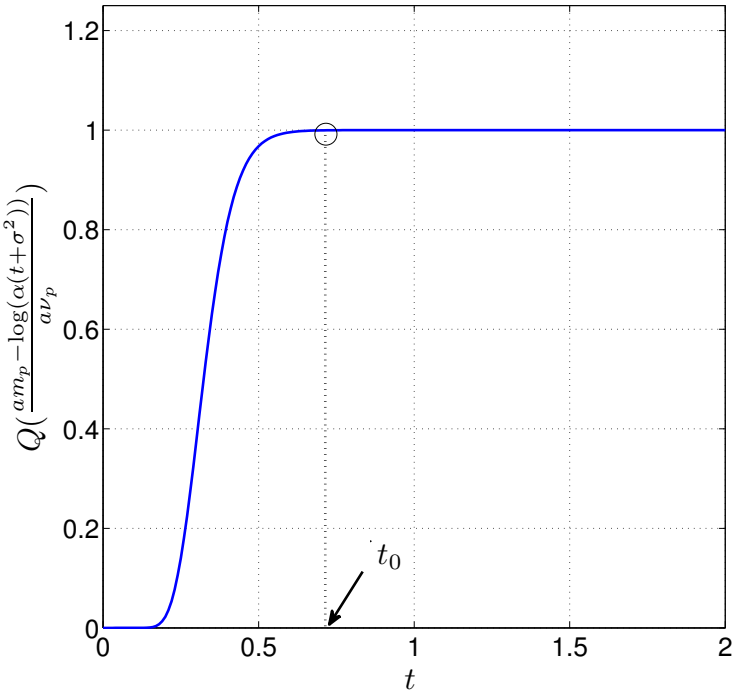

Figure 5.3: Evolution of function $Q\left(\frac{a\,m_p-\log\left(\alpha\,(t+\sigma^2)\right)}{a\,\nu_p}\right)$, $a\,m_p = 0$, $a\,\nu_p = 1$, $\sigma^2 = 0.01$ and $\alpha = 3$.

close to 1 for large t. In the example of Fig. 5.3 , we can see that from $t_0 = 0.7$ to $t \to +\infty$ we can reasonably approximate $Q\left(\frac{a\,m_p-\log\left(\alpha\,(t+\sigma^2)\right)}{a\,\nu_p}\right)$ by 1, and thus, simplify the integral (5.23). In general, the limit value t_0 depends on the mean and standard deviation $a\,m_p$ and $a\,\nu_p$ of the primary link shadowing, as well as on the outage rate C_0 (via the parameter $\alpha \triangleq 2^{\mathrm{C}_0} - 1$).
The outage probability (5.23) can be approximated as

$$\begin{aligned} P_e &\approx \psi\left(t_0\right) + \int_{t_0}^{+\infty} \frac{1}{a\,\nu_{I_{\mathrm{cr}}} t\,\sqrt{2\pi}} \exp\left(-\frac{\left(\log t - a\,m_{I_{\mathrm{cr}}}\right)^2}{2\,a^2\,\nu_{I_{\mathrm{cr}}}^2}\right) dt \\ &= \psi\left(t_0\right) + 1 - Q\left(\frac{a\,m_{I_{\mathrm{cr}}} - \log(t_0)}{a\,\nu_{I_{\mathrm{cr}}}}\right) \end{aligned} \tag{5.24}$$

where

$$\begin{aligned} \psi\left(t_0\right) &= \int_0^{t_0} \frac{1}{a\,\nu_{I_{\mathrm{cr}}} t\,\sqrt{2\pi}}\, Q\left(\frac{a\,m_p - \log\left(\alpha\,(t+\sigma^2)\right)}{a\,\nu_p}\right) \\ &\times \exp\left(-\frac{\left(\log t - a\,m_{I_{\mathrm{cr}}}\right)^2}{2\,a^2\,\nu_{I_{\mathrm{cr}}}^2}\right) dt \end{aligned} \tag{5.25}$$

is a t_0-dependent function.

The lognormal distribution: when $r_i = r$, $i = 1, ..., N$, and considering identical shadowing standard deviation for each secondary link, $\nu_i = \nu_0$, $i = 1, ..., N$, the mean and the standard deviation of the natural logarithm of the sum interference I_{cr} are given by (5.11) and (5.12). The mean and the variance of I_{cr} can be expressed as

$$\mathbb{E}[I_{\text{cr}}] = \exp\left(a\, m_{I_{\text{cr}}} + \frac{1}{2}a^2\, \nu_{I_{\text{cr}}}^2\right) \tag{5.26}$$

$$\text{Var}(I_{\text{cr}}) = \left(\exp\left(a^2\, \nu_{I_{\text{cr}}}^2\right) - 1\right) \exp\left(2a\, m_{I_{\text{cr}}} + a^2\, \nu_{I_{\text{cr}}}^2\right). \tag{5.27}$$

Replacing $a\, m_{I_{\text{cr}}}$ and $a^2\, \nu_{I_{\text{cr}}}^2$ by the values in (5.11) and (5.12) allows us writing:

$$\mathbb{E}[I_{\text{cr}}] = G_0 r^{-\eta} \exp\left(\frac{1}{2}a^2\nu_0^2\right) \sum_{i=1}^{N} P_i \tag{5.28}$$

$$\text{Var}(I_{\text{cr}}) = \left(\exp\left(a^2\, \nu_0^2\right) - 1\right) G_0^2 r^{-2\eta} \exp\left(a^2\nu_0^2\right) \sum_{i=1}^{N} P_i^2. \tag{5.29}$$

Therefore, when the radius r, of primary *no-talk zone* plus guard band, increases, both the mean $\mathbb{E}[I_{\text{cr}}]$ and the variance $\text{Var}(I_{\text{cr}})$, of the sum interference, decrease. As a consequence, the probability P_e decreases (because the function $Q\left(\frac{a\, m_p - \log\left(\alpha\,(t+\sigma^2)\right)}{a\, \nu_p}\right)$ decreases). Moreover, as a result of the shadowing, for a given radius r, the mean and the variance of the sum interference increase with the standard deviation ν_0 of the secondary links, and consequently that affects the probability P_e.

It is interesting to notice that function $\psi(t_0)$ is very close to zero when the values of sum interference within $]0, t_0]$ are very unlikely to occur. That is, the probability density function of Log-$\mathcal{N}\left(a\, m_{I_{\text{cr}}},\, a^2\, \nu_{I_{\text{cr}}}^2\right)$ has relatively insignificant values within $]0, t_0]$. In the example of figure 5.4, the term $\psi(t_0 = 0.7)$ can be neglected since the values within $]0, 0.7]$ are very unlikely occurring. Consequently, for the cases similar to the example of figure 5.4 and 5.3, the outage probability can reasonably be approximated as:

$$P_e \approx 1 - Q\left(\frac{a\, m_{I_{\text{cr}}} - \log(t_0)}{a\, \nu_{I_{\text{cr}}}}\right) \tag{5.30}$$

5.3.2 Numerical examples

In figure 5.6, we plot the outage probability P_e (using its full expression (5.23)) versus the radius, of primary *no-talk zone* plus guard band, for different values of shadowing standard deviation ν_0. We set $r_i = r$, $i = 1, ..., N$ and $\nu_i = \nu_0$, $i = 1, ..., N$. The simulation settings[1] are given below:

[1] We set $G_0 = 1$ for simplicity but in the more realistic case, G_0 is function of the center frequency f of the spectrum band: $G_0 = (c/4\pi f)^2$.

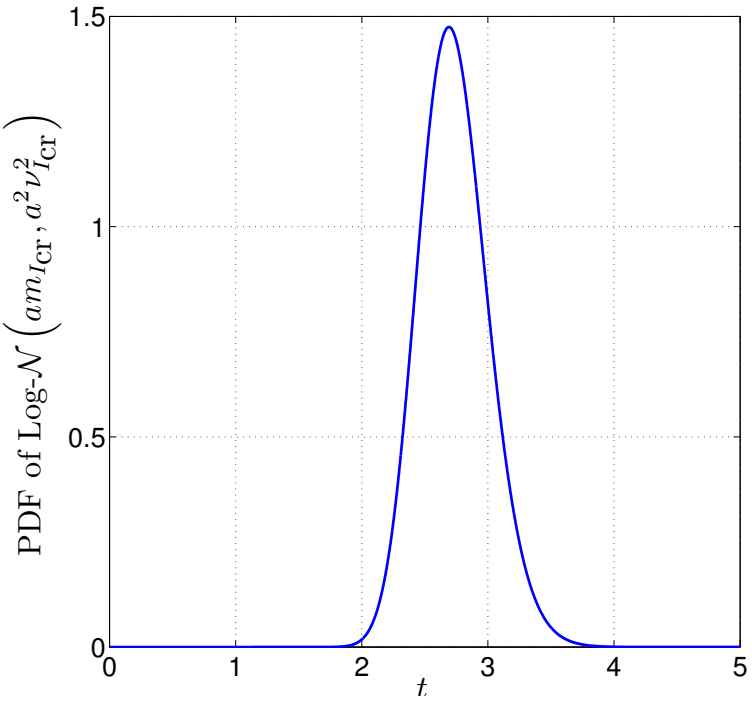

Figure 5.4: Probability density function of the random variable T, which is identically distributed with the sum interference variable $I_{\rm cr}$. $a\,m_{I_{\rm cr}} = 1$, $a\,\nu_{I_{\rm cr}} = 1/10$.

Parameters	Values
$a\,m_p$	0
$a\,\nu_p$	0dB
α	3
σ^2	0.01
G_0	1, as in [49]
η	4
N	10
P_i, $i = 1, ..., N$	0.1

Figure 5.5: Simulation settings

As the radius increases, the outage probability decreases, providing good protection to the primary transmission. As impact of shadowing, we can see that the decreasing speed depends on the spread of shadowing probability density function. For low values of shadowing standard deviation, the outage probability is low and seems to increase as the shadowing standard deviation increases.

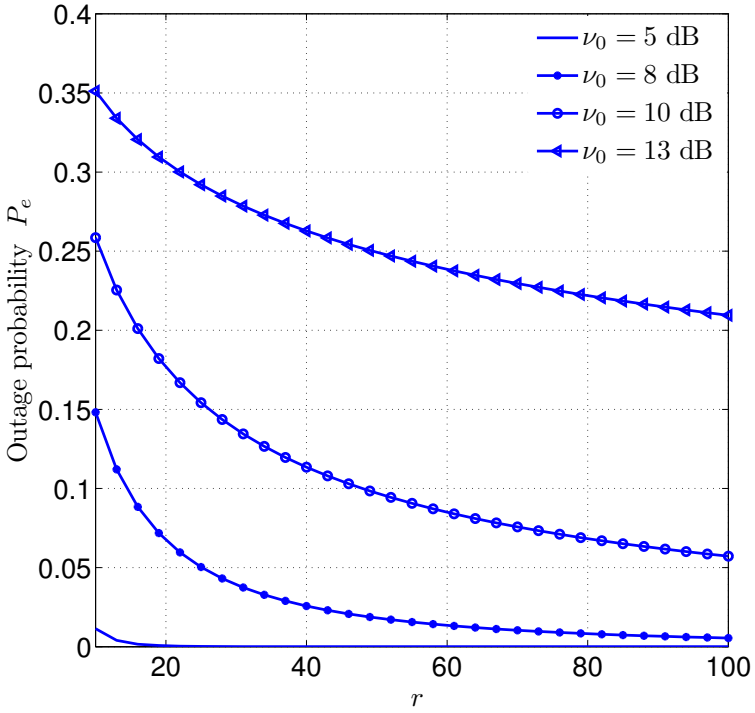

Figure 5.6: Outage probability versus radius of primary *no-talk zone* for different values of shadowing standard deviation.

5.4 Primary *no-talk zone* versus shadowing

Previously, we obtained the expression of the outage probability $\mathbf{Pr}\left(\mathrm{C_{pr}} \leq \mathrm{C_0}\right)$ for the worst case of interference, (5.23). The example of figure 5.6 shows that shadowing standard deviation impacts obviously on the radius of the primary *no-talk zone*. However it is very hard in general to study this impact via the expression (5.23). To give an insight of variation of the radius r according to the shadowing distribution, we derive an upper bound of $\mathbf{Pr}\left(\mathrm{C_{pr}} \leq \mathrm{C_0}\right)$.
The outage probability can be rewritten as

$$\mathbf{Pr}\left(\mathrm{C_{pr}} \leq \mathrm{C_0}\right) = \mathbf{Pr}\left(\frac{Y_{\mathrm{sh}}}{X_{\mathrm{sh}}} \geq \frac{1}{\alpha}\right). \tag{5.31}$$

We can apply Markov's inequality to bound $\mathbf{Pr}\left(\frac{Y_{\mathrm{sh}}}{X_{\mathrm{sh}}} \geq \frac{1}{\alpha}\right)$:

$$\mathbf{Pr}\left(\frac{Y_{\mathrm{sh}}}{X_{\mathrm{sh}}} \geq \frac{1}{\alpha}\right) \leq \alpha \mathbb{E}\left[\frac{Y_{\mathrm{sh}}}{X_{\mathrm{sh}}}\right], \tag{5.32}$$

then, outage probability is upper bounded by $p_{\text{up}} \triangleq \alpha \mathbb{E}\left[\frac{Y_{\text{sh}}}{X_{\text{sh}}}\right]$, which can also be expressed, in respect of the independence of X_{sh} and Y_{sh}, as

$$\alpha \mathbb{E}\left[\frac{Y_{\text{sh}}}{X_{\text{sh}}}\right] = \alpha \mathbb{E}\left[Y_{\text{sh}}\right] \mathbb{E}\left[\frac{1}{X_{\text{sh}}}\right] \tag{5.33}$$

Using the result (5.28), the mean of interference plus noise Y_{sh} is obtained as:

$$\begin{aligned} \mathbb{E}\left[Y_{\text{sh}}\right] &= \sigma^2 + \mathbb{E}\left[I_{\text{cr}}\right] \\ &= \sigma^2 + G_0 r^{-\eta} \exp\left(\frac{1}{2} a^2 \nu_0^2\right) \sum_{i=1}^{N} P_i. \end{aligned} \tag{5.34}$$

Moreover, since $X_{\text{sh}} \sim \text{Log-}\mathcal{N}\left(a\, m_p, a^2 \nu_p^2\right)$, $\frac{1}{X_{\text{sh}}}$ is also lognormally distributed: $\frac{1}{X_{\text{sh}}} \sim \text{Log-}\mathcal{N}\left(-a\, m_p, a^2 \nu_p^2\right)$ and

$$\begin{aligned} \mathbb{E}\left[\frac{1}{X_{\text{sh}}}\right] &= \exp\left(-a\, m_p + \frac{a^2 \nu_p^2}{2}\right) \\ &= \frac{1}{G_0 P_p r_p^{-\eta}} \exp\left(\frac{a^2 \nu_p^2}{2}\right). \end{aligned} \tag{5.35}$$

From (5.33), (5.34) and (5.35), we derive the following expression of r:

$$r^{-\eta} = \left(\frac{p_{\text{up}}}{\alpha} - \frac{\sigma^2}{G_0 P_p r_p^{-\eta}} \exp\left(\frac{1}{2} a^2 \nu_p^2\right)\right) \frac{P_p r_p^{-\eta}}{\sum_{i=1}^{N} P_i} \exp\left(-\frac{1}{2}\left(a^2\, \nu_0^2 + a^2 \nu_p^2\right)\right). \tag{5.36}$$

This result shows that the radius r, of the primary *no-talk zone* plus guard band, is increasing according to the shadowing. The decreasing slope depends on the path-loss exponent η.

Numerical examples:

In Fig. 5.7 we plot r versus shadowing standard deviation of the secondary links, with the same settings as in figure 5.5. We set $P_p = 1$ and $r_p = 1$. The primary exclusive zone grows exponentially according to the shadowing standard deviation. Fig. 5.8 shows the impact of topology (modeling here by the path-loss exponent, η) on the increasing slope of r: the lower is η, the more speedily increasing r is. Consequently, the primary *no-talk zone* is the biggest, and the most speedily increasing according to the shadowing, in free space ($\eta = 2$).

Figure 5.7: Radius of primary *no-talk zone* and guard band versus standard deviation of secondary-links shadowing for different values of the upper bound of the outage probability. $P_p = 1$, $r_p = 1$, and $\eta = 4$.

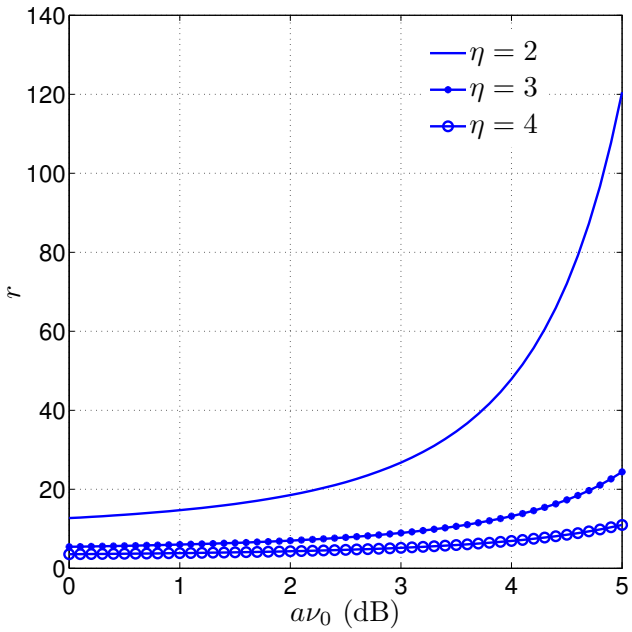

Figure 5.8: Radius of primary *no-talk zone* and guard band versus standard deviation of secondary-links shadowing for different values of path-loss exponent η. $P_p = 1$, $r_p = 1$ and $p_{\text{up}} = 0.1$.

5.5 Conclusions

In this chapter, having shown that it exists a *no-talk zone* around the primary receiver, we considered a spectrum-sharing scheme where the primary receiver is located in the center of a circle with radius R_0. In this region, there is no secondary user in order to protect the primary service against strong interference. An outage performance is also given to the primary transmission. We studied the impact of the shadowing on the primary *no-talk zone*. Our results show that the primary *no-talk zone* increases exponentially with the shadowing standard deviation and the increasing slope depends on the path-loss exponent. In particular, the lower is the path-loss exponent, the more speedily increasing according to the shadowing, is the primary *no-talk zone*. This is not surprising, since a greater path-loss exponent means a greater isolation between transmitters and receivers and therefore an easier spatial reuse of spectrum.

This contribution was published in the proceedings of the 16th *European Wireless, 2010*.

Conclusions and perspectives

Nowadays, with the continual increase of wireless services and the need of bandwidth-greedy applications, joint with electromagnetic spectrum scarcity, there is a need of smart and adequate spectral usage. Spectrum-sharing through Cognitive Radio, proposed as a promising solution for improving the spectrum efficiency, is receiving a lot of attention. In this thesis, we proposed some new contributions in the framework of spectrum-sharing systems analysis and evaluation.

We have seen, through an original characterization of the achievable rate region for the Gaussian Interference Channel (interference treated as noise), that, depending on the level of interference and the channel gains, the achievable rate region exhibits different geometrical forms. For the two-user case, the sum rate is maximal when each user transmits with own maximum permitted power in weak interference regime. Besides, it is maximal when only the best user (with maximum SNR) transmits with its maximum permitted power, the other remained off, in strong interference regime. In particular, for given performance measurement metric (utility), the proposed analytical expressions allow predicting the interference channel behavior and to determinate for what value of parameters (channel gains, transmit powers) the sharing is profitable or not. Let consider that the performance measurement metric is the sum rate of the network. Then, while for weak interference regime the sharing is profitable, in medium and strong interference regimes, cognition or sophisticated techniques (interference suppression, interference alignment with MIMO, [64], dirty paper coding etc.) could be necessary to enhance performance.

For the two-user Gaussian Interference Channel, in fading environment, we found a simple static condition that is necessary and sufficient for enabling simultaneous communication with individual outage performance for each user. After proposing and proving the condition, we gave analytical expressions for the boundaries of the set of possible allocated power pairs with which simultaneous communication is feasible. With the channel mean gains, the outage probabilities and the minimum instantaneous rates (of both the users) only, we could predict if users can share or not the same frequency band while achieving their own outage performances. Then, the proposed condition is useful when building power control, scheduling or access strategy for spectrum-sharing.

For two spectrum users with different priorities to access the spectrum (a primary user and a secondary user for instance), in order to evaluate the impact of secondary

transmission on primary rate, we have investigated secondary user power control. When there is neither collaboration between the users, nor interference or capacity loss constraint, we found that, contrary to what we could imagine, the optimal power control for the secondary link, does not cause the most harmful interference to the primary transmission. However, a constant power control does. Primary mean rate lower bound is also given when secondary user has to protect the primary transmission based on the knowledge of secondary-to-primary link gain estimation. Finally, ensuring for each user given outage performance, assuming that only direct links gains estimations (secondary-to-secondary link and secondary-to-primary link) are available at the secondary transmitter, we have proposed an original secondary power control that is useful for real-time delay-sensitive applications.

In cognitive network, the identification of spectrum opportunity should take into account both the reception quality of primary users and secondary users. So, sharing is allowed only if secondary transmission meet primary interference constraint and primary transmission allows meeting secondary interference constraint. Cognitive networks topology is then subject to at least wave propagation condition. We have seen that shadowing from obstacles affecting the wave propagation, path-loss exponent, depending on the terrain nature and on the base station antenna height, affect the network topology. Primary user *no-talk zone* grows exponentially according to the shadowing standard deviation. In particular, the increasing slope depending on the path-loss exponent. The lower is the path-loss exponent, the more speedily increasing according to the shadowing, is the primary *no-talk zone*. Then, according to the type of environment and the wave propagation conditions, it would be careful to take into account shadowing and path-loss in cognitive networks designing.

Perspectives

In this thesis, the proposed geometrical description, of the Gaussian Interference Channel, allowed us uncovering the maximum sum rate point for the two-user case. However, we have seen that the binary power allocation, that maximizes the two-user case, is not necessary the best optimization strategy for the n-user case, $n > 2$. But, we think that the proposed analytical expressions, for the boundaries of the achievable rate region, could help to find (geometrically) the optimal power allocation to achieve the maximum sum rate in the more general case. Even if several algorithms and games are proposed in the literature to optimize such a function, in general, several iterations with varied times are necessary. So, it would be interesting to investigate the problem by using expressions as those obtained in this thesis.

In chapter 3, the proposed condition to enable simultaneous communication, with individual outage performance, is for two-user case only. A perspective of this thesis could be to generalize the condition to more than two users and to investigate the problem with multiple antennas (MIMO, MISO).

To investigate the lower bounds of the primary mean rate and the secondary user power control, in chapter 4, we have assumed, for simplicity, that primary user performs a

constant power control. The effect of primary user power control scheme is not considered in the system model. However, it is known, [60], that the primary and secondary users power control schemes should be designed jointly. That is for a given licensed primary user power control scheme, we should find the optimal secondary power control strategy. So, our study could be seen as a particular case where primary user performs a constant power control. It would be interesting to approach the problem with wide view.

In this thesis, we studied only the impact of the shadowing from the secondary-to-primary links on the network topology for given value of other parameters (such as primary link shadowing). It is obvious that the primary link shadowing and path-loss affect the network topology and a complete study should take into account the variation of all the links in the network.

Appendix A

Lower bounds of the primary mean rate

In this chapter we calculate the following integrals:

$$\mathbf{C}_{1,\min}^{(1)} = \mathbb{E}\left[\log\left(1+\frac{X}{\sigma^2+Y}\right)\right] \tag{A.1}$$

$$\mathbf{C}_{1,\min}^{(2)} = \mathbb{E}\left[\log\left(1+\frac{X}{\sigma^2+\mathrm{Q}_{\mathrm{avg}}}\right)\right], \tag{A.2}$$

where $X = \bar{P}_1\, g_{11}$ and $Y = \bar{P}_2\, g_{12}$ are exponentially distributed with parameters $\frac{\lambda_{11}}{\bar{P}_1}$ and $\frac{\lambda_{12}}{\bar{P}_2}$.

A.1 Lower bounds A.1

To calculate the integral (A.1), first, we derive the probability density function of the random variable Ω defined as

$$\Omega = \frac{X}{\sigma^2+Y}. \tag{A.3}$$

Let $T = \sigma^2 + Y$. Since Y is exponentially distributed, T has a *shifted-exponential distribution* with the following probability density function:

$$f_T(t) = \begin{cases} \frac{\lambda_{12}}{\bar{P}_2}\exp\left(\frac{\lambda_{12}}{\bar{P}_2}\sigma^2\right)\exp\left(-\frac{\lambda_{12}}{\bar{P}_2}t\right) & \text{if} \quad t \geq \sigma^2 \\ 0 & \text{if} \quad \sigma^2 < t \end{cases} \tag{A.4}$$

The probability density function of the random variable Ω, for $\omega \geq 0$, can be expressed as

$$\begin{aligned} f_\Omega(\omega) &= \int_{\sigma^2}^{+\infty} t\, f_X(\omega\, t)\, f_T(t)\, dt \\ &= \frac{\lambda_{11}}{\bar{P}_1}\frac{\lambda_{12}}{\bar{P}_2}\exp\left(\frac{\lambda_{12}}{\bar{P}_2}\sigma^2\right)\int_{\sigma^2}^{+\infty} t\, \exp\left(-\left(\frac{\lambda_{11}}{\bar{P}_1}\omega + \frac{\lambda_{12}}{\bar{P}_2}\right)\, t\right)\, dt, \end{aligned}$$

thanks to the independence of X and T. After an integration by parts, we obtain

$$f_\Omega(\omega) = \begin{cases} \dfrac{1+b+\dfrac{b}{a}\omega}{a\left(1+\dfrac{1}{a}\omega\right)^2}\exp\left(-\dfrac{b}{a}\omega\right) & \text{if} \quad \omega \geq 0 \\ 0 & \text{if} \quad \omega < 0 \end{cases} \tag{A.5}$$

with [1]

$$a = \frac{\bar{P}_1}{\lambda_{11}}\frac{\lambda_{12}}{\bar{P}_2} \tag{A.6}$$

$$b = \sigma^2\,\frac{\lambda_{12}}{\bar{P}_2}. \tag{A.7}$$

The following equality holds:

$$\frac{1+b+\dfrac{b}{a}\omega}{a\left(1+\dfrac{1}{a}\omega\right)^2}\exp\left(-\frac{b}{a}\omega\right) = \left(\frac{a}{(\omega+a)^2}+\frac{b}{\omega+a}\right)\exp\left(-\frac{b}{a}\omega\right), \tag{A.8}$$

[1] In section 4.4.1.1, we set $w = \dfrac{g_{22}}{\sigma^2 + \bar{P}_1\, g_{21}}$. The probability density function f_W has the same expression as f_Ω but with $a = \dfrac{\lambda_{21}}{\bar{P}_1\,\lambda_{22}}$ and $b = \dfrac{\sigma^2\,\lambda_{21}}{\bar{P}_1}$.

therefore,

$$\begin{aligned}
\mathbf{C}_{1,\min}^{(1)} &= \mathbb{E}\left[\log\left(\Omega+1\right)\right] \\
&= \int_0^{+\infty}\left(\frac{a}{\left(\omega+a\right)^2}+\frac{b}{\omega+a}\right)\exp\left(-\frac{b}{a}\omega\right)\log\left(\omega+1\right)\,d\omega \\
&= a\int_0^{+\infty}\frac{\log\left(\omega+1\right)}{\left(\omega+a\right)^2}\exp\left(-\frac{b}{a}\omega\right)\,d\omega \qquad \text{(A.9)} \\
&+ b\int_0^{+\infty}\frac{\log\left(\omega+1\right)}{\omega+a}\exp\left(-\frac{b}{a}\omega\right)\,d\omega. \qquad \text{(A.10)}
\end{aligned}$$

Now, let

$$\mathrm{I}_1 = \int_0^{+\infty}\frac{\log\left(\omega+1\right)}{\omega+a}\exp\left(-\frac{b}{a}\omega\right)\,d\omega \qquad \text{(A.11)}$$

$$\mathrm{I}_2 = \int_0^{+\infty}\frac{\log\left(\omega+1\right)}{\left(\omega+a\right)^2}\exp\left(-\frac{b}{a}\omega\right)\,d\omega. \qquad \text{(A.12)}$$

After an integration of I_1 by parts, we obtain:

$$\mathrm{I}_1 = \frac{a}{b}\int_0^{+\infty}\frac{1}{\left(\omega+1\right)\left(\omega+a\right)}\exp\left(-\frac{b}{a}\omega\right)\,d\omega - \frac{a}{b}\mathrm{I}_2. \qquad \text{(A.13)}$$

Then, we can express $\mathrm{I}_1+\frac{a}{b}\mathrm{I}_2$ as:

$$\begin{aligned}
\mathrm{I}_1+\frac{a}{b}\mathrm{I}_2 &= \frac{a}{b}\frac{1}{a-1}\left[\int_0^{+\infty}\frac{1}{\omega+1}\exp\left(-\frac{b}{a}\omega\right)\,d\omega\right. \\
&- \left.\int_0^{+\infty}\frac{1}{\omega+a}\exp\left(-\frac{b}{a}\omega\right)\,d\omega\right], \qquad \text{(A.14)}
\end{aligned}$$

thanks to the equality

$$\frac{1}{\left(\omega+1\right)\left(\omega+a\right)} = \frac{1}{a-1}\left(\frac{1}{\omega+1}-\frac{1}{\omega+a}\right). \qquad \text{(A.15)}$$

We can rewrite (A.14) in terms of integral exponential function E_1, [68]:

$$\mathrm{I}_1+\frac{a}{b}\mathrm{I}_2 = \frac{a}{b}\frac{1}{a-1}\left[\exp\left(\frac{b}{a}\right)\,\mathrm{E}_1\left(\frac{b}{a}\right)-\exp\left(b\right)\,\mathrm{E}_1\left(b\right)\right], \qquad \text{(A.16)}$$

finally, we express the lower bounds $\mathbf{C}_{1,\min}^{(1)}$ as:

$$\begin{aligned}\mathbf{C}_{1,\min}^{(1)} &= b\left(\mathrm{I}_1 + \frac{a}{b}\mathrm{I}_2\right) \\ &= \frac{a}{a-1}\left[\exp\left(\frac{b}{a}\right)\,\mathrm{E}_1\left(\frac{b}{a}\right) - \exp\left(b\right)\,\mathrm{E}_1\left(b\right)\right].\end{aligned} \tag{A.17}$$

Replacing a and b by theirs expressions in (A.6) allows us writing:

$$\begin{aligned}\mathbf{C}_{1,\min}^{(1)} &= \frac{\bar{P}_1}{\bar{P}_1 - \dfrac{\lambda_{11}}{\lambda_{12}}\bar{P}_2}\left[\exp\left(\frac{\sigma^2\,\lambda_{11}}{\bar{P}_1}\right)\mathrm{E}_1\left(\frac{\sigma^2\,\lambda_{11}}{\bar{P}_1}\right)\right. \\ &- \left.\exp\left(\frac{\sigma^2\,\lambda_{12}}{\bar{P}_2}\right)\mathrm{E}_1\left(\frac{\sigma^2\,\lambda_{12}}{\bar{P}_2}\right)\right]\end{aligned} \tag{A.18}$$

A.2 Lower bounds A.2

Now, let $\alpha = \dfrac{1}{\sigma^2 + Q_{\text{avg}}}$. We have:

$$\begin{aligned}\mathbf{C}_{1,\min}^{(2)} &= \mathbb{E}\left[\log\left(1+\alpha\,X\right)\right] \\ &= \frac{\lambda_{11}}{\bar{P}_1}\int_0^{+\infty}\log\left(1+\alpha\,x\right)\exp\left(-\frac{\lambda_{11}}{\bar{P}_1}x\right)\,dx.\end{aligned} \tag{A.19}$$

After an integration by parts, we can express $\mathbf{C}_{1,\min}^{(2)}$ as:

$$\begin{aligned}\mathbf{C}_{1,\min}^{(2)} &= \int_0^{+\infty}\frac{\alpha}{\alpha\,x+1}\exp\left(-\frac{\lambda_{11}}{\bar{P}_1}x\right)\,dx \\ &= \exp\left(\frac{\lambda_{11}}{\alpha\,\bar{P}_1}\right)\mathrm{E}_1\left(\frac{\lambda_{11}}{\alpha\,\bar{P}_1}\right) \\ &= \exp\left(\frac{\lambda_{11}\left(\sigma^2+Q_{\text{avg}}\right)}{\bar{P}_1}\right)\mathrm{E}_1\left(\frac{\lambda_{11}\left(\sigma^2+Q_{\text{avg}}\right)}{\bar{P}_1}\right).\end{aligned} \tag{A.20}$$

Appendix B

Mean transmit power and mean interference power

In this chapter, we calculate the mean transmit power and the mean interference power of (4.29). Let $x = g_{12}$ and $y = g_{22}$, the mean transmit power of (4.29) can be expressed as:

$$\begin{aligned}\mathbb{E}\left[p_2\right] &= \int_0^{\frac{Q_{\text{peak}}}{p_{2,\text{peak}}}} \int_{\frac{K}{Q_{\text{peak}}}x}^{+\infty} \lambda_{22}\,\lambda_{12}\,p_{2,\text{peak}}\,\exp\left(-\lambda_{22}\,y\right)\,\exp\left(-\lambda_{12}\,x\right)\,dx\,dy \\ &+ \int_{\frac{Q_{\text{peak}}}{p_{2,\text{peak}}}}^{+\infty} \int_{\frac{K}{Q_{\text{peak}}}x}^{+\infty} \lambda_{22}\,\lambda_{12}\frac{Q_{\text{peak}}}{x}\,\exp\left(-\lambda_{22}\,y\right)\,\exp\left(-\lambda_{12}\,x\right)\,dx\,dy. \qquad \text{(B.1)}\end{aligned}$$

Now, let

$$\mathrm{I}_1' = \int_0^{\frac{Q_{\text{peak}}}{p_{2,\text{peak}}}} \int_{\frac{K}{Q_{\text{peak}}}x}^{+\infty} \lambda_{22}\,\lambda_{12}\,p_{2,\text{peak}}\,\exp\left(-\lambda_{22}\,y\right)\,\exp\left(-\lambda_{12}\,x\right)\,dx\,dy, \qquad \text{(B.2)}$$

$$\mathrm{I}_2' = \int_{\frac{Q_{\text{peak}}}{p_{2,\text{peak}}}}^{+\infty} \int_{\frac{K}{Q_{\text{peak}}}x}^{+\infty} \lambda_{22}\,\lambda_{12}\,\frac{Q_{\text{peak}}}{x}\,\exp\left(-\lambda_{22}\,y\right)\,\exp\left(-\lambda_{12}\,x\right)\,dx\,dy. \qquad \text{(B.3)}$$

Integral I_1' is obtained as:

$$\begin{aligned}\mathrm{I}_1' &= p_{2,\text{peak}} \int_0^{\frac{Q_{\text{peak}}}{p_{2,\text{peak}}}} \lambda_{12}\,\exp\left(-\lambda_{12}\,x\right)\left(\int_{\frac{K}{Q_{\text{peak}}}x}^{+\infty} \lambda_{22}\,\exp\left(-\lambda_{22}\,y\right)\,dy\right)dx \\ &= p_{2,\text{peak}} \int_0^{\frac{Q_{\text{peak}}}{p_{2,\text{peak}}}} \lambda_{12}\,\exp\left(-\left(\lambda_{12}+\frac{\lambda_{22}\,K}{Q_{\text{peak}}}\right)\,x\right)\,dx \\ &= \frac{p_{2,\text{peak}}}{1+\frac{\lambda_{22}}{\lambda_{12}}\,\frac{K}{Q_{\text{peak}}}}\left[1-\exp\left(-\frac{\lambda_{22}\,K+\lambda_{12}\,Q_{\text{peak}}}{p_{2,\text{peak}}}\right)\right]. \qquad \text{(B.4)}\end{aligned}$$

Integral I_2' is obtained as:

$$\begin{aligned}
\mathrm{I}_2' &= \int_{\frac{Q_{\mathrm{peak}}}{p_{2,\mathrm{peak}}}}^{+\infty} \lambda_{12}\,\frac{Q_{\mathrm{peak}}}{x}\,\exp\left(-\lambda_{12}\,x\right)\left(\int_{\frac{K}{Q_{\mathrm{peak}}}x}^{+\infty}\lambda_{22}\,\exp\left(-\lambda_{22}\,y\right)\,dy\right)\,dx \\
&= \int_{\frac{Q_{\mathrm{peak}}}{p_{2,\mathrm{peak}}}}^{+\infty} \lambda_{12}\,\frac{Q_{\mathrm{peak}}}{x}\,\exp\left(-\left(\lambda_{12}+\frac{\lambda_{22}\,K}{Q_{\mathrm{peak}}}\right)\,x\right)\,dx \\
&= \lambda_{12}\,Q_{\mathrm{peak}}\,\mathrm{E}_1\left(\frac{\lambda_{22}\,K+\lambda_{12}\,Q_{\mathrm{peak}}}{p_{2,\mathrm{peak}}}\right). \qquad \text{(B.5)}
\end{aligned}$$

Finally, we have:

$$\begin{aligned}
\mathbb{E}\left[p_2\right] &= \frac{p_{2,\mathrm{peak}}}{1+\frac{\lambda_{22}}{\lambda_{12}}\frac{K}{Q_{\mathrm{peak}}}}\left[1-\exp\left(-\frac{\lambda_{22}\,K+\lambda_{12}\,Q_{\mathrm{peak}}}{p_{2,\mathrm{peak}}}\right)\right] \\
&+ \lambda_{12}\,Q_{\mathrm{peak}}\,\mathrm{E}_1\left(\frac{\lambda_{22}\,K+\lambda_{12}\,Q_{\mathrm{peak}}}{p_{2,\mathrm{peak}}}\right). \qquad \text{(B.6)}
\end{aligned}$$

The mean interference power is expressed as:

$$\mathbb{E}\left[p_2\,\hat{g}_{12}\right] = \mathrm{I}_1'' + \mathrm{I}_2'', \qquad \text{(B.7)}$$

with:

$$\begin{aligned}
\mathrm{I}_1'' &= \int_0^{\frac{Q_{\mathrm{peak}}}{p_{2,\mathrm{peak}}}}\int_{\frac{K}{Q_{\mathrm{peak}}}x}^{+\infty}\lambda_{22}\,\lambda_{12}\,x\,p_{2,\mathrm{peak}}\,\exp\left(-\lambda_{22}\,y\right)\,\exp\left(-\lambda_{12}\,x\right)\,dx\,dy, \\
\mathrm{I}_2'' &= \int_{\frac{Q_{\mathrm{peak}}}{p_{2,\mathrm{peak}}}}^{+\infty}\int_{\frac{K}{Q_{\mathrm{peak}}}x}^{+\infty}\lambda_{22}\,\lambda_{12}\,Q_{\mathrm{peak}}\,\exp\left(-\lambda_{22}\,y\right)\,\exp\left(-\lambda_{12}\,x\right)\,dx\,dy. \qquad \text{(B.8)}
\end{aligned}$$

Integral I_1'' is obtained as follows:

$$\begin{aligned}
\mathrm{I}_1'' &= p_{2,\mathrm{peak}}\int_0^{\frac{Q_{\mathrm{peak}}}{p_{2,\mathrm{peak}}}}\lambda_{12}\,x\,\exp\left(-\lambda_{12}\,x\right)\left(\int_{\frac{K}{Q_{\mathrm{peak}}}x}^{+\infty}\lambda_{22}\,\exp\left(-\lambda_{22}\,y\right)\,dy\right)\,dx \\
&= p_{2,\mathrm{peak}}\int_0^{\frac{Q_{\mathrm{peak}}}{p_{2,\mathrm{peak}}}}\lambda_{12}\,x\,\exp\left(-\left(\lambda_{12}+\frac{\lambda_{22}\,K}{Q_{\mathrm{peak}}}\right)\,x\right)\,dx \\
&= \frac{p_{2,\mathrm{peak}}/\lambda_{12}}{\left(1+\frac{\lambda_{22}}{\lambda_{12}}\frac{K}{Q_{\mathrm{peak}}}\right)^2}\left[1-\left(1+\frac{\lambda_{12}\,Q_{\mathrm{peak}}+\lambda_{22}\,K}{p_{2,\mathrm{peak}}}\right)\exp\left(-\frac{\lambda_{12}\,Q_{\mathrm{peak}}+\lambda_{22}\,K}{p_{2,\mathrm{peak}}}\right)\right],
\end{aligned}$$

and integral I_2'' as:

$$\begin{aligned}\mathrm{I}_2'' &= Q_{\mathrm{peak}} \int_{\frac{Q_{\mathrm{peak}}}{p_{2,\mathrm{peak}}}}^{+\infty} \lambda_{12}\, \exp\left(-\lambda_{12}\, x\right) \left(\int_{\frac{K}{Q_{\mathrm{peak}}} x}^{+\infty} \lambda_{22}\, \exp\left(-\lambda_{22}\, y\right)\, dy \right) dx \\ &= \frac{Q_{\mathrm{peak}}}{1 + \frac{\lambda_{22}}{\lambda_{12}} \frac{K}{Q_{\mathrm{peak}}}} \exp\left(- \frac{\lambda_{12}\, Q_{\mathrm{peak}} + \lambda_{22}\, K}{p_{2,\mathrm{peak}}} \right).\end{aligned}$$

Finally, the mean interference power is expressed as:

$$\mathbb{E}\left[p_2\, \hat{g}_{12}\right] = \frac{p_{2,\mathrm{peak}}/\lambda_{12}}{\left(1 + \frac{\lambda_{22}}{\lambda_{12}}\, \frac{K}{Q_{\mathrm{peak}}}\right)^2} \left[1 - \exp\left(- \frac{\lambda_{12}\, Q_{\mathrm{peak}} + \lambda_{22}\, K}{p_{2,\mathrm{peak}}} \right) \right]. \tag{B.9}$$

Bibliography

[1] J. Mitola, "Cognitive radio: An integrated agent architecture for software defined radio," Ph.D. dissertation, KTH, Stockholm, Sweden, Dec. 2000.

[2] Spectrum Policy Task Force, "Spectrum Policy Task Force Report," *Federal Communications Commission ET Docket 02-135*, 2002.

[3] M. M. Buddhikot, "Understanding dynamic spectrum access: models, taxonomy and challenges," *in proceedings of IEEE DysPAN Dublin*, April 17-21, 2007.

[4] A. Shukla, A. Alptekin, J. Bradford, E. Burdidge, D. Chandler, M. Kennett, P. Levine and S. Weiss, " Cognitive Radio Technology: a study for Ofcom ", *QinetiQ*, vol. 1, February 2007.

[5] A. Shukla, A. Alptekin, J. Bradford, E. Burdidge, D. Chandler, M. Kennett, P. Levine and S. Weiss, " Cognitive Radio Technology: a study for Ofcom ", *QinetiQ*, vol. 2, December 2006.

[6] " Cisco Visual Networking Index: Global Mobile Data Traffic Forecast Update, 2009-2014 ", February 9, 2010. Online, available: http://www.cisco.com/en/US/solutions/collateral/ns341/ns525/ns537/ns705/ns827/white_paper_c11-520862.pdf

[7] "Cisco Visual Networking Index: Global Mobile Data Traffic Forecast Update," January 29, 2009. Online, available: http://www.mobiletvworld.com/resources/documents/documentvault/GlobalMobileDataTraffic2009.pdf

[8] A. Goldsmith, S. A. Jafar, I. Maric and S. Srinivasa, "Breaking spectrum gridlock with cognitive radios: an information theoretic perspective," *Proceedings of the IEEE*, vol. 97, no. 5, pp. 894-914, May 2009.

[9] P. J. Kolodzy, "Cognitive radio fundamentals," *in Proc. SDR Forum,* Singapore, Apr. 2005.

[10] J. M. Peha, "Sharing Spectrum Through Spectrum Policy Reform and Cognitive Radio," *Proceedings of the IEEE,* 2008.

[11] S. Haykin, "Cognitive Radio: Brain-Empowered Wireless Communications," *IEEE Journal on Selected Areas in Communications,* vol. 23, no.2, February 2005.

[12] Federal Communications Commission, "Report and Order (FCC 03-287): Revision of Parts 2 and 15 of the Commission's Rules to Permit Unlicensed National Information Infrastructure (U-NII) devices in the 5 GHz band," *ET Docket No. 03-122,* 18 November 2003.

[13] Wireless World Research Forum, "Cognitive Radio and Management of Spectrum and Radio Resources in Reconfigurable Networks," *Working Group 6 White Paper,* 2005.

[14] P. J. Kolodzy, "Interference temperature: A metric for dynamic spectrum utilization," *Int. J. Netw. Manage.,* pp. 103-113, Mar. 2006.

[15] F. K. Jondral, "Software-Defined Radio–Basics and Evolution to Cognitive Radio," *EURASIP Journal on Wireless Communications and Networking,* vol. 3, pp. 275-283, April 2005.

[16] T. X. Brown, "An Analysis of Unlicensed Device Operation in Licensed Broadcast Service Bands," *Proc. IEEE 1st Symp. Dynamic Spectrum Access Networks,* Baltimore, pp. 11-29, Nov. 2005.

[17] A. B. Carleial, "A case where interference does not reduce capacity," *IEEE Trans. Inform. Theory,* vol. IT-21, no. 5, p. 569, Sept. 1975.

[18] H. Sato, "Two user communication channels," *IEEE Trans. Inf. Theory,* vol. IT-23, pp. 295-304, May 1977.

[19] A. B. Carleial, "Interference channels," *IEEE Trans. Inf. Theory,* vol. IT-24, pp. 60-70, Jan. 1978.

[20] H. Sato, "On the capacity region of a discrete two-user channel for strong interference," *IEEE Trans. Inform. Theory,* vol. IT-24, no. 3, p. 377, May 1978.

[21] T. S. Han and K. Kobayashi, "A new achievable rate region for the interference channel," *IEEE Trans. Inf. Theory,* vol.27, no.1, pp. 49-60, Jan. 1981.

[22] H. Sato, "The capacity of the Gaussian interference channel under strong interference," *IEEE Trans. on Inf. Theory,* vol. 27, no. 6, pp. 786-788, Nov. 1981.

[23] M. H. M. Costa and A. E. Gamal, "The capacity region of the discrete memoryless interference channel with strong interference," *IEEE Trans. Inf. Theory,* vol. IT-33, pp. 710-711, Sep. 1987

[24] I. Sason, "On achievable rate regions for the Gaussian interference channel," *Proc. IEEE International Symposium on Information Theory (ISIT),* June 2004.

[25] G. Kramer, "Review of rate regions for interference channels ," *Proc. 2006 Int. Zurich Seminar on Communications,* Zurich, Switzerland, pp. 162-165, Feb. 22-24, 2006.

[26] A. Gjendemsjø, D. Gesbert, G. E. Øien and S. G. Kiani, "Optimal power allocation and scheduling for two-cell capacity maximization, " *4th International Symposium on Modeling and Optimization in Mobile, Ad Hoc and Wireless Networks,* pp.1-6, 03-06 April 2006.

[27] R. H. Etkin, D. N. C. Tse and H. Wang, "Gaussian Interference Channel Capacity to Within One Bit: the General Case," *IEEE International Symposiunm on Information Theory (ISIT),* pp.2181-2185, June 2007.

[28] M. Charafeddine and A. Paulraj, "Sequential Geometric Programming for 2 X 2 Interference Channel Power Control," *IEEE 41st Annual Conference on Information Science and Systems (CISS'07),* pp. 185-189, March 2007.

[29] H. Mahdavi-Doost, M. Ebrahimi and A. K. Khandani, "Characterization of rate region in interference channels with constrained power," *IEEE International Symposium on Information Theory,* pp.2441-2445, 24-29 June 2007.

[30] A. Gjendemsjø, D. Gesbert, G. E. Øien and S. G. Kiani, "Binary power control for sum rate maximization over multiple interfering links," *IEEE Transactions on Wireless Communications,* vol.7, no. 8, pp.3164-3173, August 2008

[31] A. S. Motahari and A. K. Khandani, "Capacity bounds for the Gaussian interference channel," *IEEE International Symposium on Information Theory,* vol.55, no.2, pp.620-643, Feb. 2009.

[32] A. Bagayoko, P. Tortelier and I. Fijalkow "Simultaneous outage performance in a spectrum-sharing fading environment," *IEEE SPAWC,* Marrakeck, Morocco, June 2010.

[33] R. Francisco and A. Pandharipande "Spectrum Occupancy in the 2.36-2.4 GHz Band: Measurements and Analysis," *European Wireless 2010*, Lucca, Italy, April 2010.

[34] A. Carniani, L. Giupponi and R. Verdone "Evaluation of spectrum opportunities in the GSM band," *European Wireless 2010*, Lucca, Italy, April 2010.

[35] A. Ghasemi and E. S. Sousa, "Spectrum Sensing in Cognitive Radio Networks: Requirements, Challenges and Design Trade-offs," *IEEE Communications Magazine*, vol. 46, no.4, pp. 32-39, April 2008.

[36] A. Ghasemi and E. S. Sousa, "Fundamental limits of spectrum-sharing in fading environments," *IEEE Trans. Wireless Commun.*, vol. 6, no. 2, pp. 649-658, Feb. 2007.

[37] A. Ghasemi and E. S. Sousa, "Capacity of fading channels under spectrum-sharing constraints, " *Communications, 2006. ICC '06. IEEE International Conference on*, vol.10, pp.4373-4378, June 2006.

[38] A. J. Goldsmith and P. P. Varaiya, "Capacity of fading channels with channel side information, " *Information Theory, IEEE Transactions on*, vol.43, no.6, pp.1986-1992, Nov 1997.

[39] M. Gastpar, "On Capacity Under Receive and Spatial Spectrum-Sharing Constraints, " *IEEE Transactions on Information Theory*, 53(2):471-487, February 2007.

[40] R. C. Pereira, R. D. Souza and M. E. Pellenz, "Overlay Cognitive Radio with Multiple Secondaries and its Application to Wireless Mesh Networks," *IEEE 69th Vehicular Technology Conference, VTC,* pp.1-5, 26-29 April 2009.

[41] W. Wu, S. Vishwanath and A. Arapostathis, "On the capacity of the interference channel with degraded message sets," *IEEE Trans. Inf. Theory,* vol. 53, pp. 4391-4399, Nov. 2007.

[42] A. Jovicic and P. Viswanath, "Cognitive radio: An information-theoretic perspective" *IEEE Trans. Inf. Theory,* vol. 55, no.9, pp.3945-3958, Sept. 2009.

[43] I. Marić, R. D. Yates and G. Kramer, "Capacity of interference channels with partial transmitter cooperation," *IEEE Trans. Inf. Theory,* vol. 53, pp. 3536-3548, Oct. 2007.

[44] A. Somekh-Baruch, S. Shamai(Shitz) and S. Verdu, "Cognitive interference channels with state information," *in Proc. IEEE Int. Symp. Inf. Theory,* Jul. 2008.

[45] P. Tortelier and A. Bagayoko, "On the achievable rate region of the Gaussian interference channel: the two and three-user cases," *Annals of Telecommunications*, October 2009, Online, available: http://www.springerlink.com/content/p5524607963308m7.

[46] A. Sahai, R. Tandra, S. M. Mishra and N. Hoven, "Fundamental design tradeoffs in cognitive radio systems," *TAPAS '06: Proceedings of the first international workshop on Technology and policy for accessing spectrum,* Boston, Massachusetts, pp.2, Aug. 2006.

[47] J. M. Peha, "Approaches to spectrum sharing," *IEEE Communications Magazine*, pp. 10-11, February 2005.

[48] M. Vu, N. Devroye and V. Tarokh "The primary exclusive region in cognitive networks," *5th IEEE Consumer Communications and Networking Conference (CCNC 2008),* pp.1014-1019, 10-12 Jan. 2008.

[49] J. M. Kelif and M. Coupechoux "Impact of Topology and Shadowing on the Outage Probability of Cellular Networks ", *In IEEE International Conference on Communications, ICC,* Dresden, Germany, jun 2009.

[50] V. S. Abhayawardhana, I. J. Wassell, D. Crosby, M. P. Sellars and M. G. Brown, "Comparison of empirical propagation path loss models for fixed wireless access systems", *in proceeding of the 61st IEEE Vehicular Technology Conference (VTC'05)*, vol.1, pp.73-77, Stockholm, Sweden, May-June 2005.

[51] A. Alsawah and I. Fijalkow, "Practical Radio Link Resource Allocation for Fair QoS-Provision on OFDMA Downlink with Partial Channel-State Information ", EURASIP

Journal on Applied Signal Processing - Special Issue on Cross-Layer Design for the Physical, MAC, and Link Layer in Wireless Systems, Aug. 2008.

[52] A. Bagayoko, P. Tortelier and I. Fijalkow "Impact of shadowing on the primary exclusive region in cognitive networks," *European Wireless 2010*, Lucca, Italy, April 2010.

[53] A. J. Goldsmith and P. Varaiya, "Capacity of fading channels with channel side information," *IEEE Trans. Inform. Theory*, vol. 43, no. 6, pp. 1986-1992, Nov. 1997.

[54] E. Biglieri, J. Proakis, and S. Shamai (Shitz), "Fading channels: Information-theoretic and communications aspects," *IEEE Trans. Inform. Theory*, vol. 44, no. 6, pp. 2619-2692, Oct. 1998.

[55] M. H. M. Costa, "Writing on dirty paper," *IEEE Trans. Inf. Theory*, vol. IT-29, pp. 439-441, May 1983.

[56] R. Etkin, A. P. Parekh and D. Tse, "Spectrum Sharing in Unlicensed Bands," *IEEE Journal on Selected Areas of Communication*, vol. 25, no. 3, pp. 517-528, April 2007.

[57] L. Musavian and S. Aïssa, "Ergodic and outage capacities of spectrum-sharing systems in fading channels", *IEEE GLOBECOM 2007*, pp. 3327-3331.

[58] R. Zhang, "Optimal power control over fading cognitive radio channel by exploiting primary user CSI", *IEEE GLOBECOM 2008*.

[59] R. Zhang, "On peak versus average interference power constraints for protecting primary users in cognitive radio networks", *IEEE Transactions on Wireless Communications*, vol.8, no.4, pp.2112-2120, April 2009.

[60] W. Ren, Q. Zhao and A. Swami, "Power Control in Cognitive Radio Networks: How to Cross a Multi-Lane Highway," *IEEE journal on selected areas in communications,* vol. 27, No.7, September 2009.

[61] A. Bagayoko, P. Tortelier and I. Fijalkow, "Allocation de puissance dans le partage du spectre avec une connaissance partielle des canaux," *Gretsi 2009,* Dijon, France, September 2009.

[62] A. Bagayoko, P. Tortelier and I. Fijalkow, "Spectrum-Sharing Power Control with Outage Performance Requirements and Direct Links CSI Only," *IEEE PIMRC* Istanbul, Turkey, September 2010 (to appear).

[63] A. Bagayoko, P. Tortelier and I. Fijalkow, "Power control of spectrum-sharing in fading environment with partial channel state information," *IEEE transactions on Signal Processing, to appear.*

[64] S. M. Perlaza, N. Fawaz, S. Lasaulce and M. Debbah, "From spectrum pooling to space pooling: interference alignment in MIMO cognitive networks ," *IEEE Transactions on Signal Processing,* 2010

[65] L. Fenton,"The sum of lognormal probability distributions in scatter transmission system ", *IEEE (IRE) Transactions on Communications*, CS-8, 1960.

[66] M.K. Simon and M. Alouini, *Digital communications over fading channels*, New York: Wiley, 1995.

[67] T. Cover and J. Thomas, *Elements of Information Theory*, New York: Wiley, 1991.

[68] M. Abramowitz and I. A. Stegun, "Handbook of mathematical functions," Dover, New York, 1965.